Characterization of the yeast proteins Neo1p and Sjl2p, two highly conserved regulators of phospholipid composition within endosomal membranes

Von der Fakultät Geo- und Biowissenschaften der Universität Stuttgart
zur Erlangung der Würde eines Doktors der
Naturwissenschaften (Dr. rer. Nat.) genehmigte Abhandlung

vorgelegt von

Sidonie Wicky John
aus Schelten (Schweiz)

Hauptberichter: Priv.-Doz. Dr. Birgit Singer-Krüger
Mitberichter: Prof. Dr. Dieter H. Wolf
Tag der mündlichen Prüfung: 15.12.2004

Institut für Biochemie der Universität Stuttgart
2004

Table of contents

Abbreviations

AP	clathrin heterotetrameric adaptor protein
APL	aminophospholipid
Arf	ADP-ribosylation factor
Arl	Arf-like
$C_{12}E_9$	polyoxyethylene-9-lauryl ether
CLAP	chymostatin, leupeptin, antipain, pepstatin
CPY	carboxypeptidase Y
Cy3	indocarbocyanine
DOPC	dioleoylphosphatidylcholine
ER	endoplasmic reticulum
ERAD	ER-associated degradation
FM4-64	*N*-(3-triethylammoniumpropyl)-4-(*p*-diethylaminophenyl-hexatrienyl) pyridinium dibromide
GAP	GTPase-activating protein
GEF	guanine nucleotide exchange factor
GFP	green fluorescent protein
GGA	Golgi-associated, g-adaptin homologous, Arf-interacting protein
HA	hemagglutinin
IF	indirect immunofluorescence
IP	immunoprecipitation
KP_i	potassium phosphate buffer
MVB	multivesicular body
1NA-PP1	4-amino-1-tert-butyl-3-(1'-naphthyl)pyrazolo[3,4-d]pyrimidine
NP40	Nonidet P-40
PA	phosphatidic acid
PBS	phosphate saline buffer
PC	phosphatidylcholine
PCR	polymerase chain reaction
PE	phosphatidylethanolamine
PG	phosphatidylglycerol
PI	phosphoinositide
PPIP	polyphosphoinositide phosphatase
PS	phosphatidylserine
PtdIns	phosphatidylinositol
PtdIns(4)P	phosphatidylinositol-4-phosphate
PtdIns(4,5)P_2	phosphatidyl-inositol-4,5-bisphosphate
PVC	prevacuolar compartment
SNARE	soluble *N*-ethylmaleimide-sensitive factor attachment protein receptor
SD	synthetic growth medium
SDS-PAGE	sodium dodecyl sulfate-polyacrylamide gel electrophoresis
TAP	tandem affinity purification
TCA	trichloroacetic acid
TGN	*trans*-Golgi network
ts	temperature-sensitive
YPD	yeast complete medium

Zusammenfassung

Endozytose ist ein Internalisierungsweg für extrazelluläres Material sowie für Proteine der Plasmamembran, den alle eukaryotischen Zellen verwenden. Während der Endozytose wird ein Großteil des internalisierten Materials über frühe und späte Endosomen zur Vakuole transportiert, in welcher die endozytierten Makromoleküle schließlich abgebaut werden. Außerdem überschneidet sich der Endozytoseweg mit dem biosynthetischen Transportweg an den endosomalen Kompartimenten, über welche die neusynthetisierten, vakuolären Proteine transportiert werden, bevor sie in die Vakuole gelangen. Endozytierte Proteine, die nicht zum Abbau bestimmt sind, und Rezeptoren, die zum *trans*-Golgi Netzwerk (TGN) gehören, werden von Endosomen zurück zur Plasmamembran bzw. zum TGN rezykliert. Diese verschiedenen Transportwege werden durch Membranvesikel vermittelt. Somit sind Vesikelbildungsprozesse essentiell, um den dynamischen Austausch zwischen den Kompartimenten zu gewährleisten.

Viele strukturelle und regulierende Proteine sind bei der Vesikelbildung involviert. In dem am besten charakterisierten, endosomalen Transportweg, der Clathrin-abhängigen Endozytose, wird das Hüllprotein Clathrin über Adaptorproteine an die Membran rekrutiert. Die Adaptorproteine rekrutieren außerdem endozytotische Rezeptoren im Bereich von Clathrin-umhüllten Membrandomänen und interagieren mit Proteinen, die an verschiedenen Prozessen der Vesikelbildung beteiligt sind. Die Polymerisierung von Clathrin unterstützt vermutlich die Einstülpung und damit die Deformation der Plasmamembran bis zur endgültigen Abschnürung des fertigen endozytotischen Transportvesikels.

Auch das Aktinzytoskelett ist an frühen endozytotischen Transportschritten beteiligt, insbesondere die kortikalen Aktinflecken. Diese Flecken bestehen aus kurzen Aktinfilamenten, die mit zahlreichen Proteinen assoziieren, welche beispielsweise die Polymerisierung von Aktin regulieren. Die Aktinflecken werden durch Bindung an Proteine, die gleichzeitig mit der endozytotischen Maschinerie interagieren, an Membranbereiche rekrutiert, wo die Endozytose stattfindet. Wie die Aktinflecken mechanistisch am Prozess der Endozytose mitwirken, ist nicht bekannt. Es wird allerdings vermutet, dass die beteiligten Proteine die Polymerisierung von Aktin regulieren und dadurch die Bewegungen der endozytotischen Vesikel in die Zelle hinein nach deren Abschnürung von der Plasmamembran steuern.

Wichtige Regulatoren der Vesikelbildung in allen Membrantransportwegen inklusive des endozytotischen Weges sind die kleinen GTPasen ADP-Ribosylierungsfaktoren (Arf), die zu der Ras-Superfamilie gehören. Die Arf-Proteine werden durch Guaninnukleotid-

Austauschfaktoren (GEF) in ihre GTP-gebundene, aktive Form gebildet, die mit Membranen wechselwirkt. An den Endosomen und am TGN rekrutieren die Arf-GTPasen das Hüllprotein Clathrin, das bei der Bildung spezifischer Vesikel involviert ist (siehe oben). Außerdem aktivieren Arf-GTPasen lipidmodifizierende Enzyme, deren Produkte mit Proteinen wie Epsin interagieren, die wiederum eine Deformation von Membranen induzieren können. Nach der Vesikelabschnürung wird die Hydrolyse des Arf-gebundenen GTPs mittels eines GTPase-aktivierenden Proteins (GAP) katalysiert, was zur Dissoziation von Arf-GDP und der Clathrinhülle vom Vesikel führt.

Die Phosphoglyceride, welche die Hauptkomponenten der Membranen darstellen, spielen eine essentielle Rolle bei der Membrankrümmung. Die Phosphoglyceride sind in der Lipiddoppelschicht asymmetrisch verteilt, mit Phosphatidylcholin in der extrazellulären bzw. luminalen Seite und den Aminophospholipiden (APL) wie Phosphatidylserin und Phosphatidylethanolamin in der zytosolischen Seite. Es gibt Hinweise dafür, dass die Erzeugung der Phospholipidasymmetrie, die zur Bildung einer unterschiedlichen Oberfläche an den zwei Membranseiten führt, eine Membrankrümmung induzieren kann und somit am Prozess der Vesikelbildung teilnehmen könnte. Zusätzlich ist die Lipidasymmetrie wichtig, um Proteine, die mit APLs interagieren, spezifisch an die Membran zu rekrutieren und/oder zu aktivieren. Immer mehr Studien sprechen dafür, dass die Mitglieder einer neuen Unterfamilie von P-Typ-ATPasen, der Drs2-Familie, als Aminophospholipid-Translokasen funktionieren. In *S. cerevisiae* existieren fünf Mitglieder dieser Familie. Davon zeigen Drs2p, Dnf1p, Dnf2p und Dnf3p überlappende Funktionen in verschiedenen Membrantransportwegen. Das fünfte Mitglied, Neo1p, ist das einzige essentielle Protein der Drs2-Familie. Hinweise aus der Gruppe von B. Singer-Krüger ließen vermuten, dass dieses Protein an der Endozytose beteiligt ist (siehe unten). Der erste Teil der vorliegenden Arbeit hatte als Ziel, die Lokalisierung von Neo1p zu bestimmen und seine Funktion mittels zweier Temperatur-empfindlicher *neo1* Mutanten weiter zu charakterisieren.

Phosphatidylinositol ist ein Phosphoglycerid, das einen Inositolring enthält, der unterschiedlich phosphoryliert werden kann und damit mehrere Isoformen von phosphorylierten Inositolphospholipide bilden kann. Die phosphorylierten Inositolphospholipide sind als „sekundäre Messenger“ in verschiedenen zellulären Prozessen beteiligt und können beispielsweise Isoform-spezifische Bindungspartner an die Lipiddoppelschicht rekrutieren. Der Phosphorylierungzustand des Inositolrings wird durch verschiedene Kinasen und Lipidphosphatasen reguliert. Diese Enzyme kontrollieren die zeitliche und zelluläre Verteilung der Inositolphospholipide und dadurch auch die Inositolphospholipid-abhängigen

zellulären Prozesse. Mitglieder der Synaptojanin-Familie gehören zu den Inositolphospholipid-Phosphatasen. Mehrere Hinweise lassen vermuten, dass das am besten charakterisierte Mitglied dieser Familie, Synaptojanin 1 aus Säugern, eine Rolle bei der Entmantelung der synaptischen Clathrin-umhüllten Transportvesikeln übernimmt. Die Synaptojanin-vermittelte Dephosphorylierung der Inositolphospholipide könnte möglicherweise zu einer reduzierten Affinität der Proteinhülle für die Vesikelmembran führen. In Hefe gibt es drei Synaptojanin-Proteine, Sjl1p, Sjl2p und Sjl3p. Genetische Analysen sprechen dafür, dass diese Proteine eine überlappende Funktion haben. Aber, während Δ*sjl1*Δ*sjl3* Zellen wie Wildtyp sind, zeigen Δ*sjl1*Δ*sjl2* Zellen einen größeren Defekt bei der Endozytose und der Organisation des Aktinzytoskeletts als Δ*sjl2*Δ*sjl3* Zellen. Das lässt vermutet, dass jedes Synaptojanin-Protein eine spezifische Funktion ausüben könnte. Außerdem sprechen diese Daten dafür, dass Sjl2p das wichtigste von diesen drei Proteinen für die Endozytose sein könnte. Um weitere Hinweise für eine Funktion von Sjl2p bei der Endozytose zu finden, wurde die subzelluläre Verteilung dieser Phosphatase und deren direkten Interaktionspartner Bsp1p im zweiten Teil der vorliegenden Arbeit untersucht.

Charakterisierung von Neo1p und dessen Interaktion mit Ysl2p und Arl1p

NEO1 konnte in der Arbeitsgruppe von B. Singer-Krüger als Suppressor der Wachstums- und Endozytosedefekte von Δ*ysl2*-Zellen identifiziert werden. Ysl2p lokalisiert und spielt eine Rolle im endosomalen System. Aufgrund genetischer und biochemischer Hinweise wurde vorgeschlagen, dass Ysl2p ein GEF für die kleine GTPase Arl1p darstellt (Jochum et al., 2002). In der vorliegenden Arbeit konnte durch Koimmunopräzipitationsexperimente eine Interaktion zwischen TAP-Ysl2p und HA-Neo1p *in vivo* nachgewiesen werden. Da solubilisiertes HA-Neo1p immer noch mit TAP-Ysl2p isoliert werden konnte, ist dies ein Hinweis dafür, dass die Interaktion zwischen beiden Proteine nicht über die endosomalen Membranen, die sowohl Neo1p als auch Ysl2p enthalten, vermittelt wird. Die Wechselwirkung zwischen Ysl2p und Neo1p war hochspezifisch, da die endosomalen Proteine Pep12p und Ypt51p nicht in dem TAP-Ysl2p-Präzipitat detektiert werden konnten.

Nach Färbung von HA-Neo1p durch indirekte Immunfluoreszenz ergab sich ein punktartiges Muster, das größtenteils mit dem von frühen und späten endosomalen Markerproteinen übereinstimmte. Außerdem veränderte sich das HA-Neo1p Muster in einer *vps27* Mutante, in der Endosomen eine vergrößerte, kollabierte Struktur darstellen. Daher konnte geschlossen werden, dass Neo1p an Endosomen lokalisiert ist. In der *sec7* Mutante, in

der Membranen des Golgi Komplexes größere Klumpen formen, kollabierten auch die HA-Neo1p-positiven Strukturen. HA-Neo1p kolokalisierte aber nicht mit zwei frühen Golgi Markern im Wildtyp, ein Hinweis dafür, dass die *sec7*-empfindliche Fraktion von HA-Neo1p vermutlich am späten Golgi Kompartiment lokalisiert.

In Übereinstimmung mit der relativ breiten subzellulären Lokalisierung, wurde eine Funktion für Neo1p in mehreren Transportwegen innerhalb des Endomembransystems gefunden. In den Temperatur-empfindlichen (ts) *neo1-37* und *neo1-69* Mutanten verzögerte sich der endozytotische Transport zwischen den Endosomen und der Vakuole (B. Singer-Krüger). In meiner Arbeit wurde gezeigt, dass in beiden *neo1* Mutanten der biosynthetische Transport des vakuolären Enzyms der Carboxypeptidase Y (CPY) vom endoplasmatischen Retikulum (ER) zum Golgi Komplex und noch deutlicher vom TGN zur Vakuole verzögert war. Gleichzeitig wurde eine Missortierung der Golgi-modifizierten Form von CPY in dem extrazellulären Raum beobachtet, ein Hinweis dafür, dass Neo1p eine Rolle beim Sortieren im TGN spielen könnte.

Im Gegensatz zu den Defekten im endosomalen und biosynthetischen Transport vakuolärer Proteine, die bereits bei permissiver Temperatur (30°C) auftraten, konnte in den „*neo1-ts* Mutanten“ ein Transportdefekt im anterograden und retrograden sekretorischen Weg erst nach längerer Inkubation bei restriktiver Temperatur (37°C) detektiert werden. Nach Inkubation bei 37°C wurde ein Defekt in der Glykosylierung des sekretorischen Enzyms Invertase beobachtet, welche im ER und Golgi Kompartiment stattfindet. Weiterhin wurde GFP-Rer1p, ein Rezeptor für Membranproteine des ER, der zwischen dem frühen Golgi Kompartiment und dem ER zykliert, zur Vakuole mislokalisiert. Da der Protein-Transport zwischen ER und Golgi Komplex lediglich bei restriktiver Temperatur defekt war, könnte es sich hierbei um indirekte Effekte handeln.

Die Analyse bezüglich der Lokalisierung der mutierten Neo1 Proteine zeigte, dass HA-Neo1-69p bei 25°C an den Endosomen lokalisierte, während HA-Neo1-37p bereits im ER zurückgehalten wurde. Bei der restriktiven Temperatur von 37°C akkumulierten beide mutierten Proteine innerhalb des ER, und erzeugten somit möglicherweise Verdickungen in dem dünnen, tubulären ER-Netzwerk. Es ist zu vermuten, dass die morphologischen Defekte bezüglich des ER eine Ursache des obengenannten Transportblocks im sekretorischen Weg sein könnten.

Im Einverständnis mit den Lokalisierungsergebnissen wurde gefunden, dass im Vergleich zum Wildtyp-Protein die Stabilität von Neo1-37p deutlich reduziert war, während

Neo1-69p etwas stabiler als Neo1-37p erschien. Der Unterschied in der ER-Mislokalisierung und der Stabilität zwischen beiden mutierten Neo1 Proteinen könnte damit begründet sein, dass Neo1-37p einen stärkeren Faltungsdefekt als Neo1-69p aufweist, und folglich stärker im ER zurückgehalten und schneller abgebaut wird.

Ergebnisse von B. Singer-Krüger deuteten darauf hin, dass die GTP-gebundene und myristoylierte Form von Arl1p im Kombination mit den *neo1* Mutanten schädlich ist. Mit Hilfe von indirekter Immunfluoreszenz wurde in der vorliegenden Arbeit herausgefunden, dass in der *neo1-69* Mutante die HA-Arl1p-positiven Strukturen größer und intensiver gefärbt waren als in Wildtyp-Zellen, in denen das HA-Arl1p Muster meistens diffus und mit sehr feinen Punkten erschien. In der *neo1-37* Mutante blieb das Muster von HA-Arl1p allerdings unverändert. Somit könnte es möglich sein, dass HA-Arl1p in der *neo1-69* Mutante mehr mit endosomalen Membranen assoziiert und dadurch für die Zellen schädlich ist.

Auch konnte eine veränderte Lokalisierung von Ysl2p in der *neo1-69* Mutante beobachtet werden. Während in Wildtyp-Zellen die Markierung von HA-Ysl2p ein punktartiges Färbungsmuster ergab, wurde in den meisten *neo1-69* Zellen eine diffuse Hintergrund-Färbung wie im unmarkierten Kontrollstamm gefunden. Dieser Effekt deutet auf eine Instabilität von Ysl2p. Andererseits waren in den restlichen *neo1-69* Zellen die HA-Ysl2p-positiven Punkte größer und intensiver gefärbt, analog zum HA-Arl1p-Muster. Dies spricht für einen größeren Anteil an membranassoziierten Ysl2p. In *neo1-37* Zellen blieb das HA-Ysl2p-Färbungsmuster unbeeinflusst. Die quantitative Analyse der Ysl2p-Mengen in den löslichen und membranassoziierten Fraktionen von Zellextrakten wies tatsächlich auf eine Instabilität von Ysl2p hin, besonders in der *neo1-69* Mutante. Dazu konnte gezeigt werden, dass in dieser Mutante das restliche Ysl2p stärker mit Membranen assoziiert war als im Wildtyp. Diese Ergebnisse deuten darauf hin, dass das mutierte Neo1-69p einen Einfluss auf die Stabilität und auf die Membranassoziierung von Ysl2p hat.

Um zu bestimmen, ob der C-terminale Bereich von Neo1p die Interaktion mit Ysl2p vermittelt, wurde eine verkürzte Version von Neo1p erzeugt, bei der die letzten 21 Aminosäuren fehlten. Diese Version von Neo1p (HA-Neo1p$^{\Delta Ctail}$) war allerdings nicht funktionell, da sie weder die Letalität von Δ*neo1*–Zellen, noch den Wachstumsdefekt der Δ*ysl2*-Zellen bei 37°C komplementieren konnte. Ich konnte zeigen, dass HA-Neo1p$^{\Delta Ctail}$ im ER zurückgehalten wurde und eine verkürzte Halbwertzeit besaß. Eine mit drei HA-Epitopen C-terminal markierte Version von Neo1p, die nicht funktionell war (B. Singer-Krüger), blieb ebenfalls teilweise in ER stecken und zeigte ein schwächeres Signal als das funktionelle, N-

terminal markierte HA-Neo1p. Diese Ergebnisse deuten darauf hin, dass der C-terminale Bereich von Neo1p möglicherweise für die korrekte Faltung des Proteins und dadurch für seinen Austritt aus dem ER wichtig ist.

Die Überexpression von Neo1p^{D503N}, das einen Aminosäureaustausch im Aspartat 503 enthielt, welcher im Wildtyp-Protein während der Hydrolyse von ATP phosphoryliert wird, konnte weder die Letalität von Δ*neo1*–Zellen, noch den Wachstumsdefekt der Δ*ysl2*-Zellen bei 37°C komplementieren. Somit wurde die Vermutung bestätigt, dass die ATPase-Aktivität von Neo1p essentiell für die Funktion dieser potentiellen APL Translokase ist.

Um zu untersuchen, ob eine Reduktion der enzymatischen Aktivität die Ursache für die beobachteten Defekte der *neo1-37* und *neo1-69* Mutanten sein könnte, wurde die ATPase Aktivität der Mutanten im Vergleich zum Wildtyp bestimmt. Die Isolierung von HA-Neo1p und der anschließende Enzymtest in Anwesenheit von verschiedenen Detergenzkonzentrationen ließen erkennen, dass HA-Neo1p am besten immunopräzipitiert und aktiv war bei minimalen Detergenzkonzentrationen (0.01% NP40). Sowohl HA-Neo1-37p als auch HA-Neo1-69p besaßen im Vergleich zum Wildtyp-Protein eine reduzierte ATPase-Aktivität. Allerdings war auch die Menge der immunopräzipitierten Neo1 Mutanten geringer. Durch Vergleich der Reduktion der ATPase-Aktivität und der Proteinmenge zeigte sich, dass die ATPase Aktivität von HA-Neo1-37p nicht reduziert ist und die von Neo1-69p sogar leicht erhöht ist.

In diesem Teil meiner Arbeit konnte gezeigt werden, dass Neo1p im endosomalen/späten Golgi System weitverbreitet vorhanden ist. In Übereinstimmung damit zeigten die *neo1-ts* Mutanten sowohl Defekte bei der Endozytose (B. Singer-Krüger) als auch im Proteintransport vom TGN zur Vakuole. Der sekretorische Weg wurde erst durch indirekte Effekte beeinflusst. Es konnten auch Hinweise für eine enge funktionelle Verbindung zwischen Neo1p, Ysl2p, und Arl1p erbracht werden, die ein Modell zum Zusammenspiel von APL Translokasen mit Arf Proteine und deren Regulatoren im Membrantransport unterstützen.

Charakterisierung der Lokalisierung von Sjl2p und dessen Interaktionspartner Bsp1p

Da die Deletion von *SJL2* sowohl in Δ*sjl1*- als auch in Δ*sjl3*-Zellen zu Endozytose-Defekten führte, während die Δ*sjl1*Δ*sjl3* Mutante kein Defekt zeigte, wurde in vorangegangenen Arbeiten vorgeschlagen, dass Sjl2p möglicherweise eine Rolle bei der Endozytose spielt. Ergebnisse der Gruppe von B. Singer-Krüger zeigten, dass Sjl2p

überwiegend mit Membranen assoziiert, die in einem Dichtegradienten mit endosomalen und Golgi-Markern kofraktionieren. In meiner Arbeit zeigte funktionelles HA-Sjl2p mittels indirekter Immunfluoreszenz ein schwaches, punktartiges Färbungsmuster, das aber in der *vps27* Mutante unverändert war. Auch fand sich keine Kolokalisierung der HA-Sjl2p-positiven Strukturen mit endosomalen Markerproteinen. Dies sprach gegen eine Lokalisierung von HA-Sjl2p an frühen und späten Endosomen. HA-Sjl2p konnte ebenso nicht dem Golgi Kompartiment zugeordnet werden, was durch Lokalisierung-Experimente in der *sec7* Mutante gezeigt werden konnte.

Um die Lokalisierung von HA-Sjl2p weiter zu charakterisieren, wurde ein Stamm verwendet, in dem die Gene deletiert waren, die die beiden Aktin-regulierenden Proteinkinasen Ark1p und Prk1p kodieren (Δ*ark1*Δ*prk1).* In diesen Zellen bilden sich Aktinklumpen durch Kollabieren der kortikalen Aktinflecken. Es konnte gezeigt werden, dass HA-Sjl2p mit diesen kortikalen Aktinklumpen kolokalisiert. Diese Klumpen enthielten nicht nur Komponenten des Aktinzytoskeletts, sondern auch endosomale Membranen, die durch den lipophilen Farbstoff FM4-64 und das Hüllprotein Clathrin markiert wurden. Die Tatsache, dass das GFP-Sjl2p-Muster mit dem von FM4-64 in Klumpen in den Δ*ark1*Δ*prk1*-Zellen übereinstimmte, war ein bedeutender Hinweis dafür, dass Sjl2p wahrscheinlich an primären endozytotischen Vesikeln lokalisiert. In einer Δ*ark1* Mutante, die das *prk1-as3* Allel enthielt, welches die schnelle Inaktivierung von Prk1p mittels eines chemischen Hemmstoffs erlaubte, wurde HA-Sjl2p sofort nach Prk1p-Inaktivierung an den sich formenden Aktinklumpen gefunden. Dieses Ergebnis zeigte deutlich, dass die Sjl2p-positiven Vesikeln mit dem kortikalen Aktinzytoskelett assoziieren.

Die Charakterisierung des direkten Bindungspartners von Sjl2p, HA-Bsp1p, mittels indirekter Immunfluoreszenz zeigte ein punktartiges und polarisiertes Muster, welches deutlich mit dem von Aktin übereinstimmte. Außerdem wurde HA-Bsp1p in den kortikalen Aktinklumpen der Δ*ark1*Δ*prk1*-Zellen gefunden. Somit konnte geschlossen werden, dass sich HA-Bsp1p an kortikalen Aktinflecken befindet. Ergebnisse von B. Singer-Krüger wiesen auch darauf hin, dass ein Anteil von Bsp1p mit Membranen in Abhängigkeit von der Anwesenheit von Inositolphospholipiden assoziiert. Im Einverständnis mit einer Funktion von Inositolphospholipiden bei der Lokalisierung von Bsp1p wurde in meiner Arbeit durch indirekte Immunfluoreszenzanalysen gezeigt, dass in zwei Temperatur-sensitiven Mutanten der PtdIns(4)P Kinase Pik1p, in denen die Mengen von PtdIns(4)P und PtdIns(4,5)P_2 bei der restriktiven Temperatur reduziert sind, das Muster von HA-Bsp1p nicht mehr polarisiert und

in der Signalstärke schwächer wurde. Außerdem konnte nachgewiesen werden, dass *in vitro*-translatiertes Bsp1p ausschließlich mit Liposomen bindet, die negativ geladene Phospholipide wie z.B. Inositolphospholipide enthielten, und mit diesen Liposomen in einem Sucrosegradienten flotiert. Diese Daten deuteten darauf hin, dass Bsp1p direkt mit Membranen mittels negativ geladener Phospholipide interagieren kann.

In diesem zweiten Teil meiner Arbeit wurden Hinweise dafür erbracht, dass Sjl2p sich nicht an frühen oder späten Endosomen befindet, sondern wahrscheinlich mit primären endozytotischen Vesikeln assoziiert. Die Interaktion von Sjl2p-positiven endozytotischen Vesikeln mit der Aktinzytoskelett während der frühen Phase der Endozytose könnte teilweise durch Bsp1p vermittelt werden, das an Aktinflecken lokalisiert und direkt mit Sjl2p und Membranen interagiert.

Abstract

Endocytosis is a key membrane trafficking pathway by which all eukaryotic cells internalize extracellular material as well as portions of the plasma membrane. In the budding yeast *Saccharomyces cerevisiae*, the major fraction of the material internalized at the plasma membrane is transported through the early and late endosomal compartments to the vacuole. The endosomal compartments are highly dynamic and are connected to the plasma membrane, the late Golgi complex and the vacuole by several routes, which all involve vesicular transport. Thus, the formation of vesicles is essential to maintain the dynamic exchanges between these different compartments. In the present study, I analyzed two yeast proteins, Neo1p and Sjl2p, which are suggested to function as regulators of the phospholipid composition of endosomal organelles and thereby seem to participate in vesicle formation (Neo1p) and in vesicle uncoating (Sjl2p), two processes essential during vesicular membrane transport.

Neo1p is an essential member of the Drs2 family of P-type ATPases with proposed function as aminophospholipid (APL) translocases. Genetic and biochemical data in the laboratory of B. Singer-Krüger indicated that Neo1p might function within the endosomal system. Consistent with these findings, I could confirm by indirect immunofluorescence that the major fraction of Neo1p localizes to the endosomal compartments, while a smaller part associates with late Golgi membranes. In agreement with this localization, two temperature-sensitive *neo1* mutants were shown to be defective in endocytosis (B. Singer-Krüger's laboratory) and in vacuolar protein sorting (my studies). While these defects were already observed at permissive temperature, at nonpermissive temperature the *neo1-ts* mutants exhibited additional impairments in membrane transport between the ER and the early Golgi compartment. However, these defects were most likely a consequence of the accumulation of mutant Neo1 proteins in the ER under these conditions. In support of previous results in the laboratory of B. Singer-Krüger, I identified further links between Neo1p and the endosomal proteins Ysl2p and Arl1p. I could show that Neo1p interacts *in vivo* with Ysl2p and that the subcellular localization and the stability of Ysl2p are affected in the *neo1-69* mutant. Furthermore, the subcellular distribution of Arl1p was also found to be impaired in *neo1-69* cells at permissive temperature. Based on these findings and the work of B. Singer-Krüger, Neo1p was proposed to act together with Ysl2p and Arl1p in membrane trafficking within the endosomal/late Golgi system.

In the second part of this work, the subcellular localization of Sjl2p, a polyphosphoinositide- and 5'-inositide phosphatase of the synaptojanin family, was

examined. Based on genetic analyses, Sjl2p has been suggested to participate in early steps of endocytic transport. Here, I determined by indirect immunofluorescence that the Sjl2p-positive punctate structures were distinct from those containing typical early and late endosomal marker proteins and were not sensitive to mutations affecting the structure of either the endosomal compartments or the Golgi complex. Sjl2p did not show a typical plasma membrane staining pattern either. However, Sjl2p colocalized with cortical actin patch components found within clumps that accumulated in cells lacking the two actin-regulating kinases Prk1p and Ark1p. Within these aberrant structures, Sjl2p also colocalized with FM4-64 endocytosed for a short time, suggesting that Sjl2p localized to primary endocytic vesicles that interact with the cortical actin cytoskeleton. This interaction may at least to some extent be mediated by Bsp1p, a binding partner of Sjl2p isolated in B. Singer-Krüger's laboratory, which in my studies was found to be part of the cortical actin cytoskeleton. In cells deficient for the PtdIns(4)P kinase (*pik1-ts*), the staining pattern of Bsp1p was changed, suggesting that the subcellular distribution of Bsp1p is dependent on the levels of phosphoinositides. Consistent with that, Bsp1p was found to flotate with liposomes containing acidic phospholipids including phosphoinositides. Thus, Bsp1p may act as an adapter that directly connects Sjl2p-containing vesicles to the cortical actin cytoskeleton during early stages of endocytosis via interactions with Sjl2p (B. Singer-Krüger) and with a subset of phospholipids within the vesicle membrane (B. Singer-Krüger and my results).

In summary, the results of my PhD thesis brought new insights into the localization and function of Neo1p and Sjl2p within the endosomal system. These data are relevant for future studies to elucidate the precise mechanism of Neo1p and Sjl2p during endocytosis.

1 Introduction

1.1 Endocytosis in the budding yeast *Saccharomyces cerevisiae*

1.1.1 Yeast as a model for studying endocytosis

Endocytosis is a membrane trafficking process by which all eukaryotic cells internalize extracellular ligands and soluble molecules as well as plasma membrane proteins and lipids. During endocytosis, vesicles formed by invagination of the plasma membrane are transported toward the endosomal compartments. From these compartments, internalized material is either directed to the lysosome/vacuole or is recycled back to the plasma membrane. A wide array of cellular processes requires the participation of endocytosis, including the uptake of extracellular nutrients, the regulation of cell surface expression of signalling receptors and cell surface transporters, and the control of the cell surface area.

Considerable progress has been made toward understanding the highly complex processes underlying endocytic internalization and trafficking events by studying the endocytic pathway in the budding yeast *Saccharomyces cerevisiae*. The ease of combining biochemical analyses with genetic studies in this organism allowed the isolation and characterization of a number of mutations affecting endocytosis (reviewed by D'Hondt et al., 2000). The recent determination of the complete nucleotide sequence of the *S. cerevisiae* genome (Goffeau et al., 1996) greatly facilitated the identification of homologs of yeast genes implicated in endocytosis in other eukaryotic species. Furthermore, the organelles present in yeasts and the yeast cell physiology are remarkably similar to that of higher eukaryotes. For these reasons, yeast cells have become a powerful model system for the investigation of endocytosis.

1.1.2 The endocytic compartments

The endocytic pathway is constituted of at least three compartments, two kinds of endosomes and the vacuole. The endosomal compartments have originally been characterized as early and late endosomes depending on the kinetics with which they are loaded with endocytosed material (Singer and Riezman, 1990; Singer-Krüger et al., 1993). Early and late endosomes are biochemically separable by centrifugation on a density gradient, since the early endosomes have a higher density than the late endosomes (Singer-Krüger et al., 1993). At the ultrastructural level, early endosomes, which are located at the cell periphery, display a highly complex and pleiomorphic organization that consists of cisternal regions from which thin tubules and vesicles seem to emanate (Prescianotto-Baschong and Riezman, 1998; Mulholland et al., 1999). A recent study suggests that two tubulo-vesicular compartments

exist, designated as the early endosomal and the prevacuolar compartments (PVC), which are distinguishable by the kinetics of endocytosis and their protein content (Prescianotto-Baschong and Riezman, 2002; see below). Late endosomes, which are located close to the vacuole, exhibit a more spherical organization and are described as multivesicular bodies (MVB), since they contain internal membranes formed by the invagination of the limiting membrane (Prescianotto-Baschong and Riezman, 1998; Mulholland et al., 1999). The internal membranes enclose cargo molecules destined for degradation in the vacuole (Odorizzi et al., 1998a).

In addition to their particular morphology, the endosomal compartments are also characterized by the presence of specific proteins within their membranes, like SNARE (soluble *N*-ethylmaleimide-sensitive factor attachment protein receptor) proteins. In general, the pair-wise combination of a particular v-SNARE, which localizes to a vesicular membrane, and a t-SNARE, present on a target membrane, promotes the specific docking and fusion of vesicles with their respective acceptor compartment (reviewed by Pelham, 1999). Since SNAREs exhibit specific subcellular localizations, they are used as markers to identify distinct organelles. Tlg1p and Pep12p represent endosomal t-SNAREs (Holthuis et al., 1998; Becherer et al., 1996), while Vam3p is a vacuolar t-SNARE (Darsow et al., 1998) (Fig. 1). At the ultrastructural level, both Tlg1p- and Pep12p-positive endosomes have a tubulo-vesicular appearance, but upon endocytic internalization with colloidal gold, Tlg1p-positive structures are stained before the Pep12p-positive ones (Prescianotto-Baschong and Riezman, 2002). Thus, Tlg1p is used as marker for early endosomes and Pep12p for the prevacuolar compartment. Since Tlg1p cycles between early endosomes and the late Golgi complex (Holthuis et al., 1998), a fraction of Tlg1p is also found in this latter compartment (Fig. 1).

The vacuole, which is generally composed of up to three structures, is the terminal compartment for most of the endocytosed material. Apparently, late endosomes deliver their content into the vacuole directly by fusion with the vacuolar membrane (Odorizzi et al., 1998a). The vacuole contains a wide variety of acidic hydrolases, which degrade the endocytosed proteins (reviewed by Jones, 1984). The amino acids, which result from the hydrolysis of such proteins, are exported to the cytosol, from where they can be reused by the cell. In addition to this role in the degradation of internalized material, the vacuole participates in buffering the pH of the cytoplasm and in the regulation of water and ion homeostasis (reviewed by Davis, 1986; Nelson, 1989).

1.1.3 The transport pathways within the endomembrane system

Endocytic internalization takes place at the plasma membrane, where extracellular material and plasma membrane proteins become enclosed into transport vesicles by invagination of the plasma membrane. Depending on whether a receptor is implicated in the internalization or fluid is taken up, endocytosis has been defined as receptor-mediated or fluid-phase endocytosis (Riezman et al., 1985; Chvatchko et al., 1986; Jenness and Spatrick, 1986). However, both pathways are time-, temperature- and energy-dependent and most endocytic mutants are defective both in receptor-mediated and in fluid-phase endocytosis, suggesting that these pathways share most of their machinery (reviewed by D'Hondt et al., 2000). After internalization, the primary endocytic vesicles fuse with the early endosomal compartment and most of the endocytosed material is subsequently transported via the PVC to the late endosomal compartment before being delivered to the vacuole, where it is degraded (Fig. 1, solid thick arrows). This pathway is the principal route for material internalized by bulk phase endocytosis and for proteins signalized for downregulation such as the pheromone α-factor receptor Ste2p (Chvatchko et al., 1986; Jenness and Spatrick, 1986).

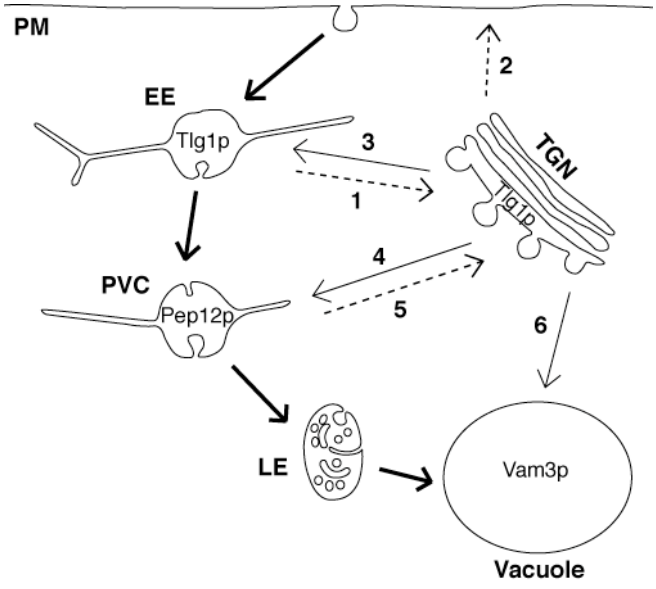

Fig. 1. Overview of the transport pathways in the endomembrane system of yeast. Solid thick arrows represent the endocytic pathway followed by most of the proteins and material internalized at the plasma membrane. Solid thin arrows depict pathways followed by resident proteins of the TGN (3, 4) or newly synthesized vacuolar proteins (3, 4, 6). Dashed arrows illustrate recycling pathways from early endosomes or the PVC to the TGN (1, 5) or from early endosomes to the plasma membrane via the TGN (1, 2).
The cellular compartments are indicated: plasma membrane (PM), early endosome (EE), prevacuolar compartment (PVC), late endosome (LE), vacuole, and *trans*-Golgi network (TGN). SNARE proteins are indicated inside the compartment they define.

Some endocytosed proteins are not transported to the vacuole, but recycle to the plasma membrane. This process has been well studied in mammalian cells, in which many proteins follow this pathway (reviewed by Gruenberg, 2003). In yeast cells, only few proteins are known to return to the plasma membrane, among which are the a-factor receptor Ste3p, the v-SNARE protein Snc1p, and the chitin synthase Chs3p (Chen and Davis, 2000; Lewis et

al., 2000; Ziman et al., 1996; Holthuis et al., 1998). After delivery to early endosomes (Fig. 1, solid thick arrows), these proteins transit to the *trans*-Golgi network (TGN) (arrow 1) and return to the cell surface via the secretory pathway (arrow 2).

The biosynthetic delivery of proteins and membranes from the TGN to the vacuole also occurs via endosomal intermediates, like the early and/or the prevacuolar compartments, as shown for the vacuolar protease carboxypeptidase Y (CPY) (reviewed by Pelham, 2002) (Fig. 1, arrows 3 and 4). Resident proteins of the TGN, like the CPY receptor Vps10p and the endopeptidase Kex2p, that reach endosomes are recycled back to the TGN (reviewed by Conibear and Stevens, 1998; Cooper and Stevens, 1996) (Fig. 1, arrows 1 and 5). An alternative direct pathway from the TGN to the vacuole bypassing endosomal compartments has been described for the vacuolar membrane protein alkaline phosphatase (ALP) (Odorizzi et al., 1998b) (Fig. 1, arrow 6).

1.2 Structural and regulatory proteins involved in endocytic vesicle formation

1.2.1 Role of the clathrin coat in vesicle formation

To maintain the compartmentalized state of the cell, traffic between membrane-bound organelles occurs via vesicular membrane carriers. The formation of such vesicles, including those generated by endocytosis, requires the recruitment of a proteinaceous coat to the membrane from which the vesicle is formed. The best-characterized endocytic transport vesicles are clathrin-coated vesicles (CCVs). In solution, clathrin forms a heterohexamer three-legged structure, the triskelion, which consists of three heavy and three light chains (Ungewickell and Branton, 1981). Oligomerization of triskelia into polyhedral cages below the plasma membrane was traditionally thought to provide a mechanical force to promote vesicle budding by imposing a curvature on the donor membrane (Heuser and Keen, 1988; reviewed by Rothman, 1994). However, recent theoretical considerations revealed that the rigidity of the clathrin coat is not sufficient to promote the bending of the membrane, arguing against an active participation of clathrin in this process. The clathrin coat may rather maintain an already curved membrane structure and by this may prevent the regeneration of a planar structure (Nossal, 2001).

Recruitment and assembly of clathrin on membranes is facilitated by the presence of clathrin heterotetrameric adaptor proteins (APs), which interact directly with clathrin (Gallusser and Kirchhausen, 1993; Dell'Angelica et al., 1998). These adaptor complexes also recruit specific receptors into clathrin-coated pits by binding to sorting signals within the receptor tails (Ohno et al., 1995; Rapoport et al., 1998). In addition, the AP complexes

interact with numerous accessory factors, which regulate or participate directly in clathrin-coated vesicle formation (reviewed by Slepnev and De Camilli, 2000). For instance, the AP-2 complex (see below) binds to epsin and amphiphysin, which both are able to deform lipid bilayers *in vitro* and may accordingly induce membrane bending during an early stage of clathrin-coated vesicle formation (see section 1.2.3; Ford et al., 2002; Takei et al., 1999).

In yeast, there are three AP complexes. While AP-1 is implicated in clathrin-mediated transport of proteins like Kex2p from the TGN to endocytic intermediates (Stepp et al., 1995; Deloche et al., 2001) (Fig. 1, arrows 3 and 4), AP-3 is required for a clathrin-independent transport pathway from the TGN to the vacuole that bypasses endosomes (Cowles et al., 1997) (Fig. 1, arrow 6). Cells lacking the AP-2 complex exhibit no observable membrane trafficking defects and AP-2 does neither interact physically nor genetically with clathrin (reviewed by Boehm and Bonifacino, 2002). Since in higher eukaryotes the AP-2 complex plays a critical role in clathrin-mediated endocytosis at the plasma membrane, it is possible that yeast AP-2 also participates in endocytosis. AP-2 may share redundant functions with other endocytic proteins, explaining the lack of observable phenotypes in the AP-2 deletion mutants. The GGAs (Golgi-associated, γ-adaptin homologous, Arf-interacting proteins) represent a new family of monomeric clathrin adaptors and, similar to AP-1, appear to participate in vacuolar protein sorting via endosomes (Black and Pelham, 2000). The recruitment of APs and GGAs to the membrane is mediated by the interaction of the adaptors with particular proteins, including the cargo receptors and members of the Arf family (see section 1.2.3), and with specific lipids within the membrane such as phosphatidylinositol-4,5-bisphosphate (PtdIns(4,5)P_2; see section 1.3.2).

Although the function of yeast clathrin and APs in the endocytic pathway is less well understood than in mammals, a number of evidence points to a role for clathrin in yeast endocytosis. Indeed, endocytic trafficking was significantly reduced in deletion and temperature-sensitive mutants of the heavy chain (*CHC1*) or the light chain (*CLC1*) of clathrin (Chu et al., 1996; Payne et al., 1988; Tan et al., 1993). Furthermore, independent genetic screens for mutants defective in endocytosis have all isolated proteins that bind either directly or via other endocytic factors to clathrin and have homologs required for mammalian clathrin-mediated endocytosis (reviewed by Baggett and Wendland, 2001). Thus, the clathrin-mediated endocytic pathway seems to be conserved down to yeast.

1.2.2 Function of the actin cytoskeleton in early stages of endocytosis

The cortical actin cytoskeleton represents another proteinaceous structure involved in initial steps of endocytosis. Cortical patches are discrete cytoskeletal bodies, which comprise short actin filaments and a plethora of actin-binding and regulatory proteins (reviewed by Engqvist-Goldstein and Drubin, 2003) and which localize to regions of cell growth (Adams and Pringle, 1984). The exact function of the cortical patches is not known, but these structures, in addition to being involved in secretion, are intimately connected to endocytosis. In fact, a number of proteins required for endocytic internalization, such as Sla2p and Ent1/2p, colocalize at least partially with cortical actin patches (reviewed by Engqvist-Goldstein and Drubin, 2003). Furthermore, temperature-sensitive forms of actin and of cortical patch components, such as the yeast amphiphysin homologs Rvs161p and Rvs167p, cause endocytic defects immediately after shift to the non-permissive temperature and the severity of the endocytic defects is generally correlated with the severity of the actin phenotype (reviewed by Engqvist-Goldstein and Drubin, 2003).

How cortical actin patches participate in endocytosis is however not well understood. Possibilities include cortical actin being involved in localizing and stabilizing an endocytic complex, to a more active role in driving invagination, scission, and possibly the movement of vesicles from the plasma membrane (reviewed by Qualmann et al., 2000). Analysis of the protein composition and the motility of the patches during endocytic internalization suggests that the polymerization of actin, which is achieved by the Arp2/3p complex (reviewed by Machesky and Gould, 1999), may produce a force to propel the newly formed endocytic vesicles into the cytoplasm (Kaksonen et al., 2003). The fact that many patch components are involved in actin polymerisation, such as the Arp2/3p nucleation promoting factors Las17p, Pan1p, and Abp1p (Winter et al., 1999; Duncan et al., 2001; Goode et al., 2001), supports the idea that actin dynamics are essential for endocytic internalization. Further evidence for this idea is that cells treated with the actin depolymerising drug latrunculin A exhibit endocytic defects (Ayscough et al., 1997).

The recruitment of cortical actin patches at sites of endocytosis is apparently mediated by proteins, like Sla2p, that link the endocytic machinery to the actin cytoskeleton. Sla2p binds to clathrin as well as to several cortical patch components including Sla1p and Rvs67p (Wesp et al., 1997; Henry et al., 2002). In turn, Sla1p and Rvs67p interact with a number of other patch components like Abp1p (Lila and Drubin, 1997; Warren et al., 2002), which represents one of the actin nucleation promoting factors critical for the activation of the Arp2/3p complex.

1.2.3 Arf GTPases and their role as regulators of vesicle formation

Beside structural factors, other proteins are required to regulate the processes involved in vesicle formation. ADP-ribosylation factors (Arfs) are GTPases, which constitute a subfamily of the highly conserved Ras superfamily of small GTPases. Arf proteins are recognized as critical regulators of the secretory and endocytic pathways by participating in coat assembly (reviewed by Donaldson and Jackson, 2000). The best-characterized member of the Arf family, Arf1p, regulates the assembly of the COPI coat on the *cis* Golgi complex and of clathrin, AP-1, AP-3, and GGAs at the *trans*-Golgi network (reviewed by Bonifacino and Lippincott-Schwartz, 2003).

In addition to its role in coat recruitment, Arf1p activates two lipid-modifying enzymes, phospholipase D (Jones et al., 1999) and phosphatidylinositol-4-phosphate-5-kinase (Godi et al., 1999; Jones et al., 2000), which results in the generation of phosphatidic acid and PtdIns(4,5)P_2, respectively. These phospholipids mediate the membrane recruitment of proteins involved in membrane deformation and scission, such as epsin and dynamin, respectively (Ford et al., 2002; Burger et al., 2000). Arf1p has been also proposed to participate directly in membrane transformation events in a similar way as endophilin, amphiphysin, and epsin (Farsad and De Camilli, 2003; Farsad et al., 2001; Ford et al., 2002). The insertion into the cytoplasmic face of the lipid bilayer of the N-terminal amphipathic helix of Arf^{GTP} (see below) may possibly drive a membrane deformation owing to a bilayer surface area discrepancy, as generally proposed in the bilayer couple hypothesis (Sheetz and Singer, 1974 and see section 1.3.1.2).

Like other small GTPases, Arf proteins cycle between an active GTP-bound form that is tightly membrane-associated and an inactive GDP-bound form, which is largely soluble. The exchange of GDP for GTP on Arf takes place on membranes and is catalyzed by a guanine nucleotide exchange factor (GEF) (reviewed by Cox et al., 2004). The nucleotide exchange induces a conformational change within the N-terminal helix resulting in the exposure of several hydrophobic residues and in the insertion and the tight binding of this helix to the membrane (Antonny et al., 1997). Membrane-bound Arf^{GTP} promotes coat assembly by interacting with the clathrin adaptors (Boehm et al., 2001; Austin et al., 2002) and the subunits of the COPI coatomer (Zhao et al., 1997). After vesicle scission, a vesicle-associated GTPase-activating protein (GAP) stimulates GTP hydrolysis on Arf, inducing the release of Arf^{GDP} and other vesicle-associated coat proteins (reviewed by Randazzo and Hirsch, 2004). This latter step is essential for further transport and fusion of the carrier vesicle to its target compartment.

1.3 Phospholipids and membrane deformation events

The phospholipids, which are the major constituents of biological membranes, are also thought to be involved in the process of vesicle formation. On the one hand, they mediate the recruitment and activation of proteins participating in vesicle budding and scission. On the other hand, the transport of phospholipids across the bilayer induces structural changes, which are thought to result in membrane bending. Proteins mediating phospholipid translocation across membranes or modifying phospholipids within membranes are described below.

1.3.1 Role of phospholipid asymmetry in membrane budding and regulation by the Drs2 family of P-type ATPases

1.3.1.1 Glycerophospholipid asymmetry and transport across the membrane bilayer

The predominant glycerophospholipids within eukaryotic membranes are phosphatidylcholine (PC), phosphatidylethanolamine (PE), and phosphatidylserine (PS). In the plasma membrane, in which the lipid composition has been best characterized, the choline-containing phospholipids PC and sphingomyelin (SM) are enriched in the outer leaflet, whereas the aminophospholipids PS and PE reside predominantly in the inner leaflet (Zachowski, 1993) (Fig. 2). A similar lipid asymmetry can be found in other organelles (Bollen and Higgins, 1980; Higgins, 1984).

For the major glycerophospholipids, *de novo* synthesis occurs on the cytosolic side of the endoplasmic reticulum (ER) (Bell et al., 1981), placing PS and PE on the side of the membrane, in which they are ultimately enriched within the plasma membrane. However, since the newly synthesized phospholipids are rapidly redistributed across the ER membrane to counter the instability of the membrane induced by the asymmetric addition of phospholipids (Ferrell et al., 1985; Farge and Devaux, 1992), the phospholipid asymmetry observed at the plasma membrane and other organelles has to be constantly regenerated and maintained. At least three classes of proteins are involved in the translocation of phospholipids across membranes (Fig. 2) (reviewed by Pomorski et al., 2004). The aminophospholipid (APL) translocases or flippases transport PS and PE in an ATP-dependent way from the extracellular/luminal layer of a membrane to the cytoplasmic side. The best candidates to perform this function are members of a subfamily of P-type ATPases (Tang et al., 1996; Catty et al., 1997; Halleck et al., 1998), which are described in detail below (1.3.1.3-1.3.1.5). The second class of phospholipid translocases is constituted by so-called floppases, which belong to the family of ABC (ATP-binding cassette) transporters. These proteins translocate PC and also other substrates like amphipathic drugs in an ATP-dependent

way from the cytoplasmic to the extracellular leaflet of the plasma membrane (reviewed by Borst et al., 2000). The third class of phospholipid transporters is composed of scramblases, which catalyze the transport of phospholipids bidirectionally across the lipid bilayer in a nonspecific and energy-independent way. Scramblases are found at the ER membrane to redistribute the newly synthesized phospholipids and at the plasma membrane, where they dissipate phospholipid asymmetry during processes like blood coagulation or apoptosis (reviewed by Pomorski et al., 2004).

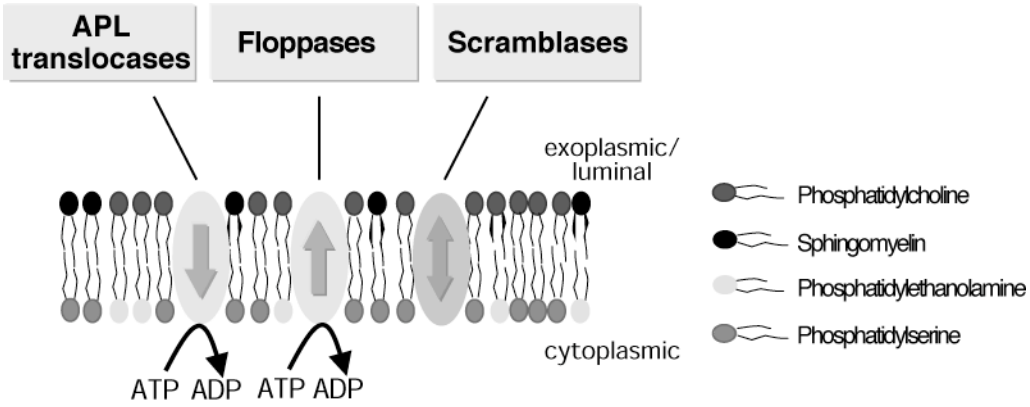

Fig. 2. Model depicting the asymmetric phospholipid distribution found at the plasma membrane and representing the three classes of phospholipid transporters and their activity. The translocation of specific phospholipids in an ATP-dependent manner toward (APL translocases) or away (floppases) from the cytoplasmic leaflet generates an asymmetric phospholipid distribution across the bilayer. Scramblases participate in the dissipation of the asymmetric distribution by transporting phospholipids in a nonspecific, bidirectional, and ATP-independent manner. APL, aminophospholipids.

1.3.1.2 Relevance of the lipid asymmetry in cellular processes

The ATP-driven transfer of aminophospholipids from one leaflet of the membrane to the other one induces a difference in the surface area between both leaflets. According to the bilayer couple hypothesis of Sheetz and Singer (1974), this asymmetry is predicted to increase the spontaneous curvature of the bilayer (Fig. 3), and thus could induce membrane budding. In support of this theory, studies revealed that a net redistribution of phospholipids from the outer to the inner leaflet of human erythrocyte ghost cells or liposome bilayers induces vesiculation (Muller et al., 1994; Farge and Devaux, 1992). Consistently, addition of aminophospholipids to the plasma membrane of living human erythrocytes, in which APL translocase activity has been demonstrated (Seigneuret and Devaux, 1984), results in a significant enhancement of the endocytic internalization of bulk membrane proteins, while addition of PC decreases endocytosis (Farge et al., 1999). Thus, the formation of endocytic vesicles may be supported by the generation of a surface area asymmetry across the plasma

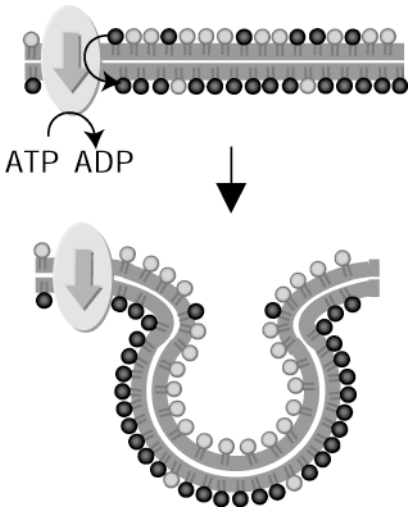

Fig. 3. Generation of a membrane curvature by the translocation of phospholipids across a bilayer. The ATP-driven translocation of phospholipids (symbolized by the arrow in an oval) may increase the concentration of lipids in one monolayer, thereby driving budding of vesicles. In particular, aminophospholipids (depicted by the dark gray rounds), but not choline-containing phospholipids (light gray rounds), may be translocated during endocytic vesicle formation.

membrane (Farge et al., 1999). A particular phospholipid composition on the cytoplasmic side of the membrane may also regulate the recruitment of proteins as well as the activation of peripheral membrane proteins that actively participate in membrane budding. For example, evidence for the involvement of PS in the membrane recruitment of clathrin, $Arf1p^{GDP}$, the Arf GEF ARNO, and in the efficient activation of $Arf1p^{GDP}$ to $Arf1p^{GTP}$ has been recently provided (Takei et al., 1998; Antonny et al., 1997; Chardin et al., 1996).

The asymmetric distribution of phospholipids is also involved in other cellular processes, such as the interaction between two membranes. While in the facing leaflets of two apposing bilayers the presence of PC is unfavorable to membrane-membrane interactions, PS and PE promote the membranes to come in closer contact and to adhere to each other (reviewed by McIntosh, 1996). In the case of interfaces containing PE, the contact seems to be facilitated by electrostatic interactions between the amino- and the phosphate groups of PE localized on the apposing bilayers. The intrabilayer hydrogen bonds between PE may in addition limit the movement of the lipid headgroups and by this decrease the steric repulsion force generated by this movement (reviewed by McIntosh, 1996). The fusion of two membranes also depends on phospholipid asymmetry, since this process requires, at least locally, the formation of a nonbilayer structure inducible by the interaction of Ca^{2+} with PS and PE but not with PC and SM (reviewed by Devaux, 1991). Thus, the presence of a high concentration of PC in the exoplasmic leaflet of plasma membranes generates a rather inert surface essential for the barrier function of this type of membrane.

The disruption of phospholipid asymmetry triggers a variety of physiological events. On the one hand, regulated exposure of PS on the platelet surface induces the reaction cascade of blood coagulation (Rosing et al., 1980) and in spermatozoa it favors fusion events that take place during the process of fertilization (Gadella and Harrison, 2002). On the other hand, the

loss of plasma membrane PS asymmetry resulting from cell injury or apoptosis causes the engulfment of these cells by macrophages bearing PS receptors (Fadok et al., 2000).

1.3.1.3 The Drs2 family of P-type ATPases and APL translocation

As mentioned before (1.3.1.1), the APL translocases are proposed to generate and maintain the asymmetry of aminophospholipids across lipid bilayers. The ATPase II of bovine chromaffin granules was the first potential APL translocase to be isolated by a biochemical approach and by the subsequent cloning of the corresponding gene (Tang et al., 1996). Sequence alignments identified Drs2p of *S. cerevisiae* as the closest ATPase II homolog (Tang et al., 1996) and an increasing number of homologs in several eukaryotes was found by genomes-wide searches (Catty et al., 1997; Gomes et al., 2000; Halleck et al., 1999). A detailed analysis of the primary sequences of the bovine ATPase II and its five *S. cerevisiae* homologs (see below) suggested that these proteins may form a novel subfamily of P-type ATPases designated as the Drs2 family (Tang et al., 1996; Catty et al., 1997). The members of this family lack negatively charged amino acids in the transmembrane domains four and six essential for cation transport in the other P-type ATPases and have hydrophobic residues at their place, arguing against a role for the Drs2 family members as cation transporters (Tang et al., 1996; Catty et al., 1997).

A considerable amount of work points to a function of the Drs2 family members as APL translocases. The first hint came from the biochemical identification of the ATPase II as being the protein mediating the ATP-dependent transport of PS across the membrane of bovine chromaffin granules (Zachowski et al., 1989; Tang et al., 1996). This finding was strengthened by functional studies with yeast cells lacking different members of the Drs2 family. In Δ*drs2* cells and in cells expressing a temperature-sensitive form of Drs2p, the translocation of PS was impaired across the plasma membrane (Tang et al., 1996; Gomes et al., 2000) and isolated late Golgi membranes (Natarajan et al., 2004), respectively. Two other yeast Drs2 family members, Dnf1p and Dnf2p, were found to be essential for the ATP-dependent inward transport of PS, PE, and PC at the plasma membrane (Pomorski et al., 2003). The reduced translocation of PE in Δ*dnf1*Δ*dnf2* cells was aggravated by the additional deletion of *DRS2*, consistent with a role for Drs2p in lipid translocation at the plasma membrane. Drs2 family members present in other organisms have also been linked to APL translocation. Expression of the *Arabidopsis thaliana ALA1* gene in Δ*drs2* yeast cells restored the PS translocation to wild-type rates *in vivo* and *in vitro* (Gomes et al., 2000). Another Drs2 family member in the protozoan parasite *Leishmania donovani*, LdMT, was found to

participate in the uptake of PC, PE, and PS in a concentration dependent way (Perez-Victoria et al., 2003). In mice spermatozoa, disruption of *SPALT*, a gene encoding a novel Drs2 family member, caused a loss of PS asymmetry, supporting a function for the SPALT protein in the maintenance of aminophospholipid asymmetry (Wang et al., 2004). In spite of these hints for a function as APL transporter for the Drs2 family members, direct evidence for this activity remains to be provided with a purified enzyme.

1.3.1.4 Localization and function of the Drs2 family members in *Saccharomyces cerevisiae*

Drs2p, Dnf1p, Dnf2p, Dnf3p, and Neo1p are the members of the Drs2 family in *S. cerevisiae*. Only Neo1p is essential and based on sequence analysis it appears to be more divergent from the other Drs2 family members (Prezant et al., 1996; Catty et al., 1997). Analysis of strains carrying all possible combinations of null alleles revealed that Drs2p, Dnf1p, Dnf2p, and Dnf3p constitute an essential subgroup with overlapping functions (Hua et al., 2002). Among the double deletion mutants, Δ*dnf1*Δ*drs2* exhibited the strongest growth and membrane trafficking defects, suggesting that these two proteins performed most of the essential functions of the Drs2/Dnf subgroup (Hua et al., 2002).

Drs2p has been the best-characterized member of the family so far. This protein is mainly localized to the late Golgi complex (Chen et al., 1999), where it is suggested to participate in the formation of a specific class of clathrin-coated secretory vesicles (Gall et al., 2002). The finding that *DRS2* exhibited strong genetic interactions with genes encoding clathrin heavy chain and Arf1p led to the proposal that the generation of lipid asymmetry could be intimately connected to the process of coat assembly during membrane budding (Chen et al., 1999). This idea was supported by the recent identification of a physical interaction between Drs2p and Gea2p, a Sec7 family Arf GEF. Disruption of this interaction resulted in defects in membrane fenestration and tubulation events along the secretory pathway that take place during the formation of secretory vesicles (Chantalat et al., 2004).

Dnf1p and Dnf2p are mainly present at the plasma membrane (Hua et al., 2002). Due to their proposed function as phospholipid translocases, these proteins are suggested to participate in endocytic vesicle formation at the plasma membrane (Pomorski et al., 2003). In addition, Dnf1p and Dnf2p might play a role in the recycling pathway from early endosomes to the TGN (Hua et al., 2002). Dnf3p localizes to the late Golgi complex and its function is less well characterized. This protein has been proposed to perform redundant functions with Dnf1p and Dnf2p in the endosomes-to-TGN pathway (Hua et al., 2002).

1.3.1.5 Neo1p is functionally connected to the endosomal proteins Ysl2p and Arl1p

The localization and function of Neo1p were only poorly characterized until recently. *NEO1* has first been identified in a screen for genes that upon overexpression confer resistance to the aminoglycoside antibiotic neomycin (Prezant et al., 1996). In the group of B. Singer-Krüger, *NEO1* was isolated in a high-copy number suppressor screen for its ability to rescue the temperature sensitivity of Δ*ysl2* cells and has also been found to represent a low-copy number suppressor of these cells. Ysl2p is peripherally associated with endosomal membranes and is required for receptor-mediated and fluid-phase endocytosis. It also participates, either directly or indirectly, in the maintenance of the vacuolar structure (Jochum et al., 2002). Sequence analysis of Ysl2p revealed homologies to the N-terminal domain of several Arf GEFs and to their catalytic Sec7 domain. In support of a function for Ysl2p as an Arf GEF, multiple genetic and biochemical evidence indicated an interaction between Ysl2p and the Arf-like protein Arl1p. The deletion of *ARL1* in Δ*ysl2* cells resulted in synthetic lethality and overexpression of *ARL1*, but not of genes encoding other Arf proteins, suppressed the defects in growth and endocytosis exhibited by Δ*ysl2* cells. A physical interaction between the N-terminal region of Ysl2p including the Sec7 domain and Arl1p was shown in an *in vitro* binding assay. Cells deleted for *ARL1* were also found to be defective in endocytic transport and in vacuolar protein sorting. These data suggested that Ysl2p could represent a Sec7 family Arf GEFs for Arl1p involved in endocytic trafficking (Jochum et al., 2002). Temperature-sensitive *neo1* mutants were generated in the lab of B. Singer-Krüger and, similar to *ysl2* mutants, several of them were shown to be impaired in endocytic transport and vacuole biogenesis. The finding that two of the *neo1-ts* alleles interacted genetically with *ARL1* (see 3.1.6) also suggested a connection between Neo1p and Arl1p. One goal of the present work was to better characterize the function of Neo1p within the endosomal system and to further study the molecular and functional interactions between Neo1p, Ysl2p, and Arl1p (see 1.4).

1.3.2 Role of phosphoinositides in membrane trafficking and their regulation by synaptojanin family members

1.3.2.1 Phosphoinositide isoforms and their subcellular distribution

Phosphoinositides (PIs) are phosphorylated derivates of phosphatidylinositol (PtdIns). The inositol headgroup of phosphatidylinositol can be reversibly phosphorylated at one or a combination of the hydroxy groups at the 3', 4' and 5' position of the inositol ring to produce distinct isoforms. The phosphorylation state of PIs is regulated by a variety of kinases, their

dephosphorylation by different phosphatases (reviewed by Odorizzi et al., 2000). Together, these enzymes regulate the temporal and spatial distribution of PIs, which act as second messengers in several cellular pathways, including vesicular traffic and actin cytoskeletal dynamics (reviewed by Martin, 2001; Simonsen et al., 2001), by recruiting isoform-specific PI-binding proteins to membranes (see below).

Phosphatidylinositol 4,5-bisphosphate (PtdIns(4,5)P_2) is the major PI found at the plasma membrane, where it participates in the recruitment of proteins involved in endocytosis (reviewed by Martin, 2001). Among these PI-interacting partners, epsins and Sla2p bind clathrin and proteins containing multiple interacting domains like Pan1p (Wendland and Emr, 1998; Wendland et al., 1999; Henry et al., 2002). In turn, Pan1p binds to a number of other proteins involved in endocytosis (Wendland and Emr, 1998). Epsins also associate with receptors destined for internalization (Shih et al., 2002). Thus, the interaction of epsins and Sla2p with PtdIns(4,5)P_2 may tether the clathrin lattice to the plasma membrane.

PtdIns(4,5)P_2 is furthermore required for the recruitment of elements of the actin cytoskeleton (reviewed by Yin and Janmey, 2003) to sites of endocytic internalization (see section 1.2.2). In particular, it has been shown that PtdIns(4,5)P_2 stimulates N-WASP, the mammalian homolog of Las17p (see 1.2.2), which in turn activates the actin nucleating Arp2/3-complex (reviewed by Yin and Janmey, 2003). Due to these multiple interactions, PtdIns(4,5)P_2 is believed to be an important factor for endocytic internalization.

PtdIns(3)P is found within endosomal membranes and participates in later stages of the endocytic pathway (reviewed by Odorizzi et al., 2000). Vac1p, one of the multiple PtdIns(3)P effectors, controls the docking of transport vesicles emanating from the Golgi complex to the prevacuolar compartment (Peterson et al., 1999). Similarly, human EEA1, another PtdIns(3)P effector, has been shown to participate in the docking of clathrin-coated vesicles to early endosomes (Rubino et al., 2000). In the late endosomal compartment, PtdIns(3)P is required for the sorting of some endocytic cargo molecules into multivesicular bodies by recruiting components of the sorting machinery of this highly complex process (Katzmann et al., 2003).

PtdIns(3,5)P_2 is synthesized on late endosomal membranes by the only PtdIns(3)P-5 kinase Fab1p, which is recruited to the membrane by PtdIns(3)P. Fab1p activity has been shown to be required for the maintenance of the vacuolar size and some of its effectors may play a role in the recycling of membranes from the vacuole to the prevacuolar compartment (Gary et al., 1998; Dove et al., 2004).

1.3.2.2 The synaptojanin family

Members of the synaptojanin family are highly conserved PI 5-phosphatases that are defined by three domains (McPherson et al., 1996): a N-terminal Sac1-like domain that resembles the polyphosphoinositide phosphatase domain of the yeast Sac1p, a central phosphoinositide 5'-phosphatase domain, and a C-terminal proline-rich domain (Fig. 4A). While the 5'-phosphatase selectively hydrolyses the phosphate group at the 5' position of the inositol ring of PtdIns(4,5)P_2, the Sac1-like domain of some synaptojanin members possesses a polyphosphoinositide phosphatase (PPIP) activity that results in the dephosphorylation of PtdIns(3)P, PtdIns(4)P, and PtdIns(3,5)P_2 to PtdIns (Guo et al., 1999) (Fig. 4B). The C-terminal proline-rich domain of the synaptojanin family members is the most variable region and may function as an interaction platform for a large number of proteins.

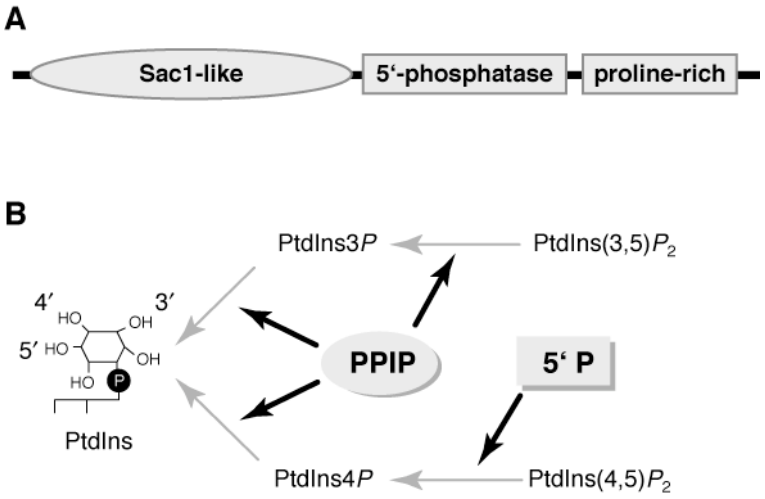

Fig. 4. Domains and enzymatic activities of the synaptojanin proteins. (A) The three domains characteristic of the synaptojanin proteins. **(B)** The Sac1-like domain of some synaptojanin proteins possesses a polyphosphoinositide phosphatase (PPIP) activity toward phosphatidylinositol (PtdIns) 3- and 4-phosphate and 3,5-bisphosphate. The 5'-phosphatase domain dephosphorylates specifically PtdIns(4,5)P_2.

Synaptojanin 1 of mice is the best-characterized member of the synaptojanin family. Synaptojanin 1-knockout mice accumulated an increased number of clathrin-coated vesicles in the nerve terminals and incubation with protein-free liposomes of the cytosol derived from the brain of these mutants resulted in an increase of clathrin-coated structures (Cremona et al., 1999). Therefore, Synaptojanin 1 has been proposed to mediate the uncoating of synaptic vesicles by dephosphorylating PtdIns(4,5)P_2 (Cremona et al., 1999). Further support of this idea was that clathrin-coated vesicles accumulated in synaptic termini of mutants of the unique synaptojanin present in *Caenorhabditis elegans* and in *Drosophila melanogaster* (Harris et al., 2000; Verstreken et al., 2003). A similar phenotype was also observed at lamprey giant synapses after disruption of synaptojanin function (Gad et al., 2000). Consistent with a role in vesicle uncoating, the mammalian Synaptojanin 1, the *Drosophila* Synj, and the *C. elegans* unc-26 proteins were all localized to coated synaptic vesicles (Haffner et al., 1997;

Schuske et al., 2003; Verstreken et al., 2003). This subcellular distribution may be at least partially mediated via the proline-rich domain. In fact, this domain of mammalian Synaptojanin 1 and *Drosophila* Synj bind to endophilin, a protein involved in clathrin-mediated endocytosis and that has been proposed to play a major role in the recruitment of synaptojanins to synaptic membranes (de Heuvel et al., 1997; Gad et al., 2000; Verstreken et al., 2003; Schuske et al., 2003).

The misregulation of PtdIns(4,5)P_2 levels and the sequestration of coat components on the accumulated vesicles in the synaptojanin mutants result in other morphological alterations. Notably, defects in the interaction of synaptic vesicles with the actin cytoskeleton were observed in the synaptojanin mutants in mice, flies, and worms (Kim et al., 2002; Verstreken et al., 2003; Harris et al., 2000). Thus, synaptojanins appear to regulate both directly and indirectly vesicle traffic after scission from the donor membrane.

1.3.2.3 Synaptojanin proteins in *Saccharomyces cerevisiae*

The yeast *Saccharomyces cerevisiae* contains three synaptojanin-like (Sjl) proteins, Sjl1p, Sjl2p, and Sjl3p (also named Inp51p, Inp52p, and Inp53p). While single disruption mutants display no obvious phenotypes, cells lacking all three synaptojanin genes are nonviable (Stolz et al., 1998), indicating that these proteins perform essential functions. Analyses by pair-wise deletion of the synaptojanin genes revealed differences among the three double deletion mutants. Receptor-mediated and fluid-phase endocytosis was impaired in Δ*sjl1*Δ*sjl2* cells (Singer-Krüger et al., 1998) and this mutant also exhibited alterations in the organization of the actin cytoskeleton and in the cell surface morphology (Srinivasan et al., 1997; Singer-Krüger et al., 1998; Stolz et al., 1998). Defects in endocytosis and in the actin cytoskeleton organization were observed in Δ*sjl2*Δ*sjl3* cells as well, but these phenotypes were less profound than in Δ*sjl1*Δ*sjl2* cells. The Δ*sjl1*Δ*sjl3* mutant displayed relatively few deficiencies (Srinivasan et al., 1997; Singer-Krüger et al., 1998; Stolz et al., 1998). The phenotypical differences among the three mutants could reflect at least partially distinct defects, rather than a difference in the penetrance of the same defects (Singer-Krüger et al., 1998) and may suggest that synaptojanins each perform specific and diverse functions in endocytosis and in the actin cytoskeleton. The fact that the Δ*sjl1*Δ*sjl3* mutant exhibited no endocytic defects suggested that Sjl2p probably represents the major player in endocytosis. A specific role was also proposed for Sjl3p in clathrin-mediating protein sorting at the TGN (Bensen et al., 2000; Ha et al., 2003).

Like their homologs in mammals, flies, and worms, the yeast synaptojanins seem to

control early steps of vesicle trafficking by regulating phosphoinositide turnover. In fact, a correlation between increased levels of PtdIns(4,5)P_2 observed in the synaptojanin mutants and the deficiencies in membrane trafficking and in the actin organization could be established (Stefan et al., 2002). Since the yeast synaptojanins all possess a similar catalytic activity, it is possible that the specificity of their individual functions is determined by a distinct localization for each synaptojanin and different interacting partners.

To find further hints for a function of Sjl2p in endocytosis, the second part of my PhD thesis addressed to some extent the subcellular localization of Sjl2p and its direct interacting partner Bsp1p.

1.4 Goal of this project

The goal of this project was to bring new insights to the function of two proteins suggested to be involved in yeast endocytosis, Neo1p (see 1.3.1.5) and Sjl2p (see 1.3.2.3). In the first part of my PhD work, the subcellular localization of Neo1p was analyzed in great detail by double immunofluorescence. The function of Neo1p was further characterized, using two *neo1-ts* mutants already shown by B. Singer-Krüger to be impaired in endocytosis and in vacuole biogenesis. These mutants were analyzed for additional membrane trafficking defects. The localization, the stabilities, and the ATPase activities of the Neo1 mutant polypeptides were compared to that of wild-type Neo1p. To further characterize the relationship between Neo1p, Ysl2p, and Arl1p (see 1.3.1.5), co-immunoprecipitation experiments were performed to address the interaction of Neo1p with Ysl2p, and the localization of Ysl2p and Arl1p was analyzed in *neo1-ts* mutants as opposed to *NEO1* cells. In the second part of this work, the subcellular distribution of Sjl2p and its interacting partner Bsp1p (see 3.2.3) was studied by indirect immunofluorescence. To check for an interaction of Sjl2p and Bsp1p with the actin cytoskeleton, microscopy was also conducted in cells, in which the cortical actin cytoskeleton aggregates into large clumps. The influence of phosphoinositides on the subcellular distribution of Bsp1p and on the binding of Bsp1p to liposomes *in vitro* was examined.

2 Materials and Methods

2.1 Materials

2.1.1 *Saccharomyces cerevisiae* strains

The *Saccharomyces cerevisiae* strains used in this study are listed below.

Yeast strain	Genotype	Source
BS64	*MAT*a *his4 ura3 leu2 lys2 bar1-1*	Singer-Krüger et al., 1994
RH1737	*MAT*a *leu2 ura3 his4 ade2 sec18 bar1-1*	H. Riezman, Switzerland
BS747	*MAT*a/α *his4/his4 ura3/ura3 leu2/leu2 lys2/lys2 ysl2::kan^r/ysl2::kan^r bar1-1/bar1-1*	Jochum et al., 2002
BS757	*MAT*a/α *his3/his3 ura3/ura3 leu2/leu2 lys2/lys2 NEO1/NEO1::3-HA-HIS5 (S. pombe) bar1-1/bar1-1*	B. Singer-Krüger (BSK)
BS811	*MAT*a/α *his4/his4 ura3/ura3 leu2/leu2 lys2/lys2 NEO1/neo1::kan^r bar1-1/bar1-1*	BSK
BS845	*MAT*a *his4 ura3 leu2 lys2 neo1::kan^r bar1-1* + pRS316-NEO1	BSK
BS862	*MAT*a *his4 ura3 leu2 lys2 neo1::kan^r bar1-1* + pRS315-HA-NEO1	BSK
BS864	*MAT*α *his4 ura3 leu2 lys2 neo1::kan^r bar1-1* + pRS315-HA-NEO1	BSK
BS912	*MAT*a *his4 ura3 leu2 lys2 YSL2::TAP-URA3 (K. lactis) neo1::kan^r bar1-1* + pRS315-HA-NEO1	BSK
BS915	*MAT*a *his4 ura3 leu2 lys2 neo1:: kan^r bar1-1* + pRS315-neo1-37	BSK
BS917	*MAT*a *his4 ura3 leu2 lys2 neo1:: kan^r bar1-1* + pRS315-neo1-69	BSK
BS993	*MAT*α *his4 ura3 leu2 lys2 YSL2::TAP-URA3 (K. lactis) neo1::kan^r bar1-1* + pRS315-HA-neo1-69	BSK
BS1001	*MAT*a *his4 ura3 leu2 lys2 YSL2::TAP-URA3 (K. lactis) neo1::kan^r bar1-1* + pRS315-HA-neo1-37	BSK
BS1088	*MAT*a *ura3 leu2 lys2 vps27 neo1:: kan^r bar1-1* + pRS315-HA-NEO1	BSK
BS1099	*MAT*a *ura3 leu2 lys2 BSP1::3-HA-HIS5 (S. pombe)*	BSK
BS1121	*MAT*α *ura3 leu2 lys2 YSL2::3-HA-HIS5 (S. pombe) bar1-1*	BSK
BS1124	*MAT*a *ura3 leu2 lys2 SJL2::3-HA-HIS5 (S. pombe) vps27*	BSK
BS1128	*MAT*α *ura3 leu2 lys2 SJL2::3-HA-HIS5 (S. pombe) bar1-1*	BSK
BS1148	*MAT*a *ura3 leu2 lys2 pik1-83::TRP1 BSP1::3-HA-HIS5 (S. pombe)*	BSK
BS1149	*MAT*a *ura3 leu2 lys2 pik1-63::TRP1 BSP1::3-HA-HIS5 (S. pombe)*	BSK
BS1175	*MAT*α *ura3 leu2 SJL2::3-HA-HIS5 (S. pombe) sec7 bar1-1*	BSK
BS1233	*MAT*α *ura3 leu2 lys2 neo1::kan^r YSL2:: 3-HA-HIS5 (S. pombe) bar1-1* + pRS315-HA-neo1-37	BSK
BS1248	*MAT*$^{\text{l}}$ *his4 ura3 leu2 lys2 SJL2::13-Myc-kan^r bar1-1*	BSK
DDY1885	*MAT*α *ura3 leu2 lys2 his3 Δark1::HIS3 Δprk1::LEU2*	BSK
BS1261	*MAT*a *ura3 leu2 lys2 BSP1::3-HA-HIS5 (S. pombe) Δark1::HIS3 Δprk1::LEU2*	BSK
BS1265	*MAT*a *his4 ura3 leu2 lys2 BSP1::13-Myc-kan^r bar1-1*	BSK

BS1270	*MAT*[1] *ura3 leu2 lys2 SJL2::3-HA-HIS5 (S. pombe)* Δ*ark1::HIS3* Δ*prk1::LEU2*	BSK
BS1279	*MAT*□ *ura3 leu2 lys2 neo1::kan*[r] *ARL1::3-HA-HIS5* (*S. pombe*) *bar1-1* + pRS316-NEO1	BSK
BS1282	*MAT*a *ura3 leu2 lys2 neo1::kan*[r] *ARL1::3-HA-HIS5 (S. pombe) bar1-1* + pRS315-neo1-37	BSK
BS1283	*MAT*a *ura3 leu2 lys2 neo1::kan*[r] *ARL1::3-HA-HIS5 (S. pombe) bar1-1* + pRS315-neo1-69	BSK
BS1285	like BS845, but + pRS315-HA-neo1-37	this study
BS1286	like BS845, but + pRS315-HA-neo1-69	this study
BS1373	*MAT*[1] *ura3 leu2 lys2 SJL1::3-HA-HIS5 (S. pombe)* Δ*ark1::HIS3* Δ*prk1::LEU2*	BSK
BS1375	*MAT*[1] *ura3 leu2 lys2 SJL3::3-HA-HIS5 (S. pombe)* Δ*ark1::HIS3* Δ*prk1::LEU2*	BSK
BS1382	*MAT*a *his4 ura3 leu2 neo1::kan*[r] *sec7 bar1-1* + pRS315-HA-NEO1	this study
BS1383	*MAT*a *ura3 leu2 lys2 vps27 neo1::kan*[r] *bar1-1* + pRS315-HA-neo1-69	this study
BS1402	*MAT*a *ura3 leu2 lys2 neo1::kan*[r] *YSL2::3-HA-HIS5 (S. pombe) bar1-1* + pRS315-HA-neo1-69	BSK
BS1417	*MAT*[1] *ura3 leu2 lys2 SJL2::3-HA-HIS5 (S. pombe)* Δ*ark1::HIS3* Δ*prk1::LEU2* + pRS316-prk1-as3	BSK
BS1423	*MAT*a *his3 ura3 leu2 met15 CHC1::GFP-HIS3*	Invitrogen
BS1439	*MAT*[1] *his3 ura3 leu2 CHC1::GFP-HIS3-MX6* Δ*ark1::HIS3* Δ*prk1::LEU2*	BSK
BS1446	*MAT*[1] *ura3 leu2 lys2 SJL2::GFP-kan*[r] Δ*ark1::HIS3* Δ*prk1::LEU2* + pRS316-prk1-as3	BSK
Y190	*MAT*a *gal4 gal80 his3 trp1-901 ade2-101 ura3-52 leu2-3,-112 +URA3::GAL*□ *lacZ, LYS2::GAL*□ *HIS3 cyh*[r]	S. Elledge, USA

[1] not determined

2.1.2 *Escherichia coli* strains

The DH5□ strain was used for all plasmid amplifications and DNA ligations, except for the generation of *NEO1*$^{\Delta Ctail}$ (see section 2.2.1), for which BMH 71-18 *mut*S and JM109 strains were used.

DH5□	F'/endA1 hsdR17($r_{k-}m_{k+}$) supE44 thi-1 recA1 gyrA (Nal_r) relA1 Δ(lacZYA-argF)$_{U169}$ (□80lacZΔM15)	Hanahan, 1983
BMH 71-18 *mut*S	thi supE Δ(lac-proAB) [*mut*S:Tn10] [F' proAB $lacI^qZ$ΔM15]	Promega
JM109	endA1 hsdR17($r_{k-}m_{k+}$) supE44 thi recA1 gyrA96, relA1 □- relA1 Δ(lac-proAB) [F' traD36 proAB $lacI^qZ$ΔM15]	Promega

2.1.3 Plasmids

The plasmids used in this study are listed below.

Plasmid name	Characteristics	Source
pRS425-NEO1	contains *Spe*I/*Eco*RI fragment of *NEO1*, cloned by *Spe*I/*Sal*I	B. Singer-Krüger (BSK)
pRS315-NEO1	contains *Spe*I/*Eco*RI fragment of *NEO1*, cloned by *Spe*I/*Sal*I	BSK
pRS316-NEO1	contains *Spe*I/*Eco*RI fragment of *NEO1*	BSK
pRS315-HA-NEO1	contains *Spe*I/*Sal*I fragment of *3-HA-NEO1*	BSK
pRS425-NEO1^{D503N}	contains *NEO1*^{D503N}	this study
pRS315-HA-NEO1$^{\Delta Ctail}$	carries *3-HA-NEO1*$^{\Delta Ctail}$	this study
pRS315-neo1-37	carries *neo1-37*, derived from pRS315-NEO1 by PCR mutagenesis	BSK
pRS315-neo1-69	carries *neo1-69*, derived from pRS315-NEO1 by PCR mutagenesis	BSK
pRS315-HA-neo1-37	contains *3-HA-neo1-37*	BSK
pRS315-HA-neo1-69	contains *3-HA-neo1-69*	BSK
pDD667	contains *GFP-ACT1*, *URA3*, CEN	D. Drubin, USA
pmycTLG1	*myc-TLG1* in pRS316	J. Holthuis, The Netherlands
pmycTLG2	*myc-TLG2* in pRS316	J. Holthuis, The Netherlands
pSKY5RER1-0	*GFP-RER1*, *URA3*, CEN	Sato et al., 2001
pBS-ADH-Ypt51Q66L	*YPT51Q66L* in pBPH1	Singer-Krüger et al., 1995
pJK59	*GFP-SEC63*, *URA3*, CEN	Prinz et al., 2000
pAS1-Neo1Nterm	*Bam*HI/*Sal*I PCR fragment of *NEO1* (encodes amino acids 1-184) in pAS1	this study
pAS1-Neo1Cterm	*Bam*HI/*Sal*I PCR fragment of *NEO1* (encodes amino acids 1091-1151) in pAS1	this study
pACTII-Ysl2-Sec7-full	*Bam*HI/*Sal*I fragment of *YSL2* (encodes amino acids 211-514) in pAS1	Jochum et al., 2002
pRS316-prk1-as3	contains *Sac*I/*Sal*I *PRK1*$^{M108G, C175A}$ in pRS316	BSK

2.1.4 Antibodies

Antibodies used in this study are listed below and dilutions used for immunoblotting are specified. Dilutions and combinations of antibodies for indirect immunofluorescence analysis are indicated in section 2.2.3.3.

2.1.4.1 Antibodies used for immunoblotting

Antibodies	Dilution	Source
Mouse monoclonal purified anti-HA, clone 16B12	1:2000	Covance
Rabbit serum or purified anti-Ysl2p	1:500	Jochum et al., 2002

Mouse monoclonal anti-Pep12p	1:500	Molecular Probes
Purified rabbit anti-Ypt51p	1:50	Singer-Krüger et al., 1995
Mouse monoclonal anti-Chc1p ascites fluid	1:500	S. Lemmon, USA
Rabbit polyclonal anti-Vps10p	1:500	BSK
Rabbit polyclonal anti-Tlg2p	1:300	BSK
Rabbit polyclonal anti-Pma1p	1:2000	BSK
Rabbit polyclonal anti-GFP	1:100	Clontech
Goat anti-mouse IgG, alkaline phosphatase-conjugated	1:1000	Kirkegaard & Perry Laboratories
Goat anti-rabbit IgG, alkaline phosphatase-conjugated	1:1000	Kirkegaard & Perry Laboratories

2.1.4.2 Antibodies used for immunoprecipitations

Antibodies	**Source**
Mouse monoclonal purified anti-HA, clone 12C5	Roche
Rabbit polyclonal anti-CPY	BSK

2.1.4.3 Primary antibodies used for indirect immunofluorescence

Antibodies	**Source**
Mouse monoclonal anti-HA, clone 16B12	Covance
Rat monoclonal affinity purified anti-HA, clone 3F10	Roche
Mouse monoclonal anti-Pep12p	Molecular Probes
Affinity purified rabbit anti-Ypt51p	Singer-Krüger et al., 1995
Mouse monoclonal anti-60kDa subunit of v-ATPase	Molecular Probes
Mouse monoclonal anti-Ypt1p ascites fluid	D. Gallwitz, Germany
Mouse monoclonal anti-Chc1p ascites fluid	S. Lemmon, USA
Rabbit polyclonal anti-c-Myc (sc-789)	Santa-Cruz Biotechnology
Affinity purified mouse a-AFP (clone 3E6)	QBIOgene
Mouse monoclonal anti-GFP	Roche

2.1.4.4 Secondary antibodies used for indirect immunofluorescence

Antibodies	**Source**
Cy3-conjugated affinity purified goat anti-mouse Fab fragment	Jackson ImmunoResearch
Alexa ^{488}-conjugated goat anti-mouse IgG (H+L) highly cross-adsorbed	Molecular Probes
Alexa ^{594}-conjugated goat anti-mouse IgG (H+L) highly cross-adsorbed	Molecular Probes
Alexa ^{594}-conjugated goat anti-rat IgG (H+L) conjugate	Molecular Probes
Alexa ^{488}-conjugated goat anti-rat IgG (H+L) conjugate	Molecular Probes
Alexa ^{594}-conjugated goat anti-rabbit IgG (H+L) highly cross-adsorbed	Molecular Probes
Alexa ^{488}-conjugated goat anti-rabbit IgG (H+L) highly cross-adsorbed	Molecular Probes

2.1.5 Enzymes and kits used for molecular biology

Restriction endonucleases used in this study were provided either by Roche or by New England Biolabs (NEB). The Vent DNA polymerase (NEB) and the T4 DNA polymerase (Roche) were used for DNA amplifications by the polymerase chain reaction (PCR).

The QIAprep Spin Miniprep Kit (Qiagen) was used for DNA isolation from *Escherichia coli* cells, the QIAEX II Gel extraction Kit (Qiagen) and the GENECLEAN® Kit (QBIOgene) for DNA extraction from agarose gels, and the QIAquick PCR Purification Kit (Qiagen) for PCR fragment purification.

2.1.6 Chemicals

Unless otherwise indicated, the chemicals used in this study were provided by the companies Genaxxon, Merck, Roth, and Sigma.

2.1.7 Media

Yeast strains were propagated either in complete medium (YPD) (1% (w/v) Bacto® yeast extract, 2% (w/v) Bacto® peptone, 2% (w/v) glucose, pH 5.5) or in synthetic growth medium (SD medium) (0.67% (w/v) yeast nitrogen base, 2% (w/v) glucose, pH 5.6) containing 0.3 mM adenine, 0.4 mM tryptophan, 1 mM lysine, 0.3 mM histidine, 1.7 mM leucine, and 0.2 mM uracil (final concentration) (complete SD medium). Cells were grown to early logarithmic phase (0.1-0.3 OD_{600} units/ml) at 25°C on a rotary shaker, unless otherwise indicated. Yeast transformants carrying a plasmid were grown in SD medium lacking either leucine or uracil depending on the selection marker (*LEU2* or *URA3*, respectively) present on the plasmid (selective SD medium).

Solid medium contained 2% (w/v) Bacto® Agar in addition to the YPD or SD medium components. Plasmid shuffle in yeast transformants carrying one plasmid with the *URA3* marker and a second one with the *LEU2* marker was induced by incubation on SD plates lacking leucine and containing 1mg/ml fluoro-orotic acid (5-FOA), resulting in the loss of the plasmid carrying the *URA3* marker. Selective growth of yeast cells carrying a gene deletion marked by the kan^r gene for geneticin resistance was performed by incubation on YPD plates containing 0.2 mg/ml geneticin (G-418 sulfate).

The sporulation of diploid cells was induced by incubation on presporulation plates (0.8% (w/v) Bacto® yeast extract, 0.3% (w/v) Bacto® peptone, 10% (w/v) glucose, 2% (w/v) Bacto® Agar) for 1 day and sporulation plates (1% (w/v) potassium acetate, 0.1% (w/v) Bacto® yeast extract, 0.05% (w/v) glucose, 2% (w/v) Bacto® Agar, 0.075 mM adenine, 0.1

mM tryptophan, 0.25 mM lysine, 0.075 mM histidine, 0.42 mM leucine, 0.05 mM uracil) for 5 days.

Escherichia coli cells transformed with plasmids carrying the gene amp^r for ampicillin resistance as selection marker were propagated in LB medium (0.5% (w/v) yeast extract, 1% (w/v) Bacto trypton, 0.5% (w/v) NaCl, pH 7.5) containing 10 mg/ml ampicillin.

2.2 Methods

2.2.1 Generation of DNA constructs

All DNA manipulations were by standard techniques (Sambrook et al., 1989). Enzymes were used as suggested by the provider. *E. coli* cells were transformed by heat shock or electroporation. All PCR-amplified DNA fragments subcloned in a vector were sequenced (MWG, Ebersberg) to verify the mutations and to exclude the presence of PCR errors.

To generate pAS1-Neo1Cterm, the DNA fragment encoding the last 20 amino acids of Neo1p was amplified by PCR using the Vent DNA polymerase and as template pRS425-NEO1. The flanking primers (see below) contained restriction sites for *Bam*HI (5'Bam,NEO1,C-term) and for *Xho*I (3'Xho,Neo1,C-term), respectively. After isolation and purification, the PCR product was digested and subcloned into pAS1 opened with *Bam*HI/*Xho*I. The same strategy was used to generate pAS1-Neo1Nterm, using as flanking primers 5'Bam,NEO1,N-term and 3'Xho,Neo1,N-term (see below) to amplify the *NEO1* fragment encoding the first 184 amino acids of Neo1p. The primers were provided by MWG and are listed below.

5'Bam,NEO1,C-term: 5'-CGTCGGATCCCAAAGGCAATTTATAGAAGG-3'
3'Xho,Neo1,C-term: 5'-GCTACTCGAGTTATGGAGTGGCAAACTC-3'
5'Bam,NEO1,N-term: 5'-CTGTGGATCCCTAACCCTCCTTCATTT-3'
3'Xho,Neo1,N-term: 5'-GGTCCTCGAGTCAAGTAACGGCATTATATTTGG-3'

The DNA fragment encoding the Neo1p^{D503N} point mutation was generated by directed mutagenesis using a PCR-based protocol (Barik and Galinski, 1991). A PCR fragment was generated with the Vent DNA polymerase using pRS425-NEO1 as template, the primer 5'-CCCTGTTTTGTTGCTTAGAAG-3', which carries the codon for the D503N mutation, and 5'-TACGACCGATAACCAAAGTAC-3' (3'NEO1,SnaB1) as second primer. The purified PCR fragment was used as megaprimer together with the flanking primer 5'-CTGACTGGAAACTACGTG-3' (5'NEO1,Pac1) in another PCR using pRS425-NEO1 as

template and the Vent DNA polymerase. This PCR fragment was digested with *Sna*BI and *Pac*I and subcloned into pRS425-NEO1 opened with *Sna*BI/*Pac*I.

To generate Neo1p$^{\Delta Ctail}$, a stop codon was introduced using the GeneEditor mutagenesis kit (Promega). The *Hind*III/*Sal*I *NEO1* fragment, subcloned into pBSK, was mutagenized according to the manufacturer using the mutagenic oligonucleotide 5'-CTATAAATTGCCTAGGCCGTCCAGACAG-3'. This created a stop codon at position 3391-3393 of the *NEO1* coding sequence and a *Sty*I restriction site. The *Sal*I/*Stu*I subfragment of the mutated *Hind*III/*Sal*I fragment was excised from pBSK and used to replace the wild-type *Sal*I/*Stu*I fragment in pRS315-HA-NEO1.

2.2.2 Mating, sporulation, transformation of yeast cells, CPY missorting, and two-hybrid assays

To generate heterozygous strains, a particular strain of mating type a was mixed with a particular strain of mating type α on YPD plates. After an overnight incubation at 25°C, the mixture was streaked out at 25°C on YPD or on selective SD plates to obtain single colonies. The biggest colonies were analyzed under the light microscope for diploid cells. Colonies of such diploids were streaked out overnight on presporulation plates at 25°C and the material was transferred to sporulation plates. After incubation at 25°C for at least 4 days, cells were prepared for tetrad dissection in dissection buffer (1.2 M sorbitol, 50 mM Tris/HCl pH 7.5) containing lyticase (isolated by B. Singer-Krüger). Tetrads were separated under the light microscope using a needle for tetrad dissection (Singer Instruments) coupled to a micromanipulator.

Transformation of yeast cells was performed after the lithium acetate method (Ito et al., 1983).

CPY missorting was analyzed by growing cells for 2 days at 25°C on YPD plates covered with a nitrocellulose membrane. The membrane was washed and CPY was immunodetected (see section 2.2.3.1) using anti-CPY antibodies.

Two-hybrid assays were performed to determine whether the N-terminal or the C-terminal regions of Neo1p mediate an interaction with Ysl2p. The Gal4 DNA binding domain fused to the C-terminal tail or the N-terminal part of Neo1p (pAS1-Neo1Cterm, pAS1-Neo1Nterm, respectively) was coexpressed with the Gal4 transcriptional activation domain fused to the Sec7 domain of Ysl2p (pACTII-Ysl2-Sec7-full) in the two-hybrid reporter strain Y190. The activation of the reporter lacZ gene was analyzed using the β-galactosidase colony filter assay (Fields and Song, 1989). The activation of the reporter *HIS3* gene was tested by

incubation of the Y190 transformants on selective SD plates lacking uracil, tryptophan and histidine and containing 25 mM 3-amino-1,2,4-triazole (3AT).

2.2.3 Biochemical methods

2.2.3.1 Cell extracts, immunoblotting of proteins, and quantitative analysis of soluble Ysl2p and Neo1p

Total cell extracts were prepared by alkaline lysis as follows. One OD_{600} unit of cells grown in YPD at 25°C to early logarithmic phase (0.1-0.3 OD_{600} units/ml) was washed once with H_2O and resuspended in 1 ml H_2O. One hundred μl of 2 N NaOH/5% (v/v) β-mercaptoethanol were added and cells were lysed for 10 min on ice. Proteins were precipitated by the addition of 6% (w/v) trichloroacetic acid (TCA) (final concentration) for 30 min on ice. After a 20 min centrifugation at 13,000 rpm, pellets were washed with 1 ml –20°C cold acetone. After air-drying, pellets were resuspended in 100 μl SDS-PAGE sample buffer (see below) with or without 9 M urea (Neo1p or Ysl2p, respectively). Samples were vortexed for 20 min at 37°C and incubated either at 50°C for 10 min (Neo1 proteins) or at 95°C for 5 min (Ysl2p).

Unless otherwise indicated, proteins were denatured in SDS-PAGE sample buffer (100 mM Tris/HCl pH 6.8, 5 mM EDTA/NaOH pH 8, 2% (w/v) SDS, 10% (w/v) glycerol, 0.02% (w/v) bromophenol blue, 2.5% (v/v) β-mercaptoethanol) or in SDS-PAGE sample buffer containing 9 M urea (Neo1 proteins) and were separated by SDS-PAGE (sodium dodecyl sulfate-polyacrylamide gel electrophoresis) (Laemmli, 1970) using the Mini-PROTEAN 3 cell (Bio-Rad Laboratories). After separation, proteins were transferred to nitrocellulose membranes using the tank blot method (Towbin et al., 1979) and the Mini-Trans-Blot cell system (Bio-Rad Laboratories). Immunoblotting was performed in low fat milk buffer [2.5% (w/v) low fat milk powder, 1 x phosphate saline buffer (PBS) (2.7 mM KCl, 137 mM NaCl, 5.6 mM Na_2HPO_4, 1.4 mM NaH_2PO_4, 1.5 mM KH_2PO_4), 0.2% (v/v) Tween 20]. Secondary antibodies were conjugated to alkaline phosphatase (see section 2.1.4.1). The alkaline phosphatase-catalyzed color reaction was performed in development reaction buffer (0.1 M Tris/HCl pH 9.5, 0.1 M NaCl, 50 mM $MgCl_2$) containing 0.015% (w/v) of BCIP (5-bromo-4chloro-3-indolyl-phosphate) and 0.03 % (w/v) of NBT (nitroblue tetrazolium) (Bio-Rad Laboratories).

To determine the percentage of membrane-associated Ysl2p in wild-type cells (BS1121) and the *neo1-69* mutant (BS1402), 100,000 x g pellet and supernatant fractions were prepared using one cell aliquot (see 2.2.3.2) of each strain. Cell lysis was performed as

described in section 2.2.3.2 in the presence of protease inhibitors [1 x PIC (0.1 μg/ml leupeptin, 0.5 mM phenanthroline, 0.5 μg/ml pepstatin, 0.1 mM pefabloc, each final concentration), 1 mM phenylmethylsulfonylfluoride (PMSF), 1 x Complete (protease inhibitor cocktail tablet, Roche, used as suggested by the manufacturer)]. Lysates were immediately precleared at 13,000 rpm for 20 min. The low-speed supernatants (880 μl) were centrifuged at 100,000 x g for 1 h in a TLA 120.2 rotor (Beckman Instruments). Pellets were resuspended in 250 μl IP buffer (see section 2.2.3.2) and the protein concentrations in the pellet and the supernatant fractions were determined using the Microassay Bradford procedure (Bradford, 1976) and an IgG standard. Each fraction was prepared in SDS-PAGE sample buffer to 1-5 μg proteins/μl. Determination of the percentage of membrane-associated Ysl2p was by loading several amounts (μg) of the pellet and the supernatant fractions on a SDS-polyacrylamide gel. After immunoblotting, the intensity of the Ysl2p bands derived from the pellet fractions was compared to that derived from the supernatant fractions. The amounts of pellet and supernatant fractions showing the same intensity of the Ysl2p band for a given strain were determined. These values were divided by the total protein amounts of the pellet and supernatant fractions, respectively. The two ratios were expressed using a common denominator, allowing the determination of the percentage of total Ysl2p that is present in each fraction (see example in Fig. 5). The same method was used to calculate the percentages of total Neo1p and Ysl2p that are present in the supernatant of cell lysates extracted with 0.01% (w/v) NP40, precleared at 13,000 rpm for 20 min, and recentrifuged for 1 h at 100,000 x g (see section 2.2.3.2).

2.2.3.2 Co-immunoprecipitation experiments using TAP-tagged Ysl2p and HA-tagged Neo1p

Cells used for co-immunoprecipitation experiments were separately prepared as follows. Cells grown in 1.6 l of YPD to 0.8-1 OD_{600} units/ml at 25°C (*neo1* mutants) or 30°C were harvested by centrifugation for 5 min at 4000 rpm. Cell pellets were washed twice with 200 ml H_2O and once with 50 ml cold IP buffer (115 mM KCl, 5 mM NaCl, 2 mM $MgCl_2$, 1 mM EDTA/NaOH pH 8, 20 mM HEPES/KOH pH 7.8). Cells were resuspended in IP buffer to a concentration of 50 OD_{600} units of cells in 300 μl of cell suspension. Aliquots containing 300 μl of cell suspension were frozen in liquid nitrogen and stored at –80°C.

The procedure used to purify TAP-Ysl2p assemblies was based on the tandem affinity purification (TAP) method described by Rigaut et al. (1999). One aliquot of BS862 and BS912 cells were lysed with glass beads (200 mg) in the presence of protease inhibitors (1 x

CLAP; chymostatin, leupeptin, antipain, pepstatin, each 5 μg/ml final concentration) by vortexing for 45 sec and cooling on ice for 1 min for 10 rounds. Cell lysates were transferred to fresh precooled Eppendorf tubes and glass beads were washed with 800 μl IP buffer. DTT was added to 1 mM (final concentration) and proteins were extracted in the presence of 0, 0.01, 0.02, or 0.04% (w/v) NP40 (final concentrations) for 20 min on ice. After 20 min of centrifugation at 13,000 rpm, 60 μl of a 1:3 slurry of IgG-Sepharose beads (Pharmacia) were added to the supernatants and the affinity purification of TAP-Ysl2p assemblies was performed for 2 h at 4°C on an overhead shaker. The IgG-Sepharose beads were washed twice with 500 μl IP buffer (containing 0 to 0.04% (w/v) NP40, respectively) and twice with 500 μl TEV cleavage buffer (10 mM Tris/HCl pH 8, 150 mM NaCl, 0.5 mM EDTA/NaOH pH 8, 1 mM DTT, 0 to 0.04% (w/v) NP40). Bound proteins were eluted in 100 μl TEV cleavage buffer containing three units of TEV protease for 2 h at 15°C. The eluates were transferred to a fresh tube and the IgG-Sepharose beads were washed twice with 400 μl TEV cleavage buffer. The proteins present in the complete eluates were precipitated in the presence of 6% (w/v) TCA, 0.015% (w/v) deoxycholic acid, and 5 μg of IgG and were resuspended in 65 μl SDS-PAGE sample buffer containing 9 M urea, vortexed for 20 min at 37°C and incubated at 50°C for 10 min. Twenty μl (Ysl2p) and 5 μl (HA-Neo1p) of samples were separated by SDS-PAGE. Ysl2p and HA-Neo1p were detected by immunoblotting using as primary antibodies rabbit anti-Ysl2p (Jochum et al., 2002) and mouse anti-HA (16B12, Covance).

To perform the complete TAP method, three aliquots of cells were processed in parallel for individual conditions. In each aliquot, proteins bound to the IgG-Sepharose beads were eluted in 75 μl TEV cleavage buffer containing three units of TEV protease for 2 h at 15°C. The three eluates were transferred to a fresh tube (total volume of 225 μl) and the IgG-Sepharose beads of the three samples were washed once with 100 μl and once with 50 μl TEV cleavage buffer, resulting in a final eluate volume of 375 μl. 1.125 ml calmodulin binding buffer (10 mM Tris/HCl pH 8, 150 mM NaCl, 1 mM magnesium acetate, 1 mM imidazol, 3.5 mM $CaCl_2$, 0.07% (v/v) β-mercaptoethanol) was added to each eluate and 40 μl of a 1:3 slurry of calmodulin affinity resin (Stratagene). After incubation for 1 h at 4°C, the calmodulin affinity resin was washed three times with 300 μl calmodulin binding buffer and proteins were released from the resin in 65 μl SDS-PAGE sample buffer containing 9 M urea at 50°C for 10 min. 25 μl (Ysl2p) and 6.25 μl (HA-Neo1p) of samples were separated by SDS-PAGE.

To perform co-immunoprecipitations with proteins solubilized by 0.01% (w/v) NP40 treatment, the supernatants obtained by centrifugation of cell extracts for 20 min at 13,000 rpm were recentrifuged at 100,000 x g for 1 h at 4°C in a TLA 120.2 rotor (Beckman Instruments). Fifty µl of the supernatants and the pellets resuspended in a total volume of 250 µl IP buffer were kept to determine the degree of solubilization of Neo1p and Ysl2p (see section 2.2.3.1). The 100,000 x g supernatants were subjected to immunoprecipitation using IgG-Sepharose beads and proteins were eluted with the TEV protease as described above. The eluates (100 µl) of five samples were pooled and the IgG-Sepharose beads were washed twice with 350 µl TEV cleavage buffer, resulting in a final eluate volume of 1.2 ml. The eluted proteins were precipitated, and finally denatured in 70 µl SDS-PAGE sample buffer containing 9 M urea as described before. The volumes separated by SDS-PAGE were 5 µl (Ysl2p), 10 µl (HA-Neo1p and Chc1p) and 20 µl (Tlg2p).

2.2.3.3 Fluorescence microscopy

To carry out indirect immunofluorescence (IF), cells were grown overnight at 25°C in YPD medium or in selective SD medium to early logarithmic phase (0.1-0.3 OD_{600} units/ml). In most cases, cells were directly fixed and processed for IF (see below). In the case of *neo1-ts* mutants, approximately 4 OD_{600} units of cells were transferred to prewarmed YPD medium of 37°C and incubated for determined times (30 min and 3 h for *neo1-37* cells, 1 h and 3 h for *neo1-69* cells) prior to fixation. The *sec7* cells were incubated in prewarmed YP medium containing 0.01% (w/v) glucose for 1 h at 37°C before fixation and processing for IF. BS1417 cells, which express an adenine analog-sensitive form of Prk1p were incubated either with 1NA-PP1 (4-amino-1-tert-butyl-3-(1'-naphthyl)pyrazolo[3,4-d]pyrimidine, 40 µM final concentration) for 5, 10, and 20 min to inhibit Prk1p, or with DMSO for 5 min before fixation and processing for indirect immunofluorescence.

Four OD_{600} units of cells were fixed for 4 h at room temperature in growth medium containing additionally 100 mM potassium phosphate buffer (KP_i, pH 6.5) (final concentration) and 4% formaldehyde (final concentration). Cells were harvested (5 min, 2000 rpm), washed three times with 1 ml sorbitol buffer (1.2 M sorbitol, 100 mM KP_i pH 6.5) and resuspended in 1 ml sorbitol buffer containing 20 mM β-mercaptoethanol. Cell walls were digested for 30 min at 30°C using Zymolyase 100T (Seigagaku Kyogo, Japan; 20 µg/ml final concentration). Spheroplasts were washed twice with 1 ml sorbitol buffer (5 min, 1000 rpm), resuspended in 400 µl sorbitol buffer and stored at 4°C for up to two days.

The fixed cells were labeled on 10-well immunofluorescence microscope slides (Polysciences, Inc.). Slides were coated with poly-L-lysine by placing 15μl of 1 mg/ml poly-L-lysine solution (in 10 mM NaN_3, stored at 4°C) in each well. After 1 min, the solution was aspirated and slides were allowed to dry. Each well was washed five times with 20 μl H_2O. Fixed cells (10-15 μl/well) were applied to the dried wells and allowed to settle for 15 min. The unbound cells were removed by washing three times with PBS-IF (53 mM Na_2HPO_4, 13 mM NaH_2PO_4, 75 mM NaCl). To reduce the unspecific binding of antibodies, cells were preincubated for 30 min in PBT (PBS-IF, 1% (w/v) BSA, 0.1% (w/v) Tween 20). PBT was aspirated and 10-15 μl of primary antibody diluted in PBT and centrifuged for 2 min at 13,000 rpm before use to pellet possible antibodies aggregates were applied. After a 1 h incubation in a humid chamber, each well was washed ten times with PBT. The secondary antibody diluted in PBT and centrifuged as described before was applied (10-15 μl/well) and incubated in the dark as described for the primary antibody. After washing each well with PBT and PBS (six times each), cells were covered with one drop of 99% glycerin for immunofluorescence (Fluka). Coverslips were sealed to the slides using nail polish and stored at 4°C in the dark for several days.

For the single staining of HA-epitope tagged proteins, the mouse monoclonal α-HA (16B12, Covance) was used as primary antibody (diluted to 1:1000, except for HA-Arl1p [1:8000] and HA-Sjl3p [1:2000]) and the indocarbocyanine (Cy3)-conjugated goat anti-mouse Fab fragment (Jackson ImmunoResearch) as secondary antibody (diluted to 1:1000).

Double indirect immunofluorescence was performed using the antibody combinations and concentrations given in Table I. GFP-Sec63p in *neo1-ts* mutants and GFP-Act1p in Δ*ark1*Δ*prk1* cells were directly observed with appropriate filter sets.

To observe GFP-tagged proteins by direct fluorescence, cells were grown at 25°C to early logarithmic phase (0.1-0.2 OD_{600} units/ml) in selective or complete SD medium. Transformants expressing GFP-Rer1p were transferred to 30°C and 37°C prewarmed SD medium and incubated for 1 h and for 2 h, respectively. The GFP-tagged proteins were viewed in the fluorescence microscope on cover slips coated with concanavalin A (for GFP-Rer1p) by spreading 5 μl/cm^2 of a 2.5 mg/ml concanavalin A solution or on Polysine™ slides (Menzel-Gläser, Germany) (for GFP-Chc1p) using the appropriate filter for GFP.

FM4-64 labeling was performed essentially as described by Jochum et al. (2002). After growth at 25°C to 0.2-0.3 OD_{600} units/ml in SD medium, 2 OD_{600} units of cells were harvested (5 min, 1000 rpm), resuspended in 100 μl SD medium and cooled on ice for 15 min. After addition of FM4-64 to 0.01 mM (final concentration), cells were incubated for 30

min at 0°C. Cells were harvested (10 sec, 13,000 rpm) and resuspended in 20 μl SD medium containing either 40 μM of 1NA-PP1 or DMSO. After 10 min of incubation at 25°C, cells were viewed under the fluorescence microscope using the appropriate filters for FM4-64 and GFP-Sjl2p.

Double staining	**First layer**	**Second layer**
HA-Neo1p/Ypt51p □	a. mouse anti-HA 1:1000 b. Alexa 488 anti-mouse 1:1000	a. rabbit anti-Ypt51p 1:100 b. Alexa 594 anti-rabbit 1:1000
HA-Neo1p/Pep12p □	a. rat anti-HA 1:100 b. Alexa 488 anti-rat 1:1000	a. mouse anti-Pep12p 1:100 b. Alexa 594 anti-mouse 1:1000
HA-Neo1p/60kDa v-ATPase □	a. rat anti-HA 1:100 b. Alexa 488 anti-rat 1:1000	a. mouse anti-60kDa 1:2000 b. Alexa 594 anti-mouse 1:2000
HA-Neo1p/Tlg1p-myc □	a. mouse anti-HA 1:1000 b. Alexa 594 anti-mouse 1:1000	a. rabbit anti-myc 1:300 b. Alexa 488 anti-rabbit 1:1000
HA-Neo1p/Tlg2p-myc □	a. mouse anti-HA 1:1000 b. Alexa 594 anti-mouse 1:1000	a. rabbit anti-myc 1:150 b. Alexa 488 anti-rabbit 1:1000
HA-Neo1p/Ypt1p □	a. rat anti-HA 1:100 b. Alexa 488 anti-rat 1:1000	a. mouse anti-Ypt1p 1:5 b. Alexa 594 anti-mouse 1:250
HA-Neo1p/GFP-Rer1p □	a. mouse anti-AFP 1:1000 b. Alexa 488 anti-mouse 1:1000	a. rat anti-HA 1:100 b. Alexa 594 anti-rat 1:1000
HA-Sjl2p/Ypt51p □	a. rabbit anti-Ypt51p 1:50 b. Alexa 488 anti-rabbit 1:1000	a. mouse anti-HA 1:1000 b. Cy3 anti-mouse 1:1000
myc-Sjl2p/GFP-Act1p □	a. rabbit anti-myc 1:100 b. Alexa 488 anti-rabbit 1:1000	a. mouse anti-GFP 1:50 b. Cy3 anti-mouse 1:1000
myc-Bsp1p/GFP-Act1p □	a. rabbit anti-myc 1:100 b. Alexa 488 anti-rabbit 1:1000	a. mouse anti-GFP 1:50 b. Cy3 anti-mouse 1:1000

Table I. Antibody combinations and concentrations used for double immunofluorescence.

2.2.3.4 Sucrose density gradient centrifugations

Sucrose density gradient centrifugations of total cell extracts of BS1285 cells transformed with GFP-Sec63p were performed according to Kölling and Hollenberg (1994) with the exception that a total of 14 fractions was collected.

2.2.3.5 Pulse-chase labeling and immunoprecipitation of HA-Neo1 proteins, HA-Ysl2p and CPY

The same protocol was used to analyze the stability of HA-Neo1 proteins (BS862, BS1001, BS993, BS64 expressing HA-Neo1p$^{\Delta Ctail}$) and of HA-Ysl2p (BS1121, BS1402, BS1233). Cells were grown overnight at 25°C in complete or selective SD medium to early logarithmic phase (0.1-0.3 OD_{600} units/ml). 5.6 OD_{600} units of cells (1 OD_{600} units/time point) were harvested and resuspended in 2.8 ml SD medium containing 50 mM KP_i (pH 5.7) and 2

mg/ml bovine serum albumin (BSA). After 15 min of preincubation at 25°C, 51 µl [^{35}S]-methionine (10 mCi/ml, Amersham, UK) were added to the culture and proteins were pulse-labeled for 30 min at 25°C. 500 µl of cells were removed (time point = 0) and the chase was induced by the addition of unlabeled methionine to 500 µg/ml (final concentration). Aliquots of cells (500 µl) were removed after 30, 60, 120, and 180 min of chase at either 25°C or 37°C and transferred to precooled tubes containing NaN_3 and NaF (10 mM final concentration, each). Cells were harvested (1 min, 13,000 rpm), washed with 1 ml 10 mM NaN_3 and resuspended in 100 µl lysis buffer (50 mM Tris/HCl pH 7.5, 1 mM EDTA/NaOH pH 8, 1 x CLAP). Glass beads (≈200 mg) were added and cells were lysed by vortexing for 1 min and cooling on ice for 1 min for five rounds. Proteins were solubilized in the presence of solubilization buffer (33 µl/sample) (4% (w/v) SDS, 600 mM NaCl, 50 mM Tris/HCl pH 7.5, 4 x CLAP) for 10 min at room temperature by rotating in an overhead shaker. Extracts were diluted with 1.2 ml IP buffer (1% (w/v) deoxycholic acid, 1% (w/v) Triton X-100, 150 mM NaCl, 50 mM Tris/HCl pH 7.5, 1 x CLAP) and centrifuged at 13,000 rpm at 4°C for 30 min. The supernatants (1.2 ml) were transferred to fresh Eppendorf tubes and incubated for 2 h at 4°C with 4 µl of anti-HA antibody (400 µg/ml, Roche). The proteins bound to anti-HA antibodies were incubated for 1 h at 4°C in the presence of 60 µl of a 1:3 slurry of Protein A-Sepharose beads. The Protein A-Sepharose beads were washed four times with 1 ml IP buffer and bound proteins were released in 65 µl SDS-PAGE sample buffer containing 9 M urea by incubation for 10 min at 50°C (Neo1 proteins) or in SDS-PAGE sample buffer (Ysl2p) for 5 min at 95°C. Twenty µl were separated by SDS-PAGE and proteins were detected by autoradiography and quantified with the phosphorimager.

Pulse-chase labeling and immunoprecipitation of carboxypeptidase Y (CPY) was performed as described previously (Singer-Krüger and Ferro-Novick, 1997).

2.2.3.6 Analysis of invertase glycosylation

To analyze the extent of glycosylation of invertase, cells (BS915, BS917, BS64, RH1737) were grown overnight in YP medium containing 5% (w/v) glucose to early logarithmic phase (0.1-0.3 OD_{600} units/ml). For each time point, 2.5 OD_{600} units of cells were harvested. Cells were washed twice with 50 ml H_2O and resuspended in YP medium containing 0.1% (w/v) glucose to 0.25 OD_{600} units/ml to derepress invertase. After 2 h at 30°C or 3 h at 37°C, 2.5 OD_{600} units of cells were harvested, washed with 5 ml 10 mM NaN_3, and resuspended in 20 µl lysis buffer (100 mM Tris/HCl pH 6.8, 10% (w/v) glycerol, 1 mM PMSF). Glass beads (≈50 mg) were added and cells were lysed by vortexing for 1 min and

cooling on ice for 1 min for six rounds. Lysates were diluted with 50 µl lysis buffer containing 0.01% (w/v) bromophenol blue and centrifuged for 15 min at 13,000 rpm at 4°C. For each sample, 7.5 µl were loaded per lane on native polyacrylamide gels (see Table II).

3 ml 1.5 M Tris/HCl pH 8.8
1.6 ml 30% acrylamide/0.8% bisacrylamide
7.4 ml H_2O
40 µl 10% (w/v) ammonium persulfate
7.9 µl N,N,N',N'-tetramethylethylenediamine(TEMED)

Table II. Composition of one native polyacrylamide gel.

Native polyacrylamide gels were run using a Tris/glycine buffer (25 mM Tris base, 200 mM glycine) until bromophenol blue reached the bottom of the gels (20 mA const., room temperature, ≈ 1.5 h). Gels were incubated in 80 ml 0.1 M saccharose/0.1 M sodium acetate/HCl (pH 4.9) for 20 min at 4°C and subsequently for 20 min at 37°C. After washing gels twice with 80 ml H_2O, 80 ml of chromophore solution (80 mg 2,3,5-triphenyltetrazolium chloride in 80 ml 0.5 M NaOH) was added and brought to boiling in the hood until the color developed (≈ 2 min). Gels were washed with H_2O and either directly dried or conserved in 10% (v/v) acetic acid.

2.2.3.7 ATPase activity assay of Neo1p

The first part of this assay included the isolation of Neo1p. Three aliquots of cells (see section 2.2.3.2) expressing either HA-Neo1p, HA-Neo1-37p, HA-Neo1-69p (BS862, BS1001, BS993, respectively) or no HA-tagged Neo1p (BS64) were lysed, extracted, and precleared by a 20 min centrifugation at 13,000 rpm as described (2.2.3.2) with the exception that the detergent conditions varied (for detail, see section 3.1.8 of the results). The affinity purification via antibodies directed against the HA-epitope was performed as described (2.2.3.5), but 6 µl of anti-HA antibody (Roche) per sample were used during an incubation of 1 h at 4°C. The Protein A-Sepharose beads were washed three times with 500 µl IP buffer and once with 500 µl ATPase assay buffer (10 mM Tris/HCl pH 8, 5 mM $MgCl_2$; detergent concentrations depended on the conditions chosen for the following ATPase assay). Triplicates of each condition were pooled and the Protein A-Sepharose beads (60 µl bed volume per condition) were resuspended in 240 µl ATPase assay buffer with or without detergent. Samples were split into five aliquots of 60 µl each (IP samples). Four aliquots were

used for the ATPase assay (see below). The fifth one was prepared for SDS-PAGE by resuspending the 12 μl bed volume of Protein A-Sepharose beads in 40 μl SDS-PAGE sample buffer containing urea. This sample was used to determine the levels of immunoprecipitated HA-Neo1p under different detergent conditions and the levels of immunoprecipitated HA-Neo1-37p, HA-Neo1-69p as compared to wild-type HA-Neo1p by immunoblotting (2.2.3.1).

In the second part of the ATPase assay, the immunoprecipitated proteins were incubated with ATP. To each 60 μl IP sample, 40 μl cold reaction mix [10 mM Tris/HCl pH 8, 5 mM $MgCl_2$, 5 mM NaN_3, 2 mM ATP (ATP disodium salt, Sigma), 5 mM phosphoenolpyruvate (Sigma) and 0.2 units of pyruvate kinase (Sigma)] were added on ice. The reaction mixes were either directly stopped on ice by the addition of 100 μl 10% (w/v) TCA (t = 0 min), or incubated for 2 h at 37°C (t = 120 min) and then stopped as described. To determine the protein-independent orthophosphate release, a reference sample (60 μl ATPase assay buffer + 40 μl reaction mix) was processed in parallel to the IP samples for each time point. Samples used to establish a standard curve (see below) were prepared by mixing 5 μl of Na_2HPO_4 solution containing 0, 0.2, 1, 2, 4, 6, 8, 10, or 12 nanomoles of Na_2HPO_4, 55 μl ATPase assay buffer and 40 μl reaction mix on ice. TCA was immediately added to 5% (w/v) (final concentration).

In the final part of the ATPase assay, the concentration of free orthophosphate was determined using a colorimetric assay. The TCA-containing samples were incubated on ice for at least 30 min and centrifuged for 5 min at 13,000 rpm at 4°C. Hundred μl of the supernatants were incubated with 750 μl of malachite green solution (0.033% (w/v) malachite green (Sigma), 1.03% (w/v) ammonium molybdate, 0.04% (w/v) Tween 40) and 50 μl 3 N H_2SO_4 at room temperature for 15 min. Extinction at 660 nm was immediately measured. A standard curve was generated by plotting the extinction value against the Na_2HPO_4 concentration of the standard probes and the concentration of free orthophosphate in the IP and reference samples was determined. For each time point (t = 0 and t = 120 min) the orthophosphate concentration generated in the reference sample was subtracted from that generated in the IP samples. The differences in free orthophosphate concentration between t = 0 and t = 120 min after the standard calculation were determined for each condition. These values were used to compare the efficiency of orthophosphate release by wild-type and mutant HA-Neo1 proteins under several detergent conditions.

2.2.3.8 Liposome floatation assay

[^{35}S]-methionine-labeled Bsp1p and Twf1p were transcribed and translated *in vitro* using a SP6 polymerase TnT^{TM} coupled transcription-translation system from a rabbit reticulocyte lysate (Promega) according to the manufacturer's instructions.

Liposomes were prepared with 1460 μg dioleoylphosphatidylcholine (DOPC, Avanti Polar Lipids) alone or with 1350 μg DOPC and 150 μg of one of the following phospholipids: phosphatidylinositol (PtdIns), phosphatidylinositol-4-phosphate (PtdIns(4)P), phosphatidylinositol-4,5-bisphosphate (PtdIns(4,5)P_2), phosphatidylserine (PS), phosphatidylethanolamine (PE), phosphatidic acid (PA), and phosphatidylglycerol (PG) (all Sigma, dissolved in chloroform). After being mixed in a glass tube, lipids were dried under a gentle N_2 stream, dissolved in 200 μl diethylether for 10 min at room temperature and dried again under N_2 in a water bath at 50°C by rapid swinging of the tube to obtain a regular film of lipids at the bottom of the tube. After 30 min under vacuum to eliminate traces of chloroform, lipids were incubated for at least 30 min at room temperature in 200 μl binding buffer (25 mM NaP_i pH 6.8, 150 mM NaCl). The suspension was homogenized in a water bath sonicator one or two times for 20 sec, until the solution became milky.

To allow the binding of Bsp1p or Twf1p to liposomes, 40 μl vesicles, 50 μl *in vitro* translated [^{35}S]-labeled Bsp1p or Twf1p and 110 μl binding buffer were mixed and incubated for 1 h at 30°C. For salt competition during binding, this mixture included 1 M NaCl (final concentration). 400 μl of 60% (w/v) sucrose were added to the reaction mix, which was transferred to an ultracentrifuged tube and overlaid with 3 ml 20% (w/v) sucrose and 200 μl binding buffer. After centrifugation at 164,000 x g for 4 h at 4°C in a SW-60 rotor (Beckman Instruments), five fractions (4 x 700 μl, 1 x 1 ml) were collected from the top of the gradient. Proteins were precipitated in the presence of 6% (w/v) TCA and 40 μg IgG, and analyzed by SDS-PAGE and autoradiography. Quantitation of [^{35}S]-labeled Bsp1p present in the top fraction, which contains the majority of liposomes, was performed with the phosphorimager.

3 Results

3.1 Characterization of wild-type and mutant Neo1 proteins and their interactions with Ysl2p and Arl1p

3.1.1 Neo1p interacts with Ysl2p *in vivo*

NEO1 was previously identified in the lab of B. Singer-Krüger as a high- and low-copy number suppressor of the temperature-sensitive (ts) growth and endocytic defects exhibited by Δ*ysl2* cells (see section 1.3.1.4). Here, I checked for an *in vivo* interaction between Neo1p and Ysl2p by co-immunoprecipitation. Ysl2p tagged C-terminally with the tandem affinity purification (TAP) epitope and Neo1p modified N-terminally with three copies of the influenza hemagglutinin (HA) epitope were functional, since cells expressing the tagged proteins exhibited normal growth (B. Singer-Krüger), while the Δ*neo1* mutation is lethal (Prezant et al., 1996) and the Δ*ysl2* mutant exhibits a growth defect (Jochum et al., 2002). Co-immunoprecipitation experiments were carried out using extracts of cells expressing either both TAP-Ysl2p and HA-Neo1p, or HA-Neo1p alone (control strain). TAP-Ysl2p assemblies were isolated from total cellular extracts by affinity purification via IgG-Sepharose and released from the matrix by the site-specific TEV protease (Rigaut et al., 1999). Immunoprecipitates were analyzed by immunoblotting using anti-Ysl2p and anti-HA antibodies (see section 2.1.4). As shown in Fig. 5A, HA-Neo1p was found in immunoprecipitates from TAP-Ysl2p expressing cells (lanes 5 to 8), but not in the control (lanes 1 to 4), suggesting that HA-Neo1p interacted specifically with Ysl2p *in vivo*. Furthermore, the association between TAP-Ysl2p and HA-Neo1p was well preserved after the second step of the tandem affinity purification (Rigaut et al., 1999) (Fig. 5B, lane 4).

Remarkably, the presence of 0.01% NP40 in the buffer during the co-immunoprecipitation enhanced the efficiency of the TAP-Ysl2p isolation as well as of the HA-Neo1p co-isolation as compared to conditions without detergent (Fig. 5A, lane 6 and 5, respectively). In contrast, higher detergent concentrations (0.02 and 0.04 % NP40) negatively affected the Ysl2p-Neo1p interaction (Fig. 5A, lane 7 and 8). To exclude the possibility of an interaction mediated via membranes including both proteins, TAP-Ysl2p assemblies were isolated from precleared cell lysates solubilized by 0.01% N40 and centrifuged for 1 h at 100,000 x g to pellet unsolubilized material. Comparison by immunoblot analysis of the amounts of Ysl2p and Neo1p present in the 100,000 x g supernatant to that in the pellet revealed that approximately 23% of Ysl2p and 18% of Neo1p were solubilized (Fig. 5C). As shown in Fig. 5D, the solubilized HA-Neo1p still co-purified specifically with TAP-Ysl2p, whereas two endosomal proteins, Pep12p and Ypt51p, were not detectable in the purified

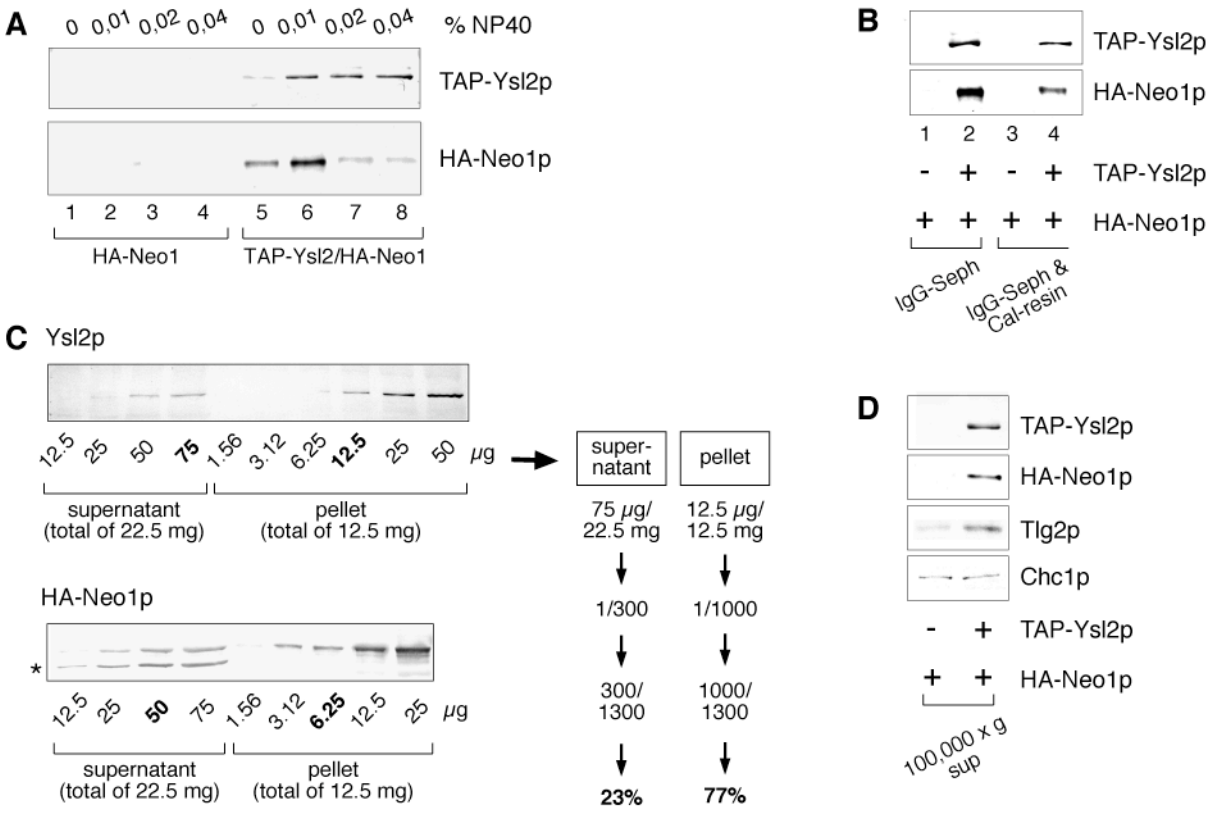

Fig. 5. Neo1p interacts with Ysl2p *in vivo*. (A) Co-immunoprecipitations were performed with lysates of cells expressing the indicated epitope-tagged proteins (lanes 1 to 4, BS862; lanes 5 to 8, BS912) in the absence (lane 1, 5) or the presence of NP40 (lanes 2 to 4 and 6 to 8; concentrations as indicated). Isolated proteins were separated by SDS-PAGE and detected by immunoblotting using rabbit anti-Ysl2p and mouse anti-HA antibodies. (B) Co-immunoprecipitations in the presence of 0.01% NP40 either after IgG-Sepharose (lane 1, 2) or after a second purification step using calmodulin resin (lane 3, 4). (C) Quantitation of Ysl2p (above) and HA-Neo1p (below) in the pellet and supernatant fractions after a 100,000 x g centrifugation of a solubilized (0.01% NP40) and precleared total cell lysate. Several quantities for each fraction were analyzed by SDS-PAGE and numbers in bold indicate the amounts in the pellet and supernatant, which are estimated to show an equivalent signal for Ysl2p or HA-Neo1p. The calculation of the percentage of Ysl2p found in each fraction is shown as example. * indicates a band unspecifically stained by the anti-HA antibody in the supernatant fraction. (D) Co-immunoprecipitation in the presence of 0.01% NP40 with a 100,000 x g supernatant. Samples were probed with anti-Ysl2p, anti-HA, anti-Tlg2p and anti-Chc1p antibodies described in section 2.1.4.

TAP-Ysl2p assemblies (data not shown). Under the same conditions of Ysl2p isolation, Tlg2p, a SNARE protein involved in recycling between endosomes and the late Golgi complex (see below), specifically co-purified with TAP-Ysl2p (Fig. 5D), although the interaction to Ysl2p was not as strong as that between Neo1p and Ysl2p. The heavy chain of clathrin (Chc1p), which is not located to endosomes, was found in equivalent amounts in both immunoprecipitates (Fig. 5D), indicating a nonspecific binding to the matrix and the presence of same quantities of proteins in the cell extracts of both strains. Together, these data indicated that the *in vivo* interactions of Ysl2p with Neo1p and also with Tlg2p are specific and are not mediated by membranes.

A two-hybrid analysis was performed to check for interactions between selected regions of Ysl2p and Neo1p. Since another Drs2p family member (Drs2p) and an Arf GEF

(Gea2p) have been found to interact directly via the Drs2p C-terminal tail and the Gea2p Sec7 domain (Chantalat et al., 2004), the corresponding domains in Neo1p and Ysl2p were chosen. The N-terminal region of Neo1p, which is cytosolic and is not related to the corresponding region of the other Drs2p family members, was also tested with the Sec7 domain of Ysl2p. No interaction was observed between the C-terminal tail of Neo1p and the Ysl2p Sec7 domain. Unfortunately, expression of the N-terminal region of Neo1p caused by itself the activation of both the lacZ and *HIS3* reporter genes, thereby making impossible the detection of an interaction with the Ysl2p Sec7 domain (data not shown). Thus, while the C-terminal tail of Neo1p appeared to not interact with the Sec7 domain of Ysl2p, the question of the binding of Neo1p to Ysl2p via its N-terminal domain remained open.

3.1.2 Neo1p localizes to endosomes and the Golgi complex

I next analyzed the intracellular localization of Neo1p by indirect immunofluorescence in a HA-Neo1p-expressing strain. While no signal was observed in an untagged strain (Fig. 6A), HA-Neo1p exhibited a punctate staining pattern over the entire cell (Fig. 6B). Spotted structures are characteristic both for endosomes and Golgi elements. To find out whether Neo1p localizes to one or both of these compartments, the HA-Neo1p distribution was examined in two mutants, which affect either the morphology of the endosomal compartment (*vps27*) or that of the Golgi complex (*sec7*). In *vps27* cells, HA-Neo1p was localized in a single, enlarged structure in proximity of the vacuole (Fig. 6C). This structure was reminiscent of the aberrant endosomal class E compartment formed in *vps27* cells by aggregation of the prevacuolar compartment (Piper et al., 1995). Upon incubation of temperature-sensitive *sec7* cells to 37°C in the presence of 0.1% glucose, aberrant Golgi structures are formed, which contain Golgi marker proteins (Segev et al., 1988). As shown in Fig. 6D, HA-Neo1p staining pattern was affected in the *sec7* mutant. Together, these results suggested that Neo1p may localize to both endosomal and Golgi compartments.

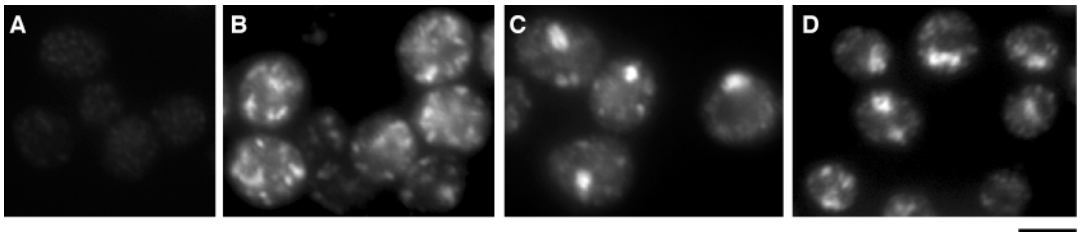

Fig. 6. HA-Neo1p localizes to punctate structures that are sensitive to mutations in *VPS27* and *SEC7*. (A-C) Cells lacking HA-Neo1p (A, BS64), wild-type cells expressing HA-Neo1p (B, BS862) and *vps27* cells expressing HA-Neo1p (C, BS1088) were grown at 25°C, fixed, and stained by indirect immunofluorescence with a monoclonal mouse anti-HA antibody as described in section 2.2.3.3. (D) *sec7* cells expressing HA-Neo1p (BS1383) were grown at 25°C and shifted for 1 h to 37°C in YP medium containing 0.1% glucose to induce the mutant phenotype. Cells were stained as in A. Bar, 5 μm.

To determine more precisely the subcellular localization of HA-Neo1p, double indirect immunofluorescence was performed with endosomal and Golgi marker proteins. The small GTPase Ypt51p regulates endocytic trafficking between early and late endosomes and localizes to both endocytic organelles (Singer-Krüger et al., 1995; Mulholland et al., 1999). Pep12p, Tlg1p, and Tlg2p represent endosomal t-SNAREs with a distinct localization (Lewis et al., 2000). Pep12p is present mainly at the prevacuolar compartment and regulates membrane transport between the Golgi complex and the vacuole (Becherer et al., 1996; Prescianotto-Baschong and Riezman, 2002). Tlg1p and Tlg2p are suggested to function in recycling between early endosomes and the late Golgi complex and localize to both compartments, with a prominence of Tlg1p on early endosomes and of Tlg2p on late Golgi structures (Abeliovich et al., 1998; Holthuis et al., 1998; Lewis et al., 2000).

Consistent with the results obtained in *vps27* and *sec7* cells, the staining patterns of HA-Neo1p and all four endosomal/late Golgi proteins were quite similar (Fig. 7A-D). The degree of colocalization of Neo1p with each marker protein was quantified by counting the total number of Neo1p-positive spots (= 100%) and determining how many of these spots contained the respective marker protein. This revealed that at least 48% of Neo1p colocalized with Pep12p (n = 1109), 35% with Ypt51p (n = 559), 54% with myc-Tlg1p (n = 611), and 40% with myc-Tlg2p (n = 685). Some Neo1p-positive spots were found in proximity of the vacuoles (Fig. 7E), similar to what has been observed for Ypt51p at the ultrastructural level (Mulholland et al., 1999). In cells expressing Ypt51Q66L, a point mutant with higher affinity

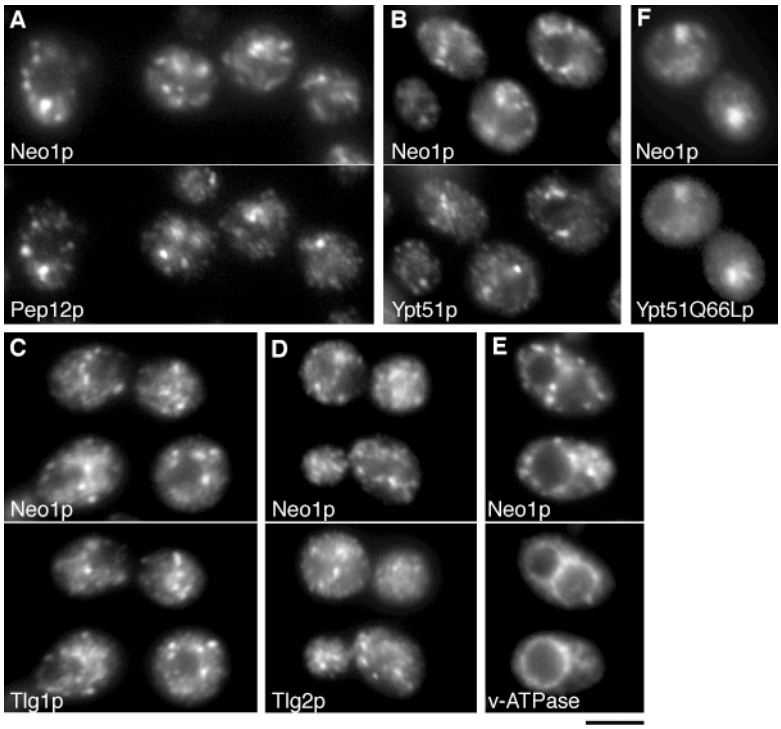

Fig. 7. HA-Neo1p colocalizes with endosomal/late Golgi markers. (A-F) Double immunofluorescence in cells expressing HA-Neo1p (BS862) (A, B, E) and in BS862 transformants expressing myc-Tlg1p (C), myc-Tlg2p (D), or Ypt51Q66L (F). Cells were grown at 25°C, fixed and stained with an anti-HA antibody to detect HA-Neo1p and either anti-Pep12p (A), anti-Ypt51p (B,F), rabbit anti-myc (C,D), or anti-60 kDa V-ATPase subunit (E) antibodies. Dilutions of the antibodies are described in section 2.2.3.3. Bar, 5 μm.

for GTP, which causes the formation of unusually large endosomes (Singer-Krüger et al., 1995), the Neo1p-positive structures were enlarged and less numerous. Under these conditions, the degree of colocalization of Neo1p with Ypt51p increased to at least 69% (Fig. 7F; n = 77).

In contrast to the large extent of colocalization with endosomal/late Golgi proteins, very little overlap was observed between the staining pattern of Neo1p and that of two early Golgi markers. Only 10% of Neo1p-positive spots coincided with that of Ypt1p (Fig. 8A; n = 990), a small GTPase found within the *cis* and *medial* Golgi complex (Segev et al., 1988), and 8% with that of GFP-Rer1p (Fig. 8B; n = 538), a retrieval receptor for endoplasmic reticulum (ER) membrane proteins, which is localized to the *cis* Golgi complex (Sato et al., 2001). Thus, the fraction of Neo1p, which is sensitive to the *sec7* mutation, most probably localizes to the late Golgi complex.

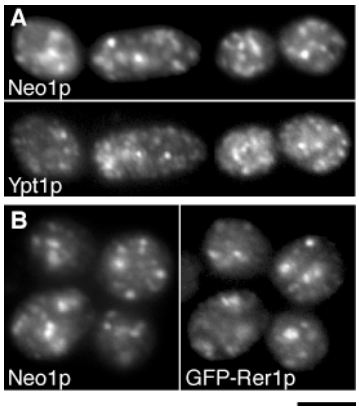

Fig. 8. HA-Neo1p does not colocalize with early Golgi markers. (A,B) Double immunofluorescence in cells expressing HA-Neo1p (BS862) (A) and in BS862 transformants expressing GFP-Rer1p (B) was performed as described in Fig. 7. Cells were stained with anti-HA to detect HA-Neo1p and either anti-Ypt1p (A) or anti-AFP (B) antibodies. Dilutions of the antibodies used are described in section 2.2.3.3. Bar, 5 μm.

Together, the localization studies clearly demonstrated that the major fraction of Neo1p is present both on early and late endosomal structures, while a smaller fraction associates with the late Golgi complex.

3.1.3 The temperature-sensitive *neo1-37* and *neo1-69* mutants are defective in vacuolar protein sorting, but not in normal secretion

To investigate the function of Neo1p in membrane trafficking, temperature-sensitive alleles of *NEO1* were generated by low fidelity PCR (B. Singer-Krüger). Two of these mutants, *neo1-37* and *neo1-69*, which grew similar to the wild type at 25°C and 30°C, but were temperature-sensitive (ts) at 37°C, were further characterized. These mutants were found by analyses of the □-factor induced degradation of the pheromone receptor Ste2p and of the uptake of the endocytic fluid phase marker Lucifer Yellow to exhibit a defect in the endocytic

transport from endosomes to the vacuole already at permissive temperature (B. Singer-Krüger).

Since most of the newly synthesized vacuolar proteins are delivered from the *trans*-Golgi network (TGN) to the vacuole (see Fig. 1) via endosomes, I tested whether the endocytic defect exhibited by the *neo1-ts* mutants impaired the vacuolar delivery of the hydrolase carboxypeptidase Y (CPY). The sorting of pulse-labeled CPY was compared between the *neo1-ts* mutants and wild-type cells under conditions that block endocytosis (30°C). CPY is synthesized in the ER in the p1 form and modified by N-linked glycosylation within the ER and the Golgi complex to form p2CPY. This form is transported to the vacuole, where it is proteolytically processed to the mature form (mCPY).

In wild-type cells, most of p1CPY synthesized during a 5 min pulse with [^{35}S]-methionine was modified to p2CPY within 5 min of chase. After 25 min of chase, all of this labeled CPY was found in its mature form (Fig. 9, lane 1 to 4). In comparison, both *neo1-ts* mutants exhibited a delay in CPY processing. In *neo1-69*, and more markedly in *neo1-37* cells, p1CPY persisted longer. Furthermore, after 25 min of chase only 52%/45% of total CPY were mature in *neo1-37*/*neo1-69* cells, respectively. Analysis of the medium fraction of the samples revealed that 8%/15% of total CPY were missorted in the p2 form to the extracellular space (*neo1-37*/*neo1-69*). In conclusion, the defects in the processing and sorting of the Golgi-modified p2CPY were consistent with a role of Neo1p in protein trafficking within the late Golgi/endosomal system.

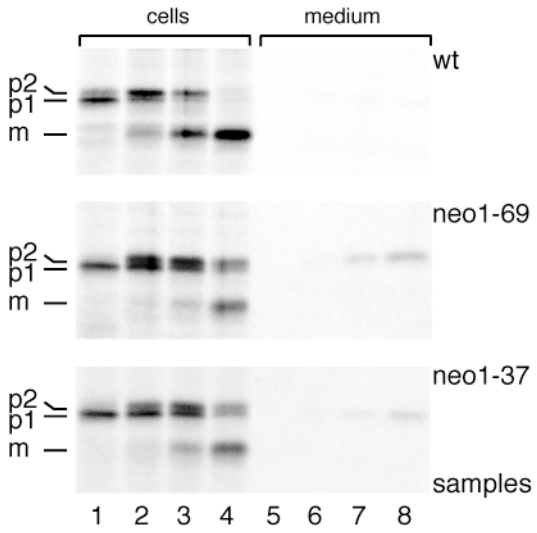

Fig. 9. *neo1-ts* mutants exhibit a delay in CPY processing and missort the Golgi-modified form of CPY to the extracellular space. Wild-type (BS64), *neo1-69* (BS917), and *neo1-37* (BS915) cells were labeled for 5 min at 30°C with [^{35}S]-methionine (lane 1 and 5). After the addition of an excess of nonlabeled methionine, cells were chased at 30°C for 5 min (lane 2 and 6), 10 min (lane 3 and 7), and 25 min (lane 4 and 8). For each sample, the medium (lanes 5 to 8) was separated from the cells, and cells were converted to spheroplasts (lanes 1 to 4). CPY was isolated from spheroplasts and the medium fractions by immunoprecipitation and analyzed by SDS-PAGE and autoradiography. p1, ER form; p2, Golgi form; m, mature form.

Although my studies clearly suggested a localization of Neo1p to endosomal and late Golgi structures, another group recently proposed a distribution and a role for Neo1p in transport between the ER and the *cis* Golgi complex (Hua and Graham, 2003). Therefore, I

also addressed the question of whether the early secretory pathway was impaired in the *neo1-37* and *neo1-69* mutants. I monitored the glycosylation of the well-characterized invertase in both *neo1-ts* mutants as compared to wild type. After derepression of invertase by low concentrations of glucose, newly synthesized invertase is core-glycosylated in the ER, transferred to the Golgi complex, where it becomes fully glycosylated (Esmon et al., 1981), and is secreted to the cell surface. Previous studies in the lab of B. Singer-Krüger indicated that at permissive temperature invertase was secreted at similar rates in *neo1-ts* mutants and wild type. Here, I also could show that both *neo1* mutants exhibited fully glycosylated internal invertase after derepression for 2 h at 30°C (Fig. 10A). This was in contrast to *sec18* cells incubated at 37°C, in which internal invertase was highly underglycosylated, consistent with a transport block from the ER to the Golgi complex observed in this strain (Novick et al., 1980). When invertase derepression was conducted in the *neo1-ts* mutants at 37°C, a slight fraction of internal invertase was found to be incompletely glycosylated (Fig. 10A, 37°C). Thus, under the nonpermissive conditions it appears that the *neo1-ts* mutants exhibit a slight defect in the secretory pathway, consistent with the delay in processing of p1CPY to p2CPY previously observed (see Fig. 9).

I also studied the localization of Rer1p, a protein mediating the retrieval of ER membrane proteins from the *cis* Golgi complex back to the ER (Sato et al., 2001). A block in the anterograde transport from the ER to the Golgi complex causes the retention of GFP-Rer1p within the ER, while a defect in the retrograde transport towards the ER results in the

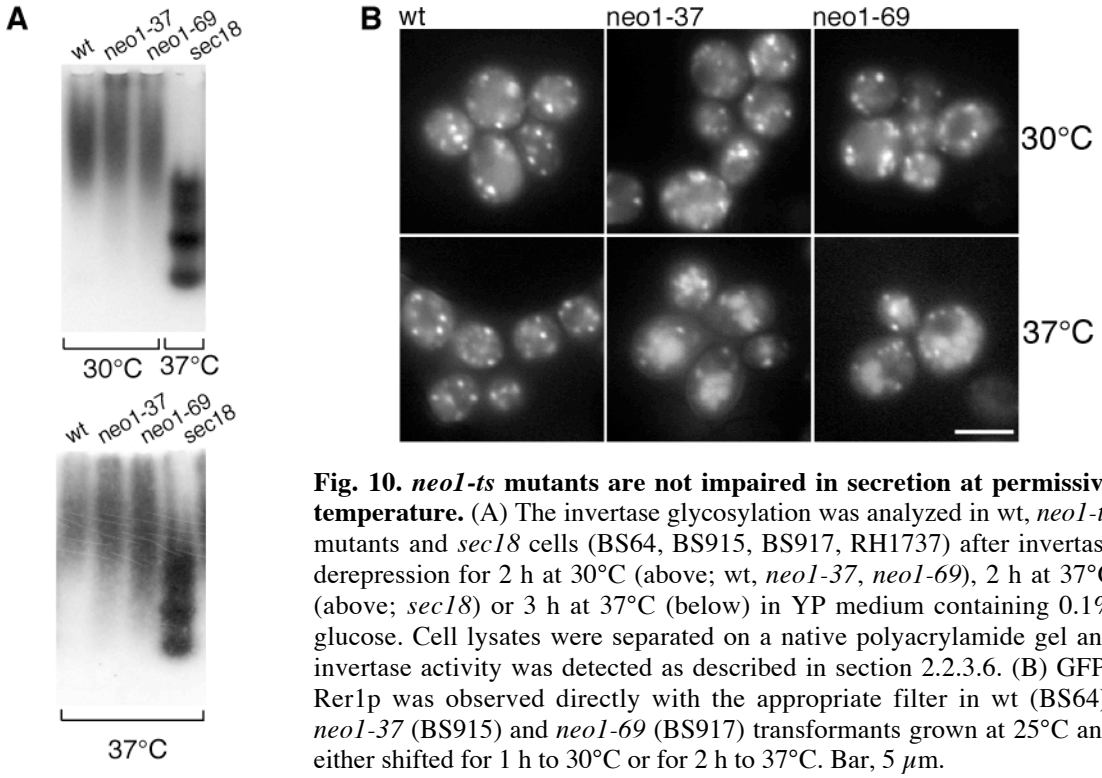

Fig. 10. *neo1-ts* mutants are not impaired in secretion at permissive temperature. (A) The invertase glycosylation was analyzed in wt, *neo1-ts* mutants and *sec18* cells (BS64, BS915, BS917, RH1737) after invertase derepression for 2 h at 30°C (above; wt, *neo1-37*, *neo1-69*), 2 h at 37°C (above; *sec18*) or 3 h at 37°C (below) in YP medium containing 0.1% glucose. Cell lysates were separated on a native polyacrylamide gel and invertase activity was detected as described in section 2.2.3.6. (B) GFP-Rer1p was observed directly with the appropriate filter in wt (BS64), *neo1-37* (BS915) and *neo1-69* (BS917) transformants grown at 25°C and either shifted for 1 h to 30°C or for 2 h to 37°C. Bar, 5 μm.

mislocalization of GFP-Rer1p to the vacuole (Sato et al., 2001). At permissive temperature, GFP-Rer1p localized to punctate structures typical for the Golgi complex in *neo1-ts* and wild-type cells (Fig. 10B, 30°C). However, incubation for 2 h at 37°C resulted in some mislocalization of GFP-Rer1p to the fragmented vacuole of both *neo1-ts* mutants, while in wild type the GFP-Rer1p staining remained unaffected (Fig. 10B, 37°C, and Hua and Graham, 2003).

In summary, the *neo1-ts* mutants were shown to display defects in vacuolar protein sorting already at permissive temperature, consistent with a role of wild-type Neo1p in protein trafficking within the late Golgi/endosomal system. In contrast, defects in anterograde and retrograde protein trafficking within the secretory pathway were observed only after incubations at 37°C and could therefore be caused by indirect effects (see below).

3.1.4 Localization and stability of the temperature-sensitive Neo1p mutants

To investigate the potential cause of the transport defects observed in the *neo1-ts* mutants, I next studied the localization of HA-Neo1-69p and HA-Neo1-37p by indirect immunofluorescence. At 25°C, HA-Neo1-69p localized to punctate structures similar to those containing wild-type Neo1p (Fig. 11A, 25°C). To verify that these structures were of endosomal nature, HA-Neo1-69p was expressed in *vps27* cells, in which the aberrant endosomal class E compartment is formed by the aggregation of the prevacuolar compartment (Piper et al., 1995). Similar to what has been observed for the wild-type HA-Neo1p in *vps27* cells (see Fig. 6C), the HA-Neo1-69p-positive spots were found to collapse into single, enlarged structures reminiscent of the class E compartment (Fig. 11B), indicating that HA-Neo1-69p indeed localized to endosomes at 25°C. At 37°C, the HA-Neo1-69p mutant polypeptide relocalized to less numerous and large, brightly stained spots (Fig. 11C, 37°C, 60 min) and after a longer shift to 37°C accumulated mostly in tubular structures (Fig. 11C, 37°C, 3 h) with a small fraction remaining on faint punctate structures.

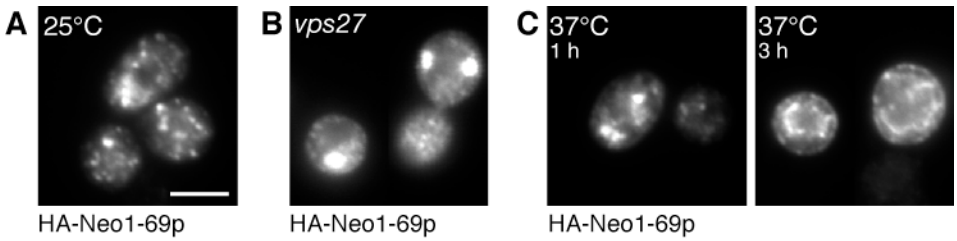

Fig. 11. HA-Neo1-69p localizes to endosomes at permissive temperature. (A, C) Indirect immunofluorescence in cells expressing HA-Neo1-69p (BS993). Cells were fixed directly after growth at 25°C (A) or after shift to 37°C for the indicated times (C), and stained with an anti-HA antibody. (B) HA-Neo1-69p in the *vsp27* strain (BS1383), in which the endosomes collapsed into the enlarged class E compartment. Cells were fixed after growth at 25 °C and processed as in A. Bar, 5 μm.

In contrast to HA-Neo1-69p, the localization of HA-Neo1-37p was clearly distinct from that of wild-type Neo1p already at permissive conditions. Instead of showing a punctate staining pattern, HA-Neo1-37p localized to tubulo-reticular structures situated along the cell periphery as well as more intracellularly (Fig. 12A, 25°C). This staining pattern is typical of the ER (see below). Shifting mutant cells to 37°C resulted in the rapid formation of intensely stained clumps within the reticular network (Fig. 12A, 37°C, 30 min). Longer incubations at the nonpermissive temperature caused HA-Neo1-37p to further accumulate in these structures, leading apparently to the deformation of tubulo-reticular to thicker bar-like structures (Fig. 12A, 37°C, 3 h).

To find out whether the reticular network stained by HA-Neo1-37p corresponded to ER membranes, mutant cells were transformed with a plasmid carrying GFP-Sec63p, a component of the ER translocon (Deshaies et al., 1991). GFP-Sec63p, detected by autofluorescence, colocalized largely with HA-Neo1-37p, indicating that the mutant protein accumulated within ER membranes already at 25°C (Fig. 12B). As expected, no signal match was observed between GFP-Sec63p and HA-Neo1-69p, since at 25°C HA-Neo1-69p still localized to endosomes (see Fig. 11B). As an additional test to determine the localization of HA-Neo1-37p, subcellular fractionation of a cell lysate using a sucrose density gradient

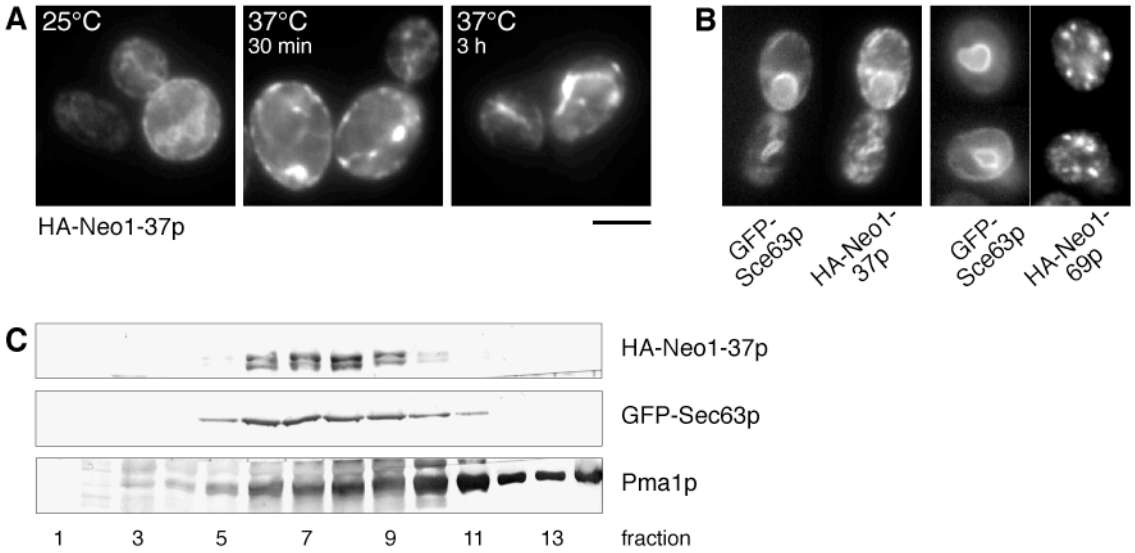

Fig. 12. HA-Neo1-37p is retained in the ER (A, B) Indirect immunofluorescence in cells expressing HA-Neo1-37p (A, BS1001) or in transformants expressing either HA-Neo1-37p (BS1285) or HA-Neo1-69p (BS1286) and carrying the GFP-Sec63p plasmid (B). Cells were fixed directly after growth at 25°C (A, 25°C; B) or after shift to 37°C for the indicated times (A), and stained with an anti-HA antibody. GFP-Sec63p was observed directly with the appropriate filter. Bar, 5 μm. (C) Subcellular fractionation of a cell lysate on a sucrose density gradient. BS1285 transformants carrying the GFP-Sec63p plasmid grown at 25°C were lyzed and subjected to sucrose density gradient fractionation as described in section 2.2.3.4. 14 fractions were collected from the top of the gradient and analyzed by immunoblotting for HA-Neo1-37p, the ER marker GFP-Sec63p and the plasma membrane Pma1p. Antibodies used are indicated in section 2.1.4.

centrifugation was performed. In the gradient, HA-Neo1-37p cofractionated with GFP-Sec63p, but not with the plasma membrane H^+-ATPase, Pma1p, which peaked in denser fractions (Fig. 12C). This indicated that the peripheral membranes stained by HA-Neo1-37p also represented ER membranes and not portions of the plasma membrane. At 37°C, the auto- and the immunofluorescence signal of GFP-Sec63p was lost, thereby preventing the simultaneous detection of mutant Neo1 proteins and GFP-Sec63p. However, since Neo1-37p failed to leave the ER already at permissive temperature, it is most likely that this defect was enhanced at nonpermissive conditions, consistent with the apparent aggregation of the mutant polypeptide (see Fig. 12A, 37°C). A substantial fraction of HA-Neo1-69p also accumulated in the ER at nonpermissive temperature, as suggested by the reticular staining pattern of HA-Neo1-69p after 3 h of incubation at 37°C (see Fig. 11A, 37°C, 3 h).

The retention of the mutant Neo1 proteins in the ER could be due to the ER quality control machinery. It was therefore possible that the Neo1-ts polypeptides were degraded more rapidly than the wild-type Neo1p. To test this possibility, the stability of the wild-type and mutant Neo1 proteins was determined by pulse-chase experiments. After pulse-labeling with [^{35}S]-methionine for 30 min at 25°C, the chase was performed at either 25°C or 37°C. At 25°C, HA-Neo1-69p was similarly stable as wild-type HA-Neo1p ($t_{1/2}$ = 257 min) with an estimated $t_{1/2}$ of 226 min, while HA-Neo1-37p was rapidly degraded with a $t_{1/2}$ of approximately 36 min (Fig. 13A). At 37°C, the stability of Neo1-69p was still comparable to that of wild-type HA-Neo1p ($t_{1/2}$ of 100 min and 90 min, respectively) (Fig. 13A). In contrast, the half-life time of HA-Neo1-37p was further decreased to 26 min (Fig. 13A).

The reduced stability of Neo1-37p was consistent with its localization to the ER. Neo1-69p, which appeared to be retained in the ER at nonpermissive temperature, exhibited a similar half-life time as wild type, but analysis at steady-state conditions in cell lysates (25°C and 37°C) revealed that the expression levels of HA-Neo1-69p were reduced to 50% of the wild-type HA-Neo1p levels (Fig. 13B and data not shown). In agreement with the results by pulse-chase, the HA-Neo1-37p steady-state levels represented only 25% of that of wild-type HA-Neo1p. The three lysates exhibited similar protein concentrations, since the amounts of a cytosolic protein, the phosphoglycerate kinase (PGK), were comparable in the three strains (Fig. 13B).

Altogether, the studies of the localization and stability of Neo1-ts proteins revealed that at permissive conditions Neo1-37p is retained within the ER, where it is rapidly degraded, while Neo1-69p exhibits a localization similar to that of wild-type Neo1p and is more stable than Neo1-37p.

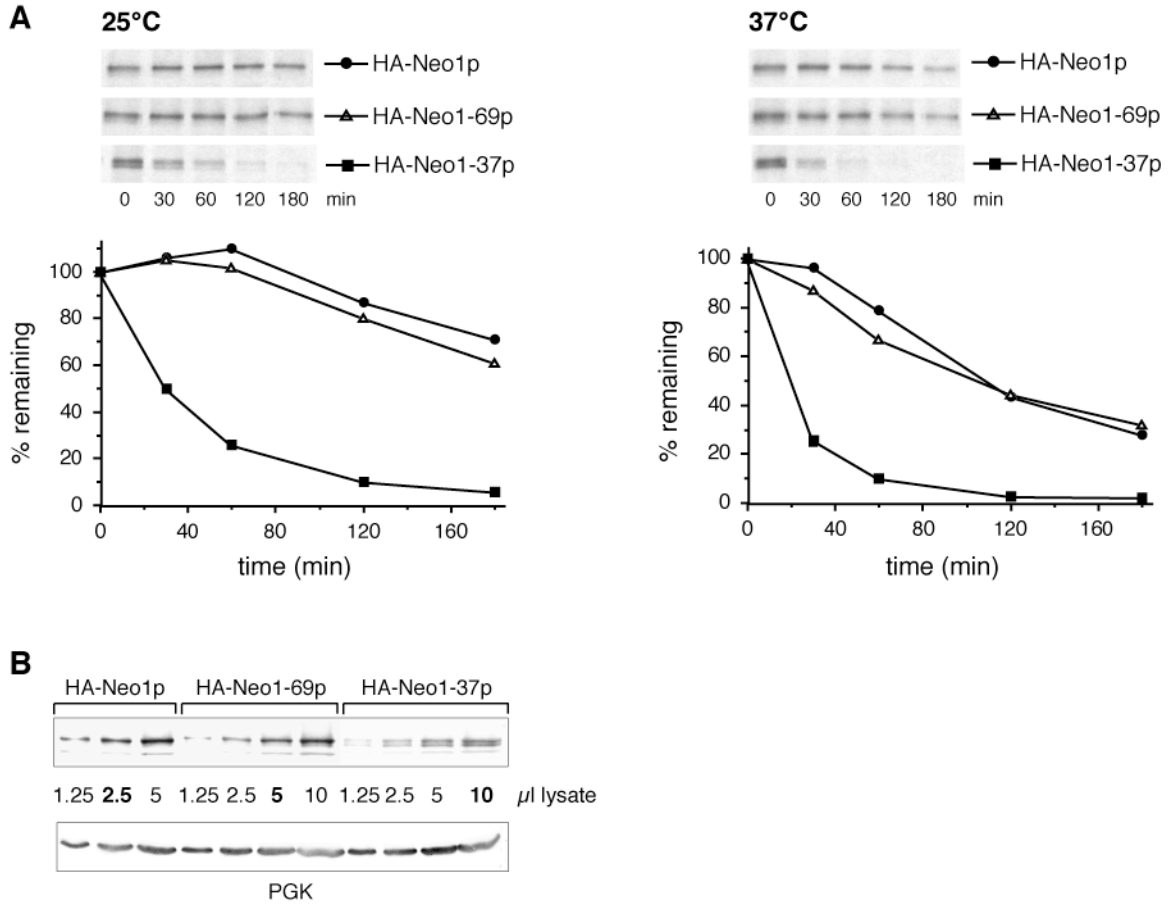

Fig. 13. Stability of Neo1-ts mutant proteins. (A) Cells expressing wild-type HA-Neo1p (BS862), HA-Neo1-37p (BS1001) or HA-Neo1-69p (BS993) were labeled with [^{35}S]-methionine for 30 min at 25°C and chased at either 25°C or 37°C for the indicated times. Aliquots were removed and Neo1 proteins were isolated by immunoprecipitation using an anti-HA antibody as described in section 2.2.3.5. HA-Neo1 protein levels were quantified with the phosphorimager and expressed as percentages of the level of labeled protein at the 0 min chase point. (B) Cells expressing wild-type HA-Neo1p, HA-Neo1-37p or HA-Neo1-69p (see A) were grown at 25°C and disrupted by alkaline lysis as described in section 2.2.3.1. Different amounts of each lysate were separated by SDS-PAGE and immunodetected for HA-Neo1 proteins and for the phosphoglycerate kinase (PGK) as control. Volumes of lysates estimated to exhibit an equivalent signal for each of the three Neo1 proteins are indicated in bold.

3.1.5 Neo1-69p affects the subcellular distribution of HA-Arl1p

The group of B. Singer-Krüger found that Ysl2p interacts genetically and physically with Arl1p, a small GTPase that could possibly be grouped with the Arf family based on sequence and structural homologies (Jochum et al., 2002; Pasqualeto et al., 2002). Because Ysl2p also revealed homologies to the Sec7 family Arf GEFs, it has been proposed that Ysl2p may represent a GEF for Arl1p (Jochum et al., 2002). B. Singer-Krüger found that the presence of *ARL1* was essential for the suppression of Δ*ysl2* cells by *NEO1*. She also showed that the deletion of *ARL1* rescued the growth at 37°C of *neo1-ts* cells and that the both myristoylated and GTP-bound form of Arl1p was harmful in the context of *neo1* mutants. In this work, I studied the localization of C-terminally HA-tagged Arl1p in the *neo1-ts* mutants

by indirect immunofluorescence. In most wild-type cells HA-Arl1p revealed a diffuse cytoplasmic staining pattern, consistent with the observation that Arl1p is predominantly soluble, and a very faint punctate pattern, probably representing the fraction of Arl1p associated with the Golgi complex and/or endosomal elements (Lee et al., 1997) (Fig. 14, wt). Only 8 % of wild-type cells (n=283) exhibited distinct punctate structures. In a significantly increased number of *neo1-69* cells (25%, n=318), the punctate HA-Arl1p structures appeared brighter and larger than in the wild type and were clearly separated from the diffuse background (Fig. 14, neo1-69, 25°C). After incubation at 37°C and in *neo1-37* cells, the HA-Arl1p staining pattern was similar to that in the wild type (Fig. 14), revealing that Arl1p apparently redistributed to bigger structures uniquely in *neo1-69* cells and surprisingly only under permissive conditions. These data suggested that the Arl1p localization may be affected uniquely under conditions at which Neo1-69p still localizes to endosomes.

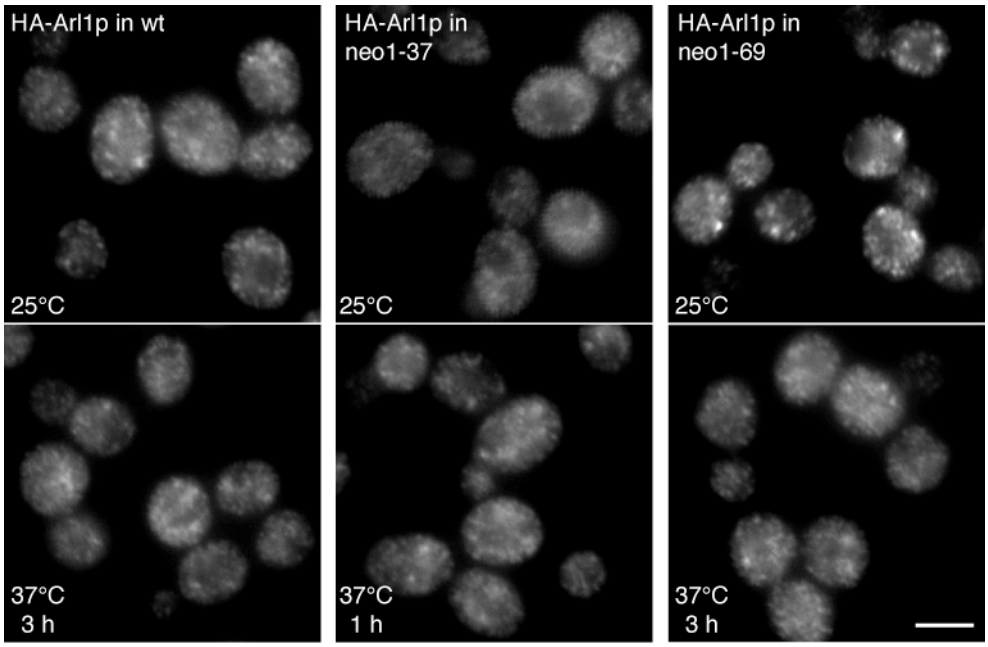

Fig. 14. HA-Arl1p localization in *neo1* mutants. Wt, *neo1-37* and *neo1-69* cells expressing HA-Arl1p (BS1279, BS1282, BS1283) were fixed directly after growth at 25°C or after shift to 37°C for the indicated times. Cells were stained by indirect immunofluorescence with an anti-HA antibody as described in section 2.2.3.3. Bar, 5 μm.

3.1.6 HA-Ysl2p localization and stability are affected in the *neo1* mutants

Because Arl1p localization was found to be affected in *neo1-69* cells, I next analyzed the effect on the distribution of Ysl2p. In wild-type cells, a functional C-terminally triple HA-tagged version of Ysl2p (HA-Ysl2p) exhibited a faint punctate staining pattern (Fig. 15, wt), consistent with the previously established endosomal localization of Ysl2p (Jochum et al., 2002). However, in the *neo1-69* mutant at 25°C, most cells (81%, n = 182) exhibited a diffuse

background staining (Fig. 15, neo1-69, 25°C) similar to that observed in an untagged control strain (Fig. 15, control). This suggested that the total levels of HA-Ysl2p were reduced in *neo1-69* cells. In the remaining 19% of the cells, the HA-Ysl2p-positive spots were brighter and larger than in the wild type, possibly indicating an abnormal association of Ysl2p with membranes. After incubation at 37°C, *neo1-69* cells exhibited either larger HA-Ysl2p-positive structures or a background staining, similar to the observed phenotypes at permissive conditions. In contrast, the HA-Ysl2p staining pattern was unaffected in *neo1-37* cells (Fig. 15, neo1-37).

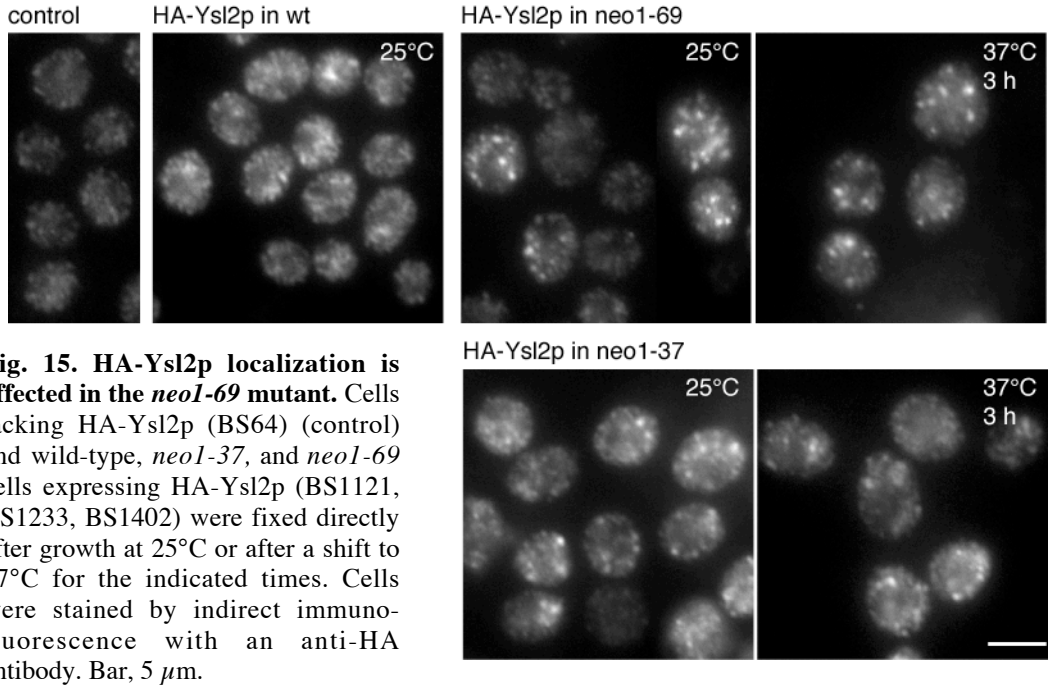

Fig. 15. HA-Ysl2p localization is affected in the *neo1-69* mutant. Cells lacking HA-Ysl2p (BS64) (control) and wild-type, *neo1-37,* and *neo1-69* cells expressing HA-Ysl2p (BS1121, BS1233, BS1402) were fixed directly after growth at 25°C or after a shift to 37°C for the indicated times. Cells were stained by indirect immunofluorescence with an anti-HA antibody. Bar, 5 μm.

The stability of Ysl2p was determined in *neo1-ts* mutants and compared to wild type by pulse-chase labeling and in total cellular extracts. Whereas [^{35}S]-labeled HA-Ysl2p exhibited a similar stability in the *neo1-ts* mutants ($t_{1/2}$ = 195/208 min in *neo1-37*/*neo169*, respectively) as compared to wild type ($t_{1/2}$ = 235 min) (Fig. 16A), in total cell extracts the levels of HA-Ysl2p were reduced to 50%/75% of the wild-type levels in *neo1-69*/*neo1-37* cells (Fig. 16B). Thus, HA-Ysl2p levels appeared to be affected in both mutants with a more profound effect in the *neo1-69* cells.

The appearance of brightly stained structures containing HA-Ysl2p in *neo1-69* cells could indicate that this HA-Ysl2p may be abnormally associated with membranes. To examine this possibility, I determined the levels of Ysl2p present in the pellet and the supernatant fractions of precleared total cellular lysates prepared from wild-type and *neo1-69* cells. At permissive temperature in wild type, 29% of HA-Ysl2p were present in the

supernatant fraction, while in *neo1-69* cells only 11% of Ysl2p was soluble (Fig. 16C). After incubation at 37°C, soluble HA-Ysl2p was further reduced in the mutant to 8.6% of total Ysl2p. These data supported the idea that HA-Ysl2p may be more membrane-associated in *neo1-69* cells than in the wild type.

Altogether, Ysl2p appears to be less stable and more membrane-associated in *neo1-69* cells as compared to the wild type. In *neo1-37* cells, the localization of Ysl2p seems to be unaffected, but the total levels of Ysl2p are slightly reduced.

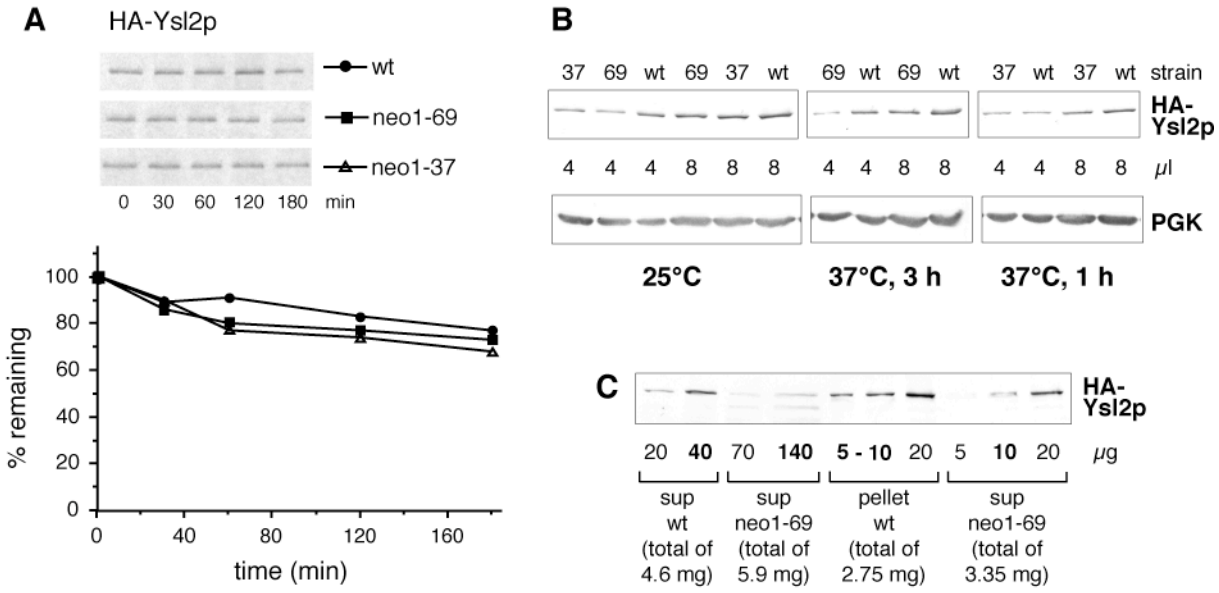

Fig. 16. Ysl2p stability and membrane-association in the *neo1* mutants. (A) Wt, *neo1-37*, and *neo1-69* cells expressing HA-Ysl2p (BS1121, BS1233, BS1402) were labeled with [^{35}S]-methionine for 30 min and chased at 25°C for the indicated times. Aliquots were removed and HA-Ysl2p was isolated by immunoprecipitation using an anti-HA antibody (2.2.3.5). HA-Ysl2p levels were quantified with the phosphorimager and expressed as percentages of the level of labeled protein at the 0 min chase point. (B) Lysates of cells (see A) grown at 25°C with or without an additional shift to 37°C for the indicated times were prepared by alkaline lysis (see section 2.2.3.1). Several amounts of each lysate were separated by SDS-PAGE and immunodetected for HA-Ysl2p and for the phosphoglycerate kinase (PGK) as control. Levels of HA-Ysl2p were compared between strains. wt, wild-type; 69, *neo1-69*; 37, *neo1-37* cells. (C) Wild-type and *neo1-69* cells expressing HA-Ysl2p (BS1121, BS1402) grown at 25°C were lyzed with glass beads. The lysates were precleared by centrifugation at 13,000 rpm prior to centrifugation at 100,000 x g for 1 h as described in section 2.2.3.1. Several amounts of the supernatant and pellet fractions were analyzed by SDS-PAGE and immunoblotting using an anti-HA antibody. Amounts of the 100,000 x g pellet and supernatant fractions estimated to exhibit an equivalent amount of Ysl2p in a given strain are indicated in bold. The percentage of Ysl2p present in each fraction was calculated as described in Fig. 5C.

3.1.7 Modifications of the Neo1p C-terminal tail affect the localization and stability of Neo1p

In contrast to the N-terminally tagged Neo1p used in this study, a version of Neo1p tagged C-terminally with a 13-myc epitope was recently shown to reside on the ER and on *cis/medial* Golgi membranes (Hua and Graham, 2003). Independently, B. Singer-Krüger

found that a C-terminally HA-tagged version of Neo1p (Neo1p-C-HA) was nonfunctional, since Neo1p-C-HA was not able to complement the lethality of Δ*neo1* cells. In this study, I tested whether the removal of the C-terminal tail of Neo1p, which is 21 amino acids in length, would affect the functionality of the protein. A plasmid encoding a version of N-terminally HA-tagged Neo1p lacking the last 21 amino acids was constructed (HA-Neo1p$^{\Delta Ctail}$) and transformed in *NEO1*Δ*neo1* cells. After sporulation and tetrad dissection, no leucine-prototroph Δ*neo1* cells carrying HA-Neo1p$^{\Delta Ctail}$ were obtained, indicating that HA-Neo1p$^{\Delta Ctail}$ was nonfunctional. In agreement to that, overexpressed HA-Neo1p$^{\Delta Ctail}$ was not able to suppress the growth defect of Δ*ysl2* cells at 37°C. To find out why the truncated version of Neo1p was nonfunctional, the localization and stability of HA-Neo1p$^{\Delta Ctail}$ were analyzed upon expression in *NEO1* cells. Indirect immunofluorescence studies revealed that HA-Neo1p$^{\Delta Ctail}$ was completely retained within the ER (Fig. 17A). Similar to Neo1-37p, the HA-Neo1p$^{\Delta Ctail}$ polypeptide was rapidly degraded with a reduced half-live time of 105 min at 25°C and 56 min at 37°C (Fig. 17B) as opposed to a half-live time of 257 min/90 min for wild-type Neo1p (25°C/37°C, see Fig. 13A).

To determine if the localization of the nonfunctional Neo1p-C-HA was also affected, indirect immunofluorescence was performed in a heterozygous strain containing Neo1p-C-HA and the wild-type untagged *NEO1* copy. Neo1p-C-HA localized to continuous reticular

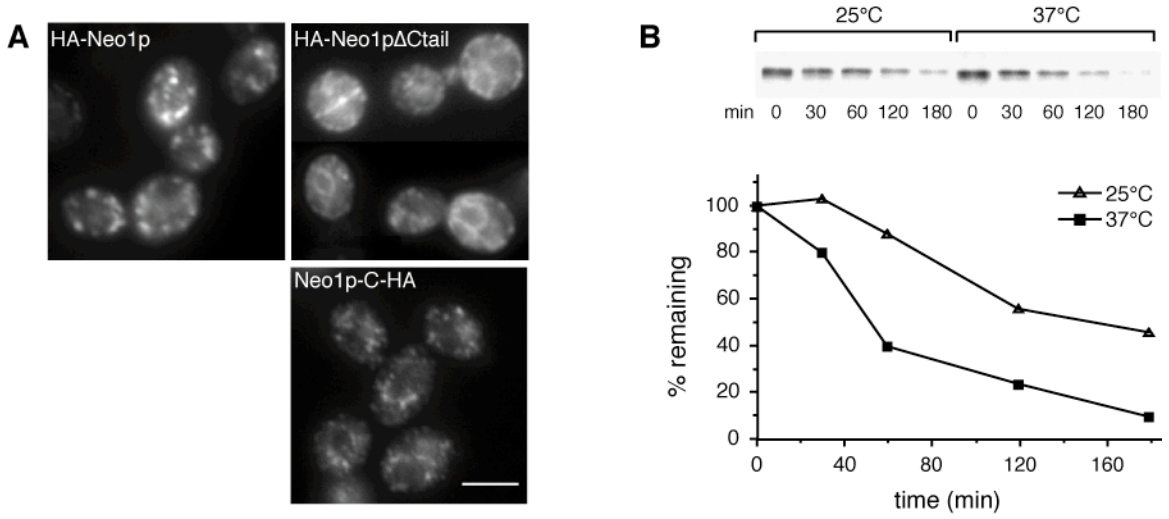

Fig. 17. C-terminal modifications of Neo1p affect its localization and stability. (A) Wild-type cells (BS64) transformed with either HA-Neo1p or HA-Neo1p$^{\Delta Ctail}$ in pRS315, and heterozygous diploids expressing C-terminally HA-tagged Neo1p (BS757, Neo1p-C-HA) were fixed after growth at 25°C and stained by indirect immunofluorescence with an anti-HA antibody as described in section 2.2.3.3. The exposure time was 3 times longer for Neo1p-C-HA as compared to HA-Neo1p and HA-Neo1p$^{\Delta Ctail}$. Bar, 5 μm. (B) BS64 cells transformed with HA-Neo1p$^{\Delta Ctail}$ were labeled with [^{35}S]-methionine for 30 min at 25 °C and chased at either 25°C or 37°C for the indicated times. Aliquots were removed and HA-Neo1p$^{\Delta Ctail}$ was isolated by immunoprecipitation using an anti-HA antibody as described in section 2.2.3.5. HA-Neo1p$^{\Delta Ctail}$ levels were quantified with the phosphorimager and expressed as percentages of the level of labeled protein at the 0 min chase point.

structures and faint punctate structures (Fig. 17A), similar to the C-terminally myc-tagged Neo1p version in the study by Hua and Graham (2003). Furthermore, the intensity of the Neo1p-C-HA staining was significantly reduced as compared to that of wild-type HA-Neo1p. Thus, similar to HA-Neo1p$^{\Delta Ctail}$, Neo1p-C-HA appeared to be, at least in part, retained in the ER and exhibited a reduced stability.

In summary, truncation as well as tagging of the C-terminal tail seems to impair the function of Neo1p. Since the C-terminally modified proteins were retained in the ER, it is possible that the C-terminal tail represents a structure essential for the correct folding of Neo1p and therefore for the exit of this protein out of the ER.

3.1.8 The Neo1p ATPase activity is essential for Neo1p function *in vivo*, but is not impaired in the *neo1* mutants

I next investigated the consequence of the inhibition of the ATPase activity of Neo1p on the functionality of this protein *in vivo*. Like all P-type ATPases, Neo1p contains the highly conserved DKTGTLT motif (see section 1.3), of which the aspartic acid side chain forms an aspartyl-phosphate catalytic intermediate, which is essential for ATP hydrolysis (Allen and Green, 1976; Fagan and Saier, 1994). This aspartic acid residue was mutated to an asparagine residue in Neo1p and the plasmid encoding Neo1p^{D503N} was transformed in a heterozygous *NEO1*Δ*neo1* strain. After sporulation and tetrad dissection, no leucine-prototroph Δ*neo1* cells carrying Neo1p^{D503N} were obtained. In addition, Neo1p^{D503N} was not able to suppress the growth defect exhibited by Δ*ysl2* cells at 37°C (Fig. 18). These data confirmed the assumption that the ATPase activity of Neo1p is essential for its function *in vivo*.

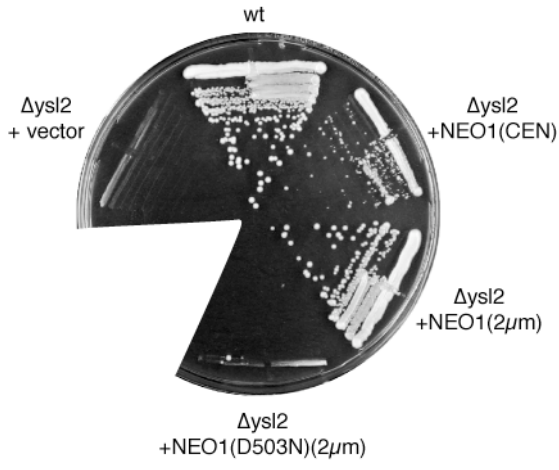

Fig. 18. *NEO1(D503N)* does not suppress the Δ*ysl2* growth defect at 37°C. Growth on YPD plates at 37°C of wt (RH1201) and Δ*ysl2* cells (BS747) transformed with the indicated CEN or 2 μm plasmids.

To determine whether the ATPase activity was impaired in the *neo1-ts* mutants, I measured this activity using an *in vitro* assay composed of two steps. Firstly, immuno-precipitated wild-type or mutant HA-Neo1 proteins were incubated with ATP. Secondly, the concentration of free inorganic orthophosphate resulting from hydrolysis of ATP was measured by a colorimetric assay (for details, see section 2.2.3.7).

First, I tried to optimize the conditions to isolate the HA-Neo1 proteins by immunoprecipitations from total cellular extracts using different detergent concentrations. As shown in Fig. 19A, HA-Neo1p was isolated most efficiently in the presence of 0.01% NP40. Analysis of the immunoprecipitates by silver staining after SDS-PAGE revealed that higher concentrations than 0.01% of NP40 did not increase the amounts of Neo1p and did not result in significantly reduced amounts of unspecifically bound proteins (Fig. 19A). Similar quantities of background were observed in a sample prepared from an untagged strain (Fig. 19B).

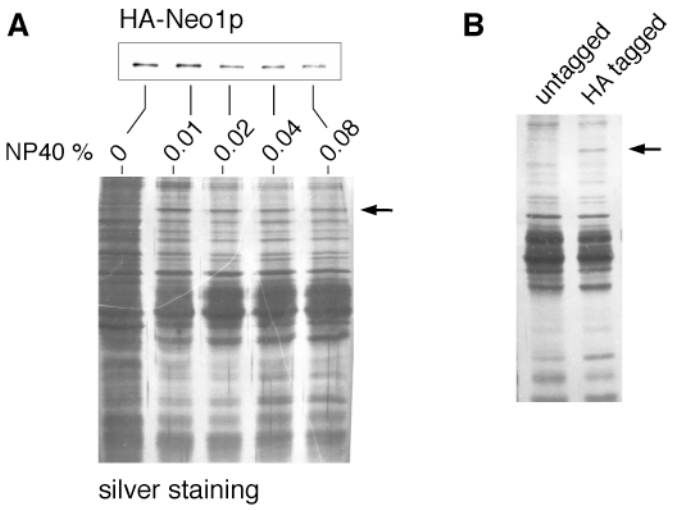

Fig. 19. Optimization of the conditions to isolate HA-Neo1p. (A) Immunoprecipitations were performed in the absence or presence of NP40 (concentrations as indicated) with an anti-HA antibody from precleared lysates of cells expressing HA-Neo1p (BS862). Proteins bound to Protein A-Sepharose were released in SDS-PAGE sample buffer, separated by SDS-PAGE, and either detected by immunoblotting using an anti-HA antibody (above) or by silver staining (below). The arrow indicates the HA-Neo1p band (B) Silver staining of proteins immunoprecipitated in the presence of 0.01 % NP40 from precleared extracts of BS862 (HA tagged) and BS64 (untagged) cells and separated by SDS-PAGE. The arrow indicates the HA-Neo1p band.

HA-Neo1p isolated in the presence of 0.01% NP40 and a control sample prepared from the untagged strain were subjected to the ATPase activity test in the absence of NP40. The release of free orthophosphate during the 2 h of incubation in the control represented 17% of that measured in the HA-Neo1p-containing sample (100%) (Fig. 20A). Since the HA-Neo1p band was the only detectable difference between the immunoprecipitates of the two cell lysates (see Fig. 19B), it is most likely that the increase in free orthophosphate corresponds to the enzymatic activity of Neo1p.

To optimize the conditions during the Neo1p ATPase assay, the reaction was carried out in the presence of 0.002, 0.004, 0.01 or 0.02% NP40. As shown in Fig. 20B, the highest ATPase activity was measured in a buffer containing 0.01% NP40.

Based on these results, the ATPase assay was performed in a buffer containing 0.01% NP40, but with immunoprecipitates generated in the presence of 0.01, 0.025, or 0.05% NP40. Almost no ATPase activity could be measured in the samples prepared in the presence of 0.025 or 0.05% NP40 (Fig. 20C), although the amounts of HA-Neo1p isolated were

comparable under the three conditions (Fig. 20D). This indicated that higher detergent concentrations during purification were harmful for the enzymatic activity of Neo1p.

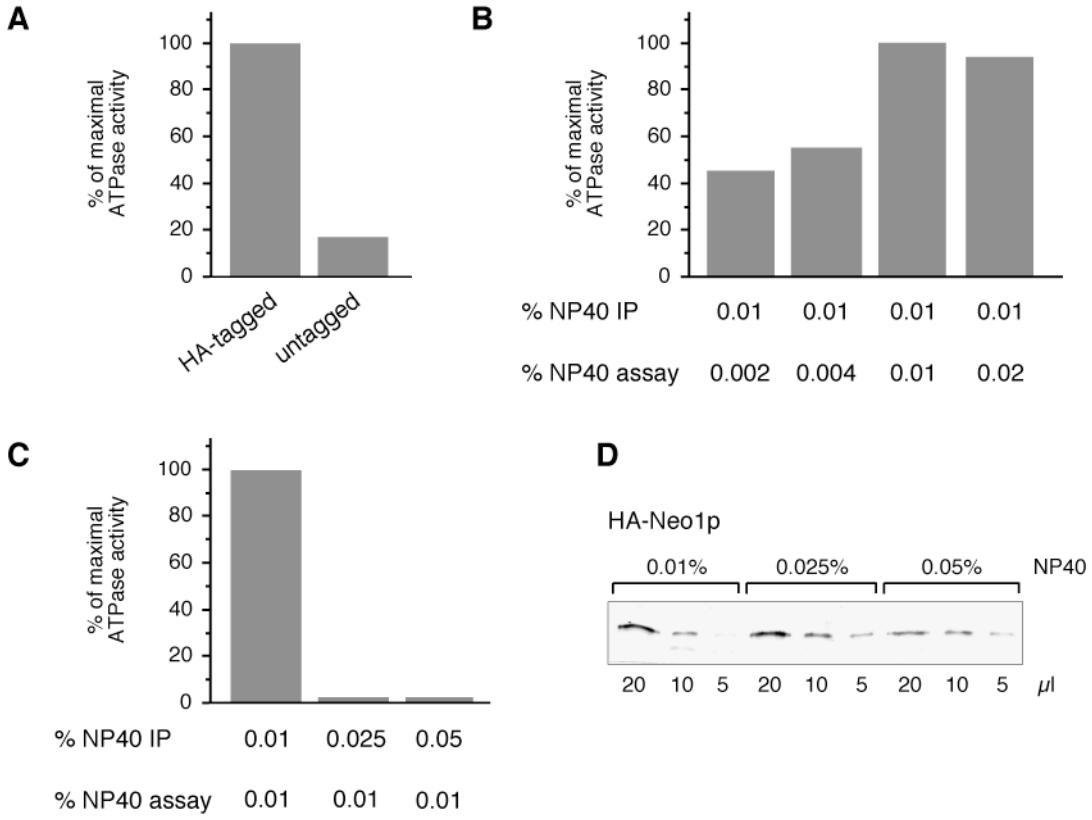

Fig. 20. ***In vitro*** **ATPase activity of HA-Neo1p immunoprecipitates.** (A) Immunoprecipitations were performed with anti-HA antibodies in the presence of 0.01% NP40 from precleared lysates of cells lacking HA-Neo1p (BS64, untagged) and of cells expressing HA-Neo1p (BS862, HA-tagged). Proteins bound to Protein A-Sepharose were resuspended in ATPase assay buffer without detergent and incubated with ATP for 0 min or 2 h at 37°C. The ATPase activity represents the increase in free orthophosphate (P_i) concentration during the 2 h of incubation (see 2.2.3.7 for details). 100% = 3.4 nmoles of P_i (mean value of 3 experiments). (B) Immunoprecipitations were performed in the presence of 0.01% NP40 from BS862 precleared cell lysates. Proteins bound to Protein A-Sepharose were resuspended in ATPase assay buffer containing NP40 (concentration as indicated) and incubated with ATP for 0 min or 2 h at 37°C. ATPase activity was determined as in (A). 100% = 5 nmoles of P_i (n = 1). (C, D) Immunoprecipitations from BS862 precleared cell lysates were performed under the indicated detergent concentrations (% NP40 IP). Proteins bound to Protein A-Sepharose were either incubated with ATP in the presence of 0.01% NP40 (C) or released in SDS-PAGE sample buffer for SDS-PAGE and Western blot analysis (D). The ATPase activity was determined as in (A). 100% = 4.4 nmoles of P_i (C, n = 1). Different volumes of each sample were separated by SDS-PAGE to compare the amounts of HA-Neo1p isolated under the different detergent conditions (D).

Since the detergent conditions seemed to dramatically influence the efficiency of the isolation as well as the ATPase activity of Neo1p, I compared the results obtained with NP40 to that acquired with another detergent, $C_{12}E_9$ (polyoxyethylene-9-lauryl ether). The amounts of immunoprecipitated HA-Neo1p after extraction with 0.02% $C_{12}E_9$ were reduced to 50% of the levels obtained after extraction with 0.01% NP40 (Fig. 21A), whereas the ATPase activity was further reduced to 10% of that measured in the immunoprecipitates

generated in the presence of 0.01% NP40. The absence of a detergent during isolation did not influence the amount of isolated Neo1p, but decreased the ATPase activity to 40% (Fig. 21B). Thus, the concentration as well as the nature of the detergent influenced dramatically the ATPase activity of Neo1p.

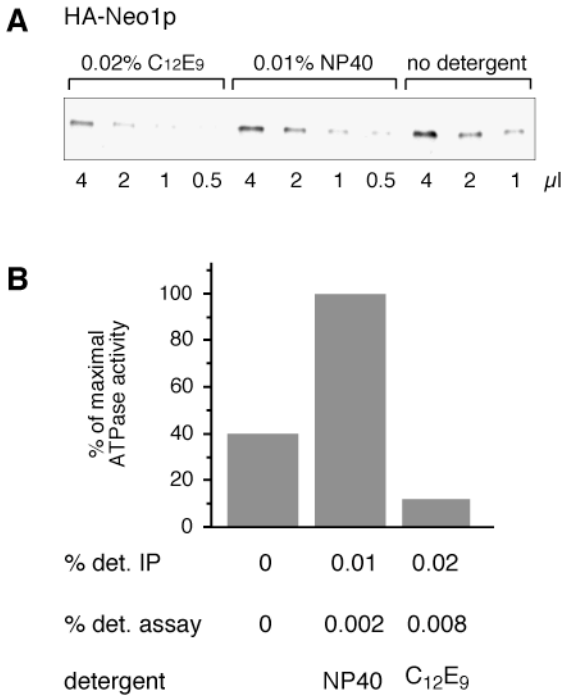

Fig. 21. Isolation of HA-Neo1p and determination of the ATPase activity in the presence of different detergents. (A) Immunoprecipitates from precleared BS862 lysates were performed under the indicated detergent conditions (% det. IP). Proteins bound to Protein A-Sepharose were released in SDS-PAGE sample buffer and several volumes of each sample were separated by SDS-PAGE and analyzed by immunoblotting to compare the amounts of HA-Neo1p isolated under the different detergent conditions. (B) Immunoprecipitates obtained as in (A) were incubated with ATP under the indicated detergents concentrations (% det. assay). ATPase activity was determined as in Fig. 20A. 100% = 3.7 nmoles of P_i (mean value of 3 experiments) (n = 1).

Finally, I analyzed whether the mutant Neo1-ts proteins were impaired in their ATPase activity. The ATPase assay was performed with HA-Neo1p, HA-Neo1-37p, and HA-Neo1-69p immunoprecipitated in the presence of 0.01% NP40. The ATPase assay was conducted in a buffer free of detergent, since the finding that the presence of 0.01% NP40 during incubation with ATP enhanced the ATPase activity of Neo1p was obtained later in time. As compared to wild-type Neo1p, both mutant proteins exhibited reduced ATPase activity, with 37% of wild-type activity for Neo1-69p and 13% for Neo1-37p (Fig. 22). However, as revealed by immunoblotting, the amounts of mutant Neo1 proteins isolated were reduced to approximately 20%/10% (HA-Neo1-69p/HA-Neo1-37p) of that of purified wild-type Neo1p (Fig. 22). This implies that the apparent reduction in the ATPase activity exhibited by the mutant Neo1-ts proteins was most likely due to less protein in the assay. Correcting for the reduced quantities of Neo1-69p even suggested that the ATPase activity of this Neo1 mutant may in fact be higher than that exhibited by wild-type Neo1p.

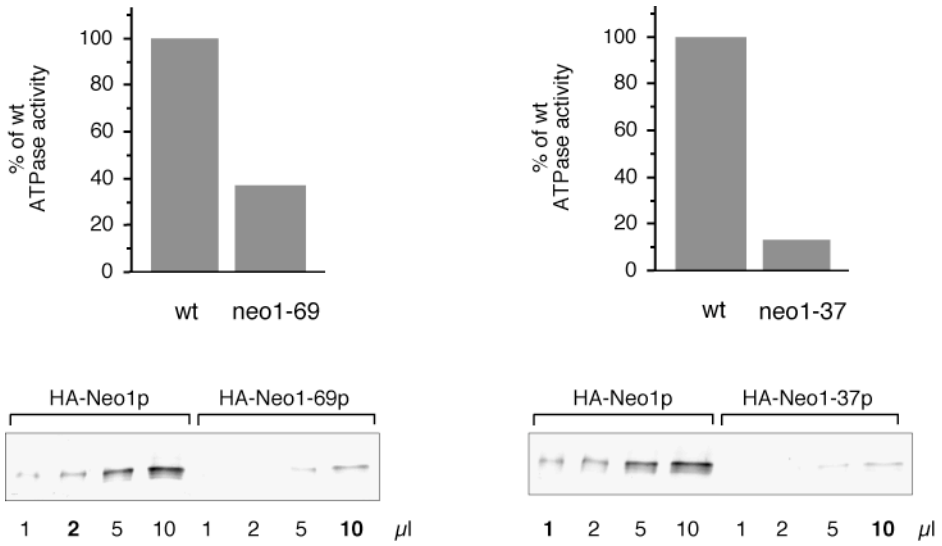

Fig. 22. The ATPase activity of Neo1-37p is similar to that of wild-type Neo1p, while the Neo1-69p activity may be increased. Immunoprecipitations from precleared lysates of cells expressing either wt HA-Neo1p (BS862), HA-Neo1-69p (BS993) or HA-Neo1-37p (BS1001) were performed in the presence of 0.01% NP40 with an anti-HA antibody. Proteins bound to Protein A-Sepharose were either resuspended in ATPase assay buffer without detergent or in SDS-PAGE sample buffer. ATPase activity was determined as in Fig. 20A. 100% = 3 nmoles of P_i (mean value of 3 experiments). Several volumes of each immunoprecipitate resuspended in SDS-PAGE sample buffer were separated by SDS-PAGE to compare the amounts of isolated HA-Neo1-69p, HA-Neo1-37p, and wild-type HA-Neo1p. Volumes exhibiting a comparable immunodetection signal for HA-Neo1 proteins were indicated in bold.

3.2 Characterization of the localization of Sjl2p and of its newly-identified interacting partner Bsp1p

3.2.1 Sjl2p localizes to punctate structures by indirect immunofluorescence

Sjl2p is a polyphosphoinositide phosphatase, which may be involved in endocytic trafficking, as suggested by genetic evidence (Singer-Krüger et al., 1998; Stefan et al., 2002). While the mutants harboring a single deletion of either one of the three synaptojanin genes displayed no obvious phenotypes (Stolz et al., 1998), double mutant analysis showed that Δ*sjl2*Δ*sjl3* and more profoundly Δ*sjl1*Δ*sjl2* cells exhibited a defect in receptor-mediated and fluid-phase endocytosis, but not Δ*sjl1*Δ*sjl3* cells (Singer-Krüger et al., 1998). Δ*sjl1*Δ*sjl2* and Δ*sjl2*Δ*sjl3* cells were also defective in the organization of the actin cytoskeleton and Δ*sjl1*Δ*sjl2* showed an aberrant cell surface morphology (Srinivasan et al., 1997; Stolz et al., 1998; Singer-Krüger et al., 1998), while the Δ*sjl1*Δ*sjl3* mutant was phenotypically like wild type. Together, these studies suggested that among the three synaptojanins Sjl2p may represent the major player in endocytosis. To find further support to this idea, I analyzed the subcellular distribution of Sjl2p by indirect immunofluorescence. The strain used in this study contained Sjl2p tagged C-terminally with three copies of the HA-epitope. This version of

Sjl2p was functional, since a Δ*sjl1*Δ*sjl3* strain expressing HA-Sjl2p grew like wild type (B. Singer-Krüger), whereas a strain impaired in the function of the three synaptojanins would be lethal (Srinivasan et al., 1997; Stolz et al., 1998; Singer-Krüger et al., 1998). HA-Sjl2p exhibited a faint punctate staining pattern, which was only slightly above the background signal observed in an untagged strain (Fig. 23A). This punctate pattern could indicate that HA-Sjl2p localizes to endosomes or the Golgi complex. However, in the *vsp27* mutant, in which the prevacuolar compartment collapses into the enlarged class E compartment (Piper et al., 1995; see section 3.1.2), the distribution of HA-Sjl2p was unaffected, suggesting that Sjl2p does not localize to this compartment (Fig. 23B). Apparently, Sjl2p does not associate with the Golgi complex either, since the HA-Sjl2p staining pattern was unchanged in temperature-sensitive *sec7* cells shifted to 37°C in the presence of 0.1% glucose (Fig. 23B), the conditions under which Golgi structures form aberrant clumps (Segev et al., 1988; see section 3.1.2).

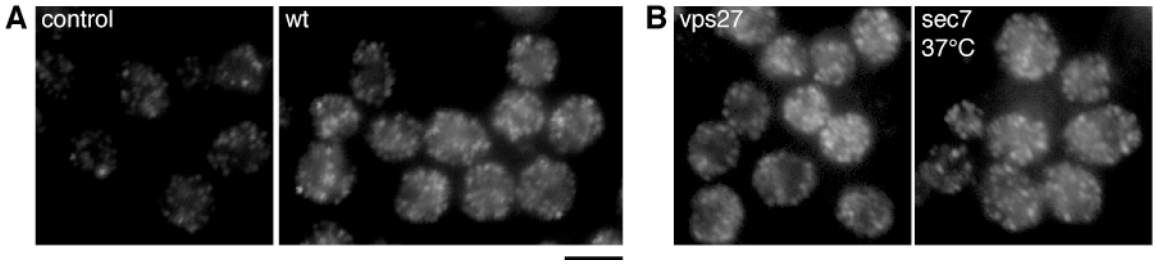

Fig. 23. HA-Sjl2p localizes to punctate structures that are not sensitive to mutations in *VPS27* and *SEC7*. (A) Cells lacking HA-Sjl2p (BS64) (control) and wild-type cells expressing HA-Sjl2p (BS1128) were grown at 25°C, fixed, and stained by indirect immunofluorescence with a monoclonal mouse anti-HA antibody as described in section 2.2.3.3. (B) Indirect immunofluorescence in *vps27* cells expressing HA-Sjl2p (BS1124) was performed as in (A). *sec7* cells expressing HA-Sjl2p (BS1175) were grown at 25°C and shifted for 1 h to 37°C in YP medium containing 0.1% glucose prior to fixation to induce the mutant phenotype. Bar, 5 μm.

To determine if at least some HA-positive spots represented endosomal structures, double indirect immunofluorescence was performed with the endosomal markers previously described (see section 3.1.2), i.e. Ypt51p, Tlg1/2p and Pep12p. However, no colocalization was observed between HA-Sjl2p and the four endosomal markers. One example is shown in Fig. 24A with Ypt51p, which localizes to both early and late endosomes. Consistent with these results, expression of the mutant Ypt51Q66L, which induces the formation of enlarged endosomes (Singer-Krüger et al., 1995; see section 3.1.2), did not lead to the collapse of the HA-Sjl2p-positive spots (Fig. 24B).

Altogether, these data indicated that Sjl2p does neither localize to the early and the late endosomal compartments defined by the typical endosomal SNARE proteins and Ypt51p nor to the Golgi complex. However, due to the punctate staining pattern exhibited by HA-

Sjl2p and the suggested role for Sjl2p in early endocytic steps, Sjl2p might localize to primary endocytic vesicles, an idea which was supported by further localization studies (see below).

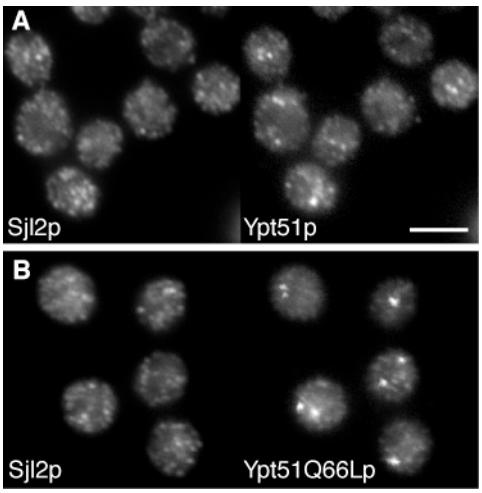

Fig. 24. HA-Sjl2p does not colocalize with the endosomal marker Ypt51p. (A,B) Double immunofluorescence of HA-Sjl2p and Ypt51p in cells expressing HA-Sjl2p and wild-type Ytp51p (A, BS1128) or in transformants expressing HA-Sjl2p and Ypt51Q66L (B, BS1128 + Ytp51Q66L in pBPH1). After growth at 25°C, cells were fixed and stained with anti-HA and anti-Ypt51p antibodies. Dilutions of the antibodies used are described in section 2.2.3.3. Bar, 5 μm.

3.2.2 The staining pattern of HA-Sjl2p is affected in cells lacking the actin-regulating kinases Ark1p and Prk1p

Since Sjl2p has been suggested to participate in the organization of the actin cytoskeleton (see above; Srinivasan et al., 1997; Singer-Krüger et al., 1998; Stefan et al., 2002) and because Sjl2p may localize to primary endocytic vesicles, it was possible that a fraction of Sjl2p interacts with the actin cytoskeleton and in particular with actin cortical patches, which are structures required during early steps of endocytosis (reviewed by Engqvist-Goldstein and Drubin, 2003). To test this idea, I performed a double labeling of myc-Sjl2p and GFP-actin (GFP-Act1p). As shown in Fig. 25A, no clear colocalization between Sjl2p and actin could be observed. However, the staining pattern of HA-Sjl2p was dramatically changed and appeared mainly as one large structure in cells lacking the two redundant actin-regulating kinases Ark1p and Prk1p (Fig. 25B). In the Δ*ark1*Δ*prk1* mutant, large cytoplasmic clumps are formed by the aggregation of components of the cortical actin patches (Cope et al., 1999). Double labeling of HA-Sjl2p and GFP-Act1p in this mutant confirmed that the large structures corresponded to the cytoplasmic actin clumps (Fig. 25C) and therefore suggested that Sjl2p may at least partially interact with the cortical actin cytoskeleton. Interestingly, the two other yeast synaptojanin proteins, HA-Sjl1p and HA-Sjl3p, did not localize to the cytoplasmic actin clumps formed in Δ*ark1*Δ*prk1* cells (Fig. 25D), although genetic evidence suggested an overlapping function between all three synaptojanins in the organization of the actin cytoskeleton and in endocytosis (see above).

The finding that, among the three synaptojanins only Sjl2p localized to the actin clumps, suggested a unique function or a different regulation of Sjl2p at these cellular sites.

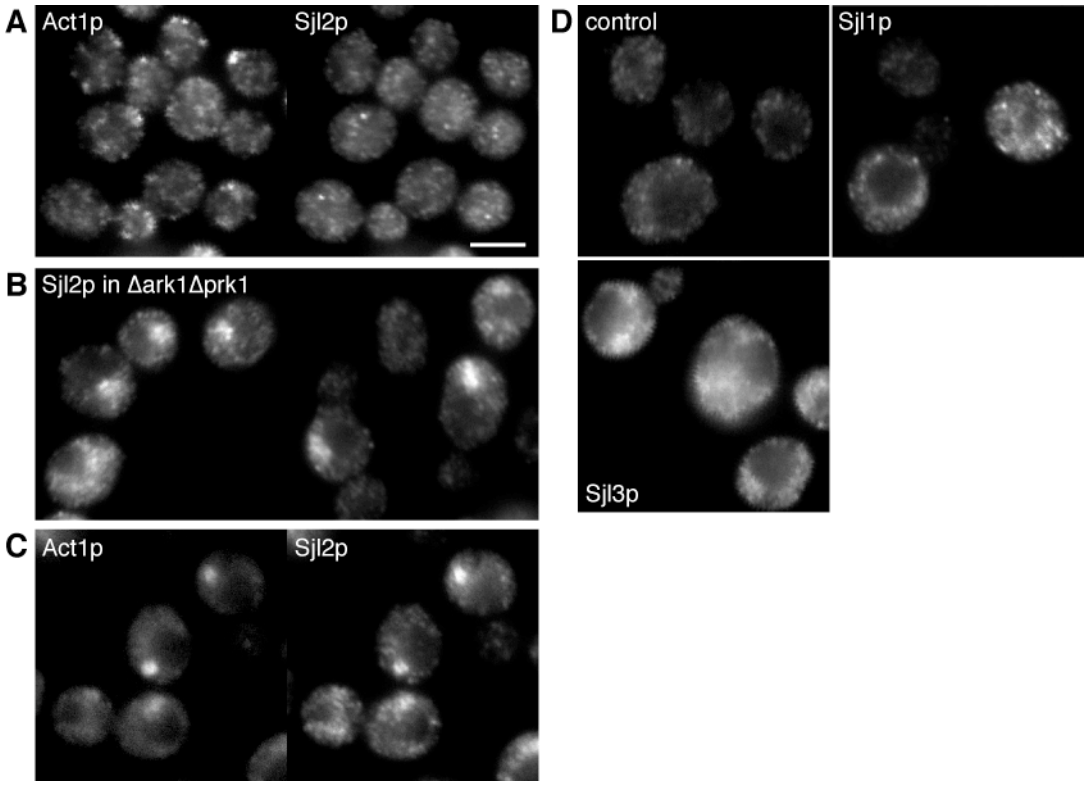

Fig. 25. HA-Sjl2p localizes to actin clumps in Δ*ark1*Δ*prk1* cells. (A) Double immunofluorescence of myc-Sjl2p and GFP-Act1p was performed in cells expressing myc-Sjl2p and GFP-Act1p (BS1248 + GFP-Act1p) grown at 25°C, fixed, and stained with anti-myc and anti-GFP antibodies (see section 2.2.3.3). Bar, 5 μm. (B,C) Δ*ark1*Δ*prk1* cells expressing HA-Sjl2p (B, BS1270) or expressing HA-Sjl2p and GFP-Act1p (C, BS1270 + GFP-Act1p) grown at 25°C were analyzed by indirect immunofluorescence using an anti-HA antibody. GFP-Act1p was observed directly using the appropriate filter sets (C). (D) Staining of Δ*ark1*Δ*prk1* cells expressing HA-Sjl1p (BS1373), HA-Sjl3p (BS1375) or of untagged Δ*ark1*Δ*prk1* cells as control (DDY1885) was performed as in (B).

To find out whether Sjl2p localized rapidly to the forming actin clumps, the distribution of Sjl2p was analyzed in a Δ*ark1*Δ*prk1* strain containing the *prk1-as3* plasmid (designated as Δ*ark1 prk1-as3*). The *prk1-as3* allele contains mutations that affect the ATP-binding pocket of Prk1p and render the kinase sensitive to the adenine analog 1NA-PP1 (4-amino-1-tert-butyl-3-(1'-naphthyl)pyrazolo[3,4-d]pyrimidine) and therefore enables the rapid and specific inactivation of Prk1p kinase activity *in vivo* (Bishop et al., 1998; Sekiya-Kawasaki et al., 2003). By inactivating this form of Prk1p in a Δ*ark1* strain, the kinetics of the formation and localization of the forming actin clumps could be followed (Sekiya-Kawasaki et al., 2003). Within 2 minutes after the addition of 1NA-PP1, the faint HA-Sjl2p-positive spots observed in cells before treatment with the inhibitor aggregated into small clumps in the

daughter cells and at the bud neck of small budded cells (Fig. 26). The HA-Sjl2p-containing clumps then moved into the mother cells (Fig. 26, 5 min). After 20 minutes of Prk1p inhibition, the clumps were still found in the mother cells and were larger (Fig. 26). The time course of the formation of the Sjl2p-containing clumps was similar to that observed for Abp1p-positive clumps (Sekiya-Kawasaki et al., 2003), suggesting that the localization of Sjl2p to these structures is most likely due to the association of Sjl2p with the cortical actin cytoskeleton and not to indirect effects caused by the disorganization of the actin cytoskeleton.

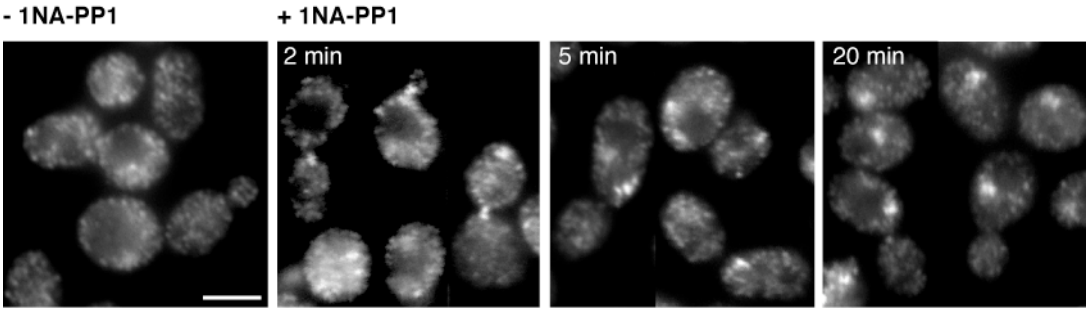

Fig. 26. HA-Sjl2p localizes rapidly to the actin clumps after inhibition of the Prk1p kinase activity. Indirect immunofluorescence was performed in Δ*ark1 prk1-as3* cells expressing HA-Sjl2p (BS1417). After growth at 25°C, cells were incubated in medium containing either DMSO for 5 min (-1NA-PP1) or 40 μM 1NA-PP1 (+1NA-PP1) for the indicated times prior to fixation. Cells were stained with an anti-HA antibody. Bar, 5 μm.

Since previous data in the lab of B. Singer-Krüger indicated that the major fraction of Sjl2p is membrane-associated (unpublished data), it was of interest to determine whether in cells lacking Ark1p and Prk1p activity the clumps-localized HA-Sjl2p was still associated with membranes and whether these membranes were derived of endocytosis. To address this question, I followed the lipophilic dye FM4-64, which marks endocytic membranes (Vida and Emr, 1995), and Sjl2p simultaneously in Δ*ark1 prk1-as3* cells. After incorporation of FM4-64 into the plasma membrane by incubation at 0°C, cells were resuspended in fresh medium with or without 1NA-PP1, incubated for 10 min at 25°C, and immediately observed under the fluorescence microscope. While in non-treated cells FM4-64 labeled punctate structures distributed throughout the cytosol, in 1NA-PP1-treated cells FM4-64 was observed in bigger and less numerous structures (Fig. 27A). They corresponded to the newly formed actin clumps, since they colocalized with GFP-Sjl2p (Fig. 27B). The presence of the clathrin coat component GFP-Chc1p in the large aggregates in Δ*ark1*Δ*prk1* cells was also consistent with the idea that plasma membrane-derived endocytic vesicles accumulate in the actin clumps (Fig. 27C).

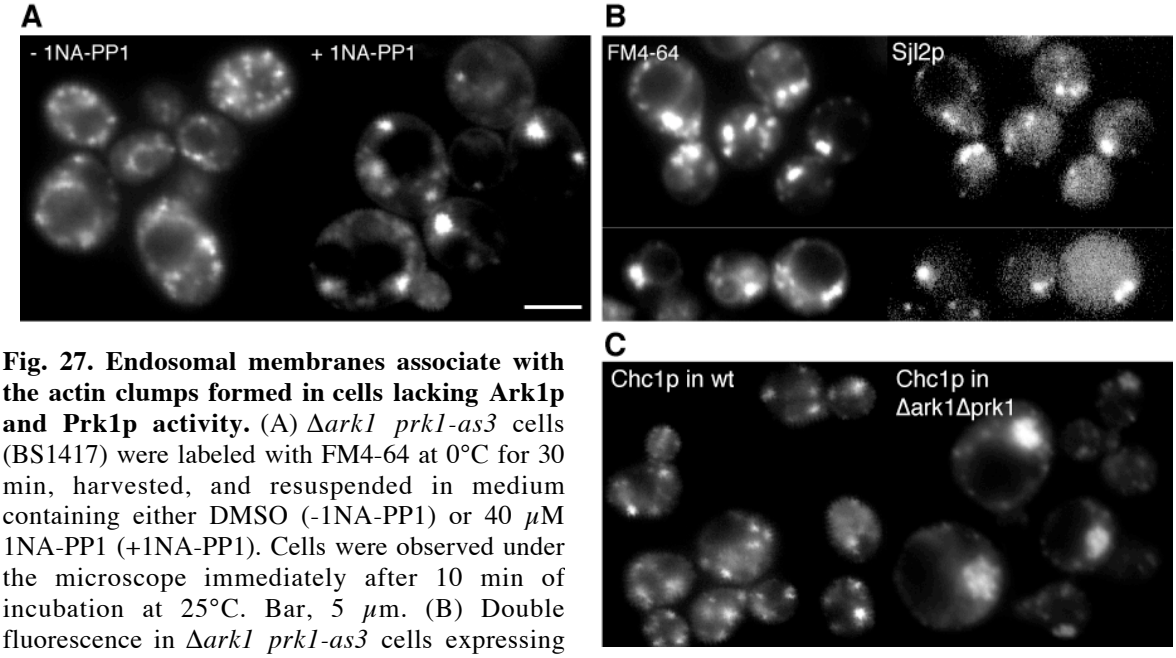

Fig. 27. Endosomal membranes associate with the actin clumps formed in cells lacking Ark1p and Prk1p activity. (A) Δ*ark1 prk1-as3* cells (BS1417) were labeled with FM4-64 at 0°C for 30 min, harvested, and resuspended in medium containing either DMSO (-1NA-PP1) or 40 μM 1NA-PP1 (+1NA-PP1). Cells were observed under the microscope immediately after 10 min of incubation at 25°C. Bar, 5 μm. (B) Double fluorescence in Δ*ark1 prk1-as3* cells expressing GFP-Sjl2p (BS1446) and labeled with FM4-64 as described in A. Cells were incubated for 10 min at 25°C in medium containing 1NA-PP1 prior visualization. (C) GFP-Chc1p in *ARK1 PRK1* cells (BS1423) or in Δ*ark1*Δ*prk1* cells (BS1439) was observed with the appropriate filter directly after cell growth at 25°C.

Altogether, these results provided strong evidence that the cytoplasmic actin clumps present in the Δ*ark1 prk1* mutants contain not only cortical patch components but also endocytic membranes, most likely primary endocytic vesicles containing Sjl2p.

3.2.3 Bsp1p, a binding partner of Sjl2p, localizes to cortical actin patches and partially associates with membranes in a phosphoinositide dependent manner

Bsp1p was identified in the lab of B. Singer-Krüger as a binding partner of the Sac1-like domain of Sjl2p in a genome-wide two-hybrid screen. Further biochemical studies in her lab confirmed the interaction between Bsp1p and Sjl2p. Since the localization of Bsp1p might give a clue to its function and the subcellular distribution of Sjl2p, indirect immunofluorescence was performed in a strain expressing a C-terminally HA-tagged version of Bsp1p. This version of Bsp1p was functional, since HA-Bsp1p retained the capacity to interact with Sjl2p (B. Singer-Krüger). HA-Bsp1p was found in faint cytoplasmic dots distributed over the entire cell similar to HA-Sjl2p (see Fig. 23A) and in addition a fraction of the HA-Bsp1p-positive structures exhibited a clear polarized pattern. In cells containing small buds, the brightly stained HA-Bsp1p-positive dots were concentrated in certain regions of the

cell periphery and at the bud tips (Fig. 28A, arrowheads). In large-budded cells, HA-Bsp1p staining was often concentrated at the bud neck (Fig. 28A, asterisks). Since this pattern was similar to the appearance of the cortical actin cytoskeleton, double indirect immunofluorescence was performed with myc-Bsp1p and GFP-Act1p. The HA-Bsp1p-positive structures colocalized to a great extent with those containing GFP-Act1p (Fig. 28B). Furthermore, HA-Bsp1p localized to the cytoplasmic actin clumps formed in the Δ*ark1*Δ*prk1* mutant (Fig. 28C; see section 3.2.2). Together, these results suggested that Bsp1p is most probably a component of the cortical actin patches.

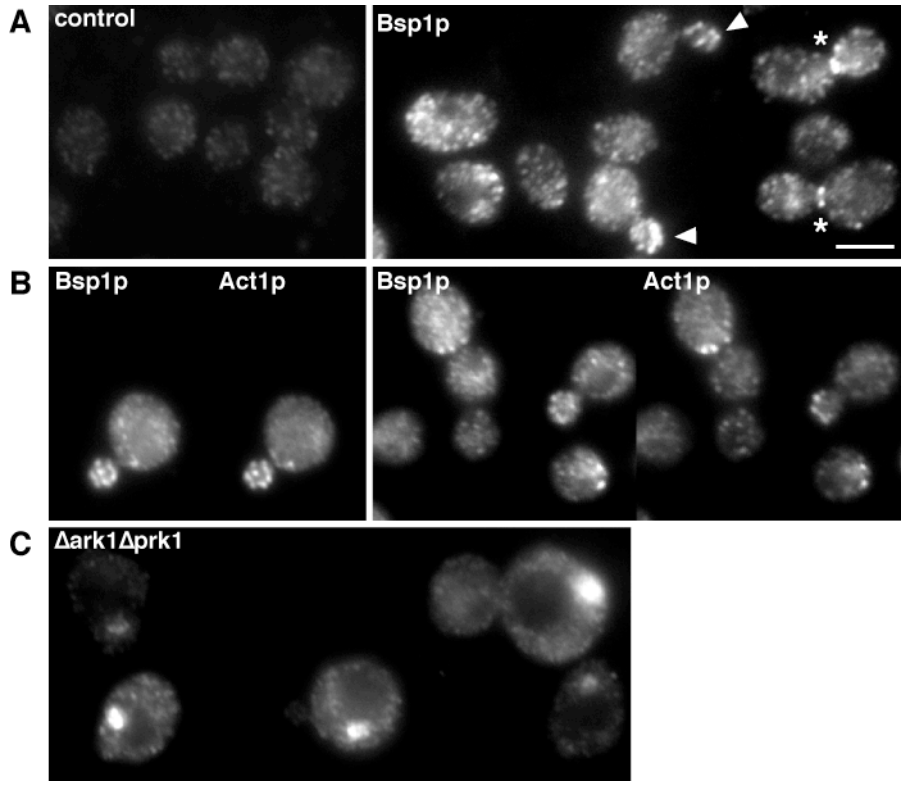

Fig. 28. HA-Bsp1p localizes to the cortical actin cytoskeleton. (A) Cells lacking HA-Bsp1p (BS64, control) and wild-type cells expressing HA-Bsp1p (BS1099, Bsp1p) were grown at 25°C, fixed, and stained by indirect immunofluorescence with an anti-HA antibody. Intensely stained structures at bud tips and at bud necks are indicated by arrowheads and asterisks, respectively. Bar, 5 μm. (B) Double immunofluorescence was performed in cells expressing myc-Bsp1p (BS1265) transformed with the GFP-Act1p plasmid using anti-myc and anti-GFP antibodies. (C) Staining of HA-Bsp1p in Δ*ark1*Δ*prk1* cells (BS1261) by indirect immunofluorescence was performed as described in (A).

Previous results in the lab of B. Singer-Krüger revealed that a fraction of Bsp1p is associated with membranes that contain endosomal and Golgi marker proteins. This fraction of Bsp1p could represent the dotted structures distributed in a non-polarized fashion (see Fig. 28A). Since Bsp1p interacts directly with the polyphosphoinositide phosphatase Sjl2p *in vivo*, I asked whether the subcellular distribution of Bsp1p was dependent on phosphoinositides. The staining pattern of HA-Bsp1p was analyzed in two mutants expressing temperature-

sensitive forms of the PtdIns(4)P kinase Pik1p. In both *pik1-63* and *pik-83* mutants, the levels of PtdIns(4)P and PtdIns(4,5)P_2 drop by 45–60% at the nonpermissive temperature of 37°C (Hama et al., 1999; Audhya et al., 2000). Indirect immunofluorescence experiments in *pik1-63* and *pik1-83* cells incubated for 2 h at 37°C revealed that the HA-Bsp1p staining pattern was no more polarized and that the signal intensity of the HA-Bsp1p-posivite dots was reduced as compared to *PIK1* cells (Fig. 29). At the permissive temperature, similar effects were observed in *pik1-83* cells. In these cells a reduction of PtdIns(4)P kinase activity was already observed at 25°C (Audhya et al., 2000). In contrast, in *pik1-63* cells the HA-Bsp1p localization was similar to that in the wild type (Fig. 29). Together, these results indicated that the subcellular localization of Bsp1p is dependent on the cellular levels of PtdIns(4)P and PtdIns(4,5)P_2.

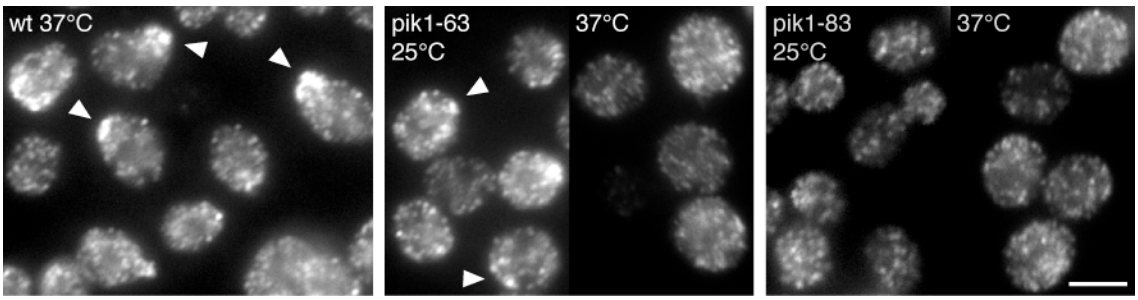

Fig. 29. HA-Bsp1p localization is dependent on phosphoinositides. Wild-type, *pik-1-63*, and *pik1-83* cells expressing HA-Bsp1p (BS1099, BS1149, BS1148, respectively) were grown at 25°C and either directly processed for indirect immunofluorescence or shifted for 2 h to 37°C prior to fixation. Staining of HA-Bsp1p was performed with an anti-HA antibody. Arrowheads indicate intensely stained structures. Bar, 5 μm.

3.2.4 Bsp1p interacts *in vitro* with phosphoinositides and other acidic phospholipids

To find out whether Bsp1p binds preferentially to one or the other phosphoinositide derivative, I carried out an *in vitro* floatation assay using liposomes of defined lipid composition. In this assay, *in vitro* translated Bsp1p using a reticulocyte lysate was incubated with liposomes and subsequently overlaid with a sucrose step gradient (see section 2.2.3.8). After centrifugation at 164,000 x g for 4 h, five fractions were collected from the top of the gradient. As shown in Fig. 30A, only a small fraction of Bsp1p floated into the gradient with liposomes constituted uniquely of dioleoylphosphatidylcholine (DOPC). In contrast, inclusion of small amounts of phosphatidylinositol-4-phosphate (PtdIns(4)P) into DOPC-based liposomes greatly enhanced the affinity of Bsp1p for liposomes. This was revealed by the presence of significantly larger amounts of Bsp1p in the gradient, in particular the top fraction, which contains the majority of the liposomes (Fig. 30A). Binding of twinfilin, a

protein known to interact with phosphoinositides (Palmgren et al., 2001), to DOPC-based liposomes was also greatly enhanced upon inclusion of PtdIns(4)P (Fig. 30A, Twf1p). The selective affinity of Bsp1p for lipids was estimated by comparing the floatation efficiency of Bsp1p with DOPC-based liposomes containing equal amounts of either one of an array of phospholipids (Fig. 30B). Quantitation of Bsp1p present in the top fraction of the gradients revealed that Bsp1p bound most efficiently to liposomes containing inositol-phospholipids and other acidic phospholipids [Fig. 30B; phosphatidylinositol (PtdIns), phosphatidylinositol-4-phosphate (PtdIns(4)P), phosphatidylinositol-4,5-bisphosphate (PtdIns(4,5)P_2), phosphatidylserine (PS), phosphatidic acid (PA), and phosphatidylglycerol (PG)], while little or no binding was observed with liposomes containing DOPC or phosphatidylethanolamine (PE). Since no further selectivity for a particular phospholipid could be determined, it was possible that the binding of Bsp1p to liposomes containing acidic phospholipids was based on ionic interactions. In agreement with this idea, the presence of 1M NaCl during incubation of Bsp1p with liposomes containing either PtdIns(4)P or PtdIns(4,5)P_2 completely inhibited the floatation of Bsp1p into the gradient. Thus, these results suggested that Bsp1p associates with membranes via ionic interactions. However, it is still possible that Bsp1p interacts preferentially with certain phosphoinositides *in vivo*.

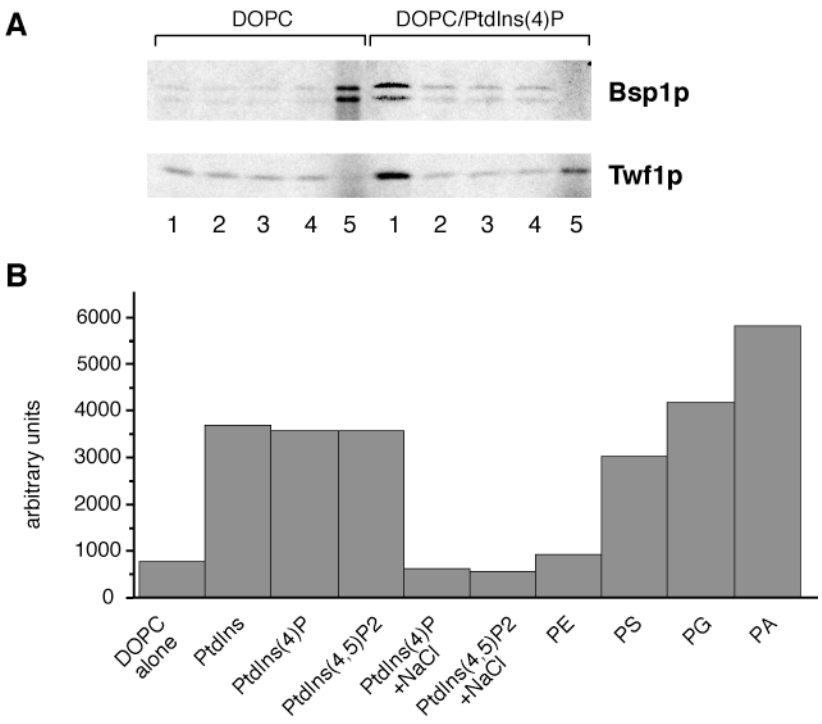

Fig. 30. Bsp1p associates with liposomes containing acidic phospholipids. (A,B) DOPC-based liposomes in the absence or presence of the indicated phospholipids (9% of total) were incubated for 1 h at 30°C with *in vitro* translated Bsp1p (A,B) or Twf1p (A). Subsequently, the reaction mixtures were subjected to floatation on a sucrose gradient. For details, see section 2.2.3.8. (A) The 5 fractions collected from each gradient were separated by SDS-PAGE and analyzed by autoradiography. 1, top fraction; 5, pellet fraction. (B) The presence of Bsp1p in the top fraction was quantified for each type of liposomes with the phosphorimager. +NaCl indicates the presence of 1 M NaCl during liposome binding. For abbreviations of lipids, see text.

4 Discussion

4.1 Neo1p functions within the endosomal system together with Ysl2p and Arl1p

4.1.1 Localization of Neo1p within the endomembrane/Golgi system and essential role of Neo1p

In the present study, Neo1p was found to localize within the endosomal system. In double labeling experiments, Neo1p colocalized to a great extent with the established endosomal marker proteins Ypt51p, Tlg1p and Pep12p. In addition, the numerous Neo1p-positive spots collapsed into large aggregates reminiscent of the aberrant class E compartment in the *vps27* mutant and in Ypt51Q66L-expressing cells. The endosomal localization of Neo1p was in accord with functional analyses, which revealed a defect in endocytic trafficking in the temperature-sensitive *neo1-37* and *neo1-69* mutants (B. Singer-Krüger) and a close connection between Neo1p and Ysl2p and Arl1p (B. Singer-Krüger and the present study), two proteins acting within the endosomal/late Golgi system (Jochum et al., 2002; Abudugupur et al., 2002; Rosenwald et al., 2002).

In addition to its role within the endosomal system, a small fraction of Neo1p may also act in the late Golgi compartment/TGN. Neo1p localized to the aberrant structures formed by Golgi membranes in *sec7* cells and colocalized to a large extent with Tlg1p and Tlg2p, which are distributed between early endosomes and the late Golgi complex (Abeliovich et al., 1998; Holthuis et al., 1998, Lewis et al., 2000). Since Neo1p did not overlap with the early Golgi marker proteins Ypt1p and Rer1p, it is most likely that the fraction of Neo1p sensitive to the *sec7* mutation associates with the late Golgi compartment. Such a localization for Neo1p may explain why the Golgi-modified p2 form of CPY was partially missorted to the extracellular space in the *neo1-ts* mutants.

Importantly, the results presented here designate Neo1p as the major member of the Drs2 family within the endosomal system. Among the other members, Dnf1p and Dnf2p are found primarily at the plasma membrane, while Dnf3p localizes to the late Golgi compartment (Hua et al., 2002; Pomorski et al., 2003). Drs2p is also primarily found and functions in the late Golgi compartment (Chen et al., 1999; Gall et al., 2002; Chantalat et al., 2004; Natarajan et al., 2004). The broad distribution of Neo1p within the endomembrane system, which exhibits a complex and highly dynamic organization (reviewed by Gruenberg, 2001; Prescianotto-Baschong and Riezman, 1998 and 2002), may explain why Neo1p function is essential. Growing evidence supports the idea that the Drs2 family members act as APL translocases and could therefore participate in the regulation of membrane shape (see section 1.3.1; Devaux, 1991; Farge et al., 1999). As the principal APL translocase within the

endosomal system, Neo1p may contribute to endosomal membrane deformations, which play a role in processes like tubule and vesicle formation. By participating in these reactions, Neo1p may be involved in a decisive manner in vesicular transport from the endosomal compartments to the vacuole and in recycling from the endosomes to the TGN (see Fig. 1).

It is intriguing that the localization of Neo1p and Drs2p at least partially overlaps: a fraction of Neo1p is found at the late Golgi complex (this study), where Drs2p localizes (Chen et al., 1999), and Drs2p has been shown to cycle via endosomes between the plasma membrane and the TGN (Saito et al., 2004). In spite of the similar localization of Neo1p and Drs2p, the lethality of Δ*neo1* cells cannot be rescued by overexpression of *DRS2* (Hua et al., 2002). In addition, Δ*drs2* cells exhibit a cold-sensitive growth defect (Chen et al., 1999), although Neo1p is present in these cells. The inactivation of Drs2p results in a reduction of translocation of fluorescently labeled PS across purified TGN membranes (Natarajan et al., 2004), which most probably also contain Neo1p. These data suggest that the Drs2p and Neo1p functions within the TGN and endosomes are likely distinct, maybe due to specific interactions of Drs2p and Neo1p with other components involved in distinct reactions at these sites. Alternatively, the fraction of Neo1p within the TGN and that of Drs2p within endosomes may not be sufficient to compensate for the absence of the major APL at these respective subcellular compartments.

4.1.2 ER localization of mutant Neo1 polypeptides and consequences on the secretory pathway

A relevant finding was that upon incubation at nonpermissive temperature the mutant Neo1 polypeptides were retained in the ER. As suggested by the enhanced intensity of the staining in tubular structures, the mutant proteins accumulated massively in the ER, resulting in the formation of abnormal enlarged structures within the tubular network. This morphological defect correlated with perturbations in the anterograde and retrograde membrane transport within the early secretory pathway at 37°C. A similar correlation between defects in the secretory pathway and the accumulation in the ER of a member of the P-type ATPase family was already observed with the H^+-ATPase Pma1p^{D378N} mutant (Wang and Chang, 1999). Thus, the perturbations of the secretory pathway observed in the *neo1-ts* mutants represent most likely indirect defects due to the buildup of the mutant proteins in the ER, rather than the result of a deficient Neo1p function in secretion.

The ER retention of the mutant Neo1 proteins may be effected by improper folding. This would be consistent with work on several Pma1 mutants showing that the mutant

proteins were misfolded, rapidly degraded, and retained in abnormal enlarged ER structures. Since a correlation could be established between poor protein folding and ER retention (DeWitt et al., 1998), it is likely that the variable extent of ER mislocalization and the distinct stabilities exhibited by Neo1-37p and Neo1-69p reflect different degrees of misfolding of these proteins. The malfolded Neo1-ts proteins are probably ubiquitinated and cleared by the ER-associated degradation (ERAD) pathway, since an ubiquitinated form of Neo1p has been found to accumulate in the ER of mutants defective in the ERAD machinery (Hitchcock et al., 2003). Another reason for the ER retention that may be linked to improper folding is that the mutant Neo1 proteins may fail to associate with a specific sorting component required for the ER exit of Neo1p. In support to this idea, interactions of the APL translocases Drs2p and Dnf1p with the sorting chaperones Cdc50p and Lem3p, respectively, were found to be essential for the ER exit and for the proper sorting of Drs2p and Dnf1p to their target compartment (Saito et al., 2004). Cdc50p and Lem3p belong to an essential family of structural homologs, which are suggested to function as subunits of the Drs2p family ATPases required for the quality control, the sorting, and even the regulation of the activity of the APL translocases (Radji et al., 2001; Saito et al., 2004). In analogy to Drs2p and Dnf1p, Neo1p might also associate with one of these chaperones to exit the ER and be sorted to endosomes. In the study by Saito et al. (2004), *NEO1* was shown to genetically interact with *CDC50*, but neither Cdc50p nor Lem3p were found to physically interact with Neo1p. However, the co-isolation experiments were performed with a C-terminally 13-myc-tagged version of Neo1p, which was most likely not functional. In fact, 13-myc-tagged Neo1p was retained partially in the ER, while my studies and work of B. Singer-Krüger clearly showed that Neo1p localizes and functions on endosomes. Thus, the question of whether Neo1p sorting relies on a mechanism dependent on these chaperones remains open.

The C-terminal region appeared to be particularly important for folding, since the truncated HA-Neo1p$^{\Delta Ctail}$ and several C-terminal tagged Neo1-variants accumulated at least partially in the ER (the present study; Hua et al., 2003; Saito et al., 2004). The ER localization can however not alone account for the total loss of function exhibited by HA-Neo1p$^{\Delta Ctail}$ and Neo1p-C-HA (the present study and B. Singer-Krüger, respectively), since Neo1-37p was retained in the ER, but *neo1-37* cells grew similar to the wild type at permissive temperature. A possibility is that the changes within the C-terminus may perturb the essential ATPase activity of Neo1p, which does not appear to be affected in Neo1-37p, at least *in vitro* (this study). In this context, it is important to state that the C-terminal tail of several P-type ATPases has been shown to constitute a regulatory domain of the ATPase activity (Enyedi et

al., 1987; Portillo et al., 1989). However, the hypothetical regulation of the Neo1p activity by its C-terminus might be quite different from that described for other P-type ATPases, since the deletion of Neo1p C-terminus rendered Neo1p nonfunctional, whereas the enzymatic activity of the ATPases mentioned above was activated by such a truncation (Portillo et al., 1989; Enyedi et al., 1993).

4.1.3 Concerted action of APL translocases, Arf GEFs and Arf proteins during vesicle formation

Results of my study together with work of B. Singer-Krüger revealed genetic and physical interactions between Neo1p and Ysl2p, and provided multiple evidence that Neo1p and Arl1p are genetically related (Fig. 31A). Furthermore, B. Singer-Krüger showed that the suppression of Δ*ysl2* cells by *NEO1* is dependent on *ARL1*. These interactions, the similar localization of the three proteins, and the resemblance of a number of phenotypes shown by mutants of the three genes strongly suggested that Neo1p, Ysl2p, and Arl1p act together in endosomal membrane trafficking. Based on sequence and structural homology, Arl1p could possibly be grouped into the Arf family (Pasqualato et al., 2002), whose members have been shown to participate in the assembly of coat components on membranes (Donaldson and Jackson, 2000). In support of a concerted action for Neo1p, Arl1p, and Ysl2p in vesicle budding, *neo1-69* cells accumulated aberrantly shaped endosomal/vacuolar membrane elongations with an increased surface to volume ratio (in collaboration with H. Schwarz, MPI, Tübingen). This mutant exhibited also an increased membrane-association of Arl1p and Ysl2p (this study). Thus, the morphological alteration of the endosomal membranes in *neo1-69* cells might reflect a lack of coordination between the activity of Neo1p, Arl1p, and Ysl2p in the process of vesicle formation, thereby resulting in endocytic trafficking defects. Significantly, another APL translocase family member (Drs2p) exhibits analogous interactions with a Sec7 family Arf GEF (Gea2p) and Arf1p. Drs2p interacts directly with Gea2p (Chantalat et al., 2004), while a connection between Drs2p and Arf1p is suggested by genetic data (Chen et al., 1999). The disruption of the interaction between Drs2p and Gea2p leads to defects in membrane deformation events required for the segregation of secretory granules (Chantalat et al., 2004). Thus, the striking similarities between the two APL translocases in their interactions with Arf proteins and Arf regulators, strongly support the idea that the generation of lipid bilayer asymmetry is intimately connected to Arf activity and coat assembly during budding reactions (Chen et al., 1999; Huijbregts et al., 2000).

Based on the present state of knowledge, the following model for the concerted action of Neo1p, Ysl2p, and Arl1p during vesicle formation is proposed (Fig. 31). Neo1p interacts with the peripherally membrane-associated Ysl2p on the endosomal membrane (Fig. 31B, 1). Cytosolic Arl1p^{GDP} is recruited to the membrane via direct interaction with Ysl2p and maybe Neo1p, and/or via binding to PS present on the cytosolic face of the membrane as a consequence of Neo1p translocase activity (see below). Once Arl1p^{GDP} is peripherally associated with endosomal membranes, nucleotide exchange on Arl1p may take place, possibly executed by Ysl2p, the candidate Arl1p GEF (Jochum et al., 2002) (Fig. 31B, 2). Tightly membrane-associated Arl1p^{GTP} may interact with effector proteins to promote a membrane deformation and Neo1p may cooperatively participate in this membrane process via its APL translocase activity (Fig. 31B, 3).

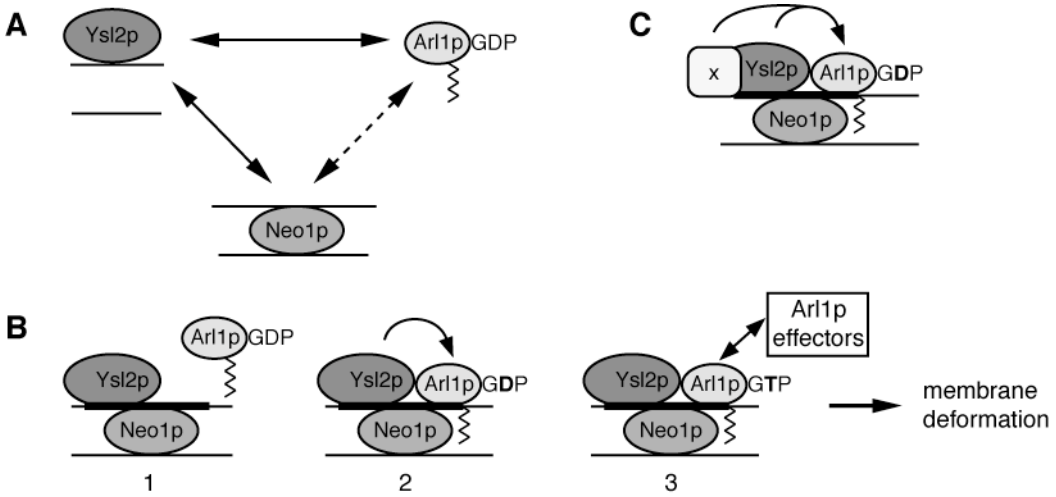

Fig. 31. Functional interactions between Neo1p, Ysl2p and Arl1p. (A) Known interactions between Ysl2p, Arl1p and Neo1p based on data of B. Singer-Krüger's lab and of the present work. Solid arrows indicate genetic and physical interactions and dashed arrows genetic interactions only. (B) Model for the concerted action of Neo1p, Ysl2p and Arl1p. For details, see text. The thick black bar represents the APLs translocated by Neo1p. (C) Potential participation of a still unidentified factor (x) acting together with Ysl2p on Arl1p-guanine nucleotide state.

The membrane association and activation of Arl1p may indeed partially depend on Neo1p activity, since evidence for the involvement of PS, one of the major substrates of APL translocases (reviewed by Daleke and Lyles, 2000), in the membrane recruitment of Arf1p^{GDP} and in the efficient activation of Arf1p^{GDP} to Arf1p^{GTP} has been recently provided (Antonny et al., 1997; Chardin et al., 1996). By analogy to Arf1p, the activation of Arl1p may also result in a conformational change within its N-terminal helix allowing the insertion of this structure with the membrane and thereby the tight membrane association of Arl1p^{GTP} (Antonny et al., 1997).

Three major points remain however to be addressed to verify the proposed model. Firstly, the role of Ysl2p as Arl1p GEF has still to be determined by biochemical analysis and one can therefore not exclude the possibility that Ysl2p required an additional component to activate Arl1p (Fig. 31C). Secondly, no Arl1p effectors have been identified so far that may act in endosomal trafficking. Finally, direct biochemical evidence for the APL activity of Neo1p and the other Drs2p family members has still to be provided. Recently, the inactivation of Drs2p has been shown to impair the translocation of fluorescently labeled PS across purified TGN membranes *in vitro*. However, in cells devoid of PS Drs2p was still required for the formation of secretory vesicles, suggesting that Drs2p *in vivo* function may be independent on PS translocation (Natarajan et al., 2004). Whether in the absence of PS Drs2p uses another phospholipid as substrate, or whether the primary function of Drs2p is not linked to APL translocation is not known. In conclusion, further analyses are required to determine the exact function of Ysl2p, Arl1p and Neo1p and their concerted role in endosomal membrane trafficking.

4.2 Evidence for a localization of Sjl2p to primary endocytic vesicles and their interaction with the cortical actin cytoskeleton

Sjl2p has been suggested to represent the major player in early steps of endocytosis among the three synaptojanins, since Δ*sjl2*Δ*sjl3* and more profoundly Δ*sjl1*Δ*sjl2* cells were defective in receptor-mediated and fluid-phase endocytosis (Singer-Krüger et al., 1998) and in the organization of the actin cytoskeleton, while the Δ*sjl1*Δ*sjl3* mutant did not displayed these defects (Srinivasan et al., 1997; Stolz et al., 1998; Singer-Krüger et al., 1998). Results in the lab of B. Singer-Krüger also revealed that Sjl2p was associated with membranes that cofractionated with small organelles such as endosomes and Golgi elements in a density gradient, suggesting that Sjl2p may localize to endosomes. Work conducted in this thesis brought clues for the localization of Sjl2p within the endosomal system. The punctate HA-Sjl2p-positive structures distributed throughout the cytoplasm did not collapse in cells carrying either the *vps27* or the *sec7* mutation and were distinct from those positive for established endosomal marker proteins (Ypt51p, Pep12p, and Tlg1p), indicating that Sjl2p does neither localize to early and late endosomes nor to the Golgi complex. Sjl2p did also not show a typical plasma membrane staining pattern, in agreement with subcellular fractionation experiments performed in the lab of B. Singer-Krüger showing that Sjl2p did not cofractionate with the plasma membrane-localized Pam1p. A key finding was that Sjl2p localized to the cytoplasmic actin clumps formed in cells lacking both Prk1p and Ark1p.

These two redundant actin-regulating kinases are proposed to couple the dynamic processes of actin cytoskeleton assembly and endocytosis, and the absence of these two proteins leads to the collapse of the cortical actin patches into actin clumps (Cope et al., 1999; reviewed by Smythe and Ayscough, 2003). The actin clumps contained both actin cortical patch components such as Abp1p, Sla1p and Pan1p (Cope et al., 1999; Watson et al., 2001; Warren et al., 2002) and vesicles (Sekiya-Kawasaki et al., 2003). Most likely these are primary endocytic vesicles rather than endosomes, since the endocytic tracer FM4-64 (Vida and Emr, 1995) also accumulated in the actin clumps (this study and Sekiya-Kawasaki et al., 2003), but not Tlg1p, Ypt51p, or Pep12p (B. Singer-Krüger's lab). The observation that Sjl2p colocalized to a great extent with FM4-64 at the actin clumps, strongly suggested that Sjl2p localizes to the primary endocytic vesicles. This subcellular distribution would explain why Sjl2p was not sensitive to the *vsp27* mutation and did not colocalize with early and late endosomal marker proteins.

The existence of endocytic vesicles distinct from the early and the late endosomal compartments was previously demonstrated by electron microscopy using endocytic tracers (Prescianotto-Baschong and Riezman, 1998; Mulholland et al., 1999). A subcellular localization of Sjl2p to primary endocytic vesicles suggests that this protein may represent the counterpart of mammalian Synaptojanin 1, *Caenorhabditis elegans UNC-26* gene product, and *Drosophila melanogaster* Synj, which all localize to synaptic coated vesicles (Haffner et al., 1997; Schuske et al., 2003; Verstreken et al., 2003).

The observation that Sjl2p localized to the forming actin clumps immediately after the inactivation of Prk1p activity in Δ*ark1* cells suggested a direct association of the Sjl2p-containing vesicles with the actin cytoskeleton. This association may be at least in part mediated by Bsp1p, a binding partner of Sjl2p identified in B. Singer-Krüger's lab. My studies revealed an association of Bsp1p with cortical actin patches. Further independent evidence designating Bsp1p as a cortical patch component ranged from two-hybrid interactions between Bsp1p and cortical patch components (Drees et al., 2001) to genetic interactions between *BSP1* and *RVS167* and *ABP1* (B. Singer-Krüger). In addition to its localization to cortical actin patches, a fraction of Bsp1p was also found to associate in a phosphoinositide-dependent manner with membranes (B. Singer-Krüger). In agreement with this finding, I could show that Bsp1p associated *in vitro* with liposomes containing acidic phospholipids, including phosphoinositides. These results suggested that Bsp1p may associate with Sjl2p-containing membranes via two attachment sites, Sjl2p itself and specific phospholipids. Thus, Bsp1p could act as an adapter that directly connects Sjl2p-containing

vesicles to the cortical actin cytoskeleton. Sjl2p has been found recently to interact with two other cortical actin patch components, Abp1p and Sla1p (Fazi et al., 2002; Stamenova et al., 2004). These interactions have still to be confirmed *in vivo*, but Abp1p and Sla1p may participate together with Bsp1p in the interaction of Sjl2p-containing vesicles with the cortical actin cytoskeleton.

In summary, results obtained in my thesis brought evidence for a localization of Sjl2p to primary endocytic vesicles and for a close connection between Sjl2p-containing vesicles and the cortical actin cytoskeleton. These data are relevant for further studies to elucidate the precise mechanism of Sjl2p during early steps of endocytosis.

4.3 Perspectives

To verify the model proposed for the concerted action of Neo1p, Ysl2p, and Arl1p, the exact functions of these three proteins and the interactions between them should be defined in detail. A key point is to examine the ability of purified Neo1p to translocate phospholipids across the endosomal lipid bilayer and to determine its substrate specificity. It will also be interesting to find out whether the activity of Neo1p influences membrane shape and in which membrane deformation events (tubulation, vesiculation) Neo1p is implicated. Putative regulators of the Neo1p translocase activity may determine where on the endosomal membranes and when vesicles will be formed. Ysl2p and Arl1p, which are possibly recruited to the membrane via Neo1p, may also be implicated in the regulation of Neo1p in order to coordinate the activities of the three proteins on the membrane. Finding new binding partners for Neo1p, Ysl2p, and effectors of Arl1p may also greatly help to better understand the function of these three proteins and the process requiring their concerted action during vesicle formation.

Results obtained in the second part of my PhD suggest that Sjl2p may localize to primary endocytic vesicles. This proposition should however be examined using additional methods. One possibility is to analyze the localization of Sjl2p by electron microscopy using double labeling of Sjl2p and endocytosed positively charged Nanogold (see Prescianotto-Baschong and Riezman, 1998). By defining the localization of Sjl2p after various time of endocytosis of Nanogold, one could determine when Sjl2p is recruited to the endocytic membranes. It would also be interesting to find the protein(s) mediating the recruitment of Sjl2p to endocytic membranes. The identification of regulators of the interaction of the Sjl2p-containing vesicles with the actin cytoskeleton and of the enzymatic activity of Sjl2p will also bring important clues to the Sjl2p function. These studies may also help to understand what

determines the specific function of Sjl2p in endocytosis as compared to the two other yeast synaptojanins, Sjl1p and Sjl3p.

Literature

Abeliovich, H., Grote, E., Novick, P., and Ferro-Novick, S. (1998). Tlg2p, a yeast syntaxin homolog that resides on the Golgi and endocytic structures. J. Biol. Chem. *273*, 11719-11727.

Abudugupur, A., Mitsui, K., Yokota, S., and Tsurugi, K. (2002). An *ARL1* mutation affected autophagic cell death in yeast, causing a defect in central vacuole formation. Cell Death. Differ. *9*, 158-168.

Adams, A.E., and Pringle, J.R. (1984). Relationship of actin and tubulin distribution to bud growth in wild-type and morphogenetic-mutant *Saccharomyces cerevisiae*. J. Cell Biol. *98*, 934-945.

Allen, G., and Green, N.M. (1976). A 31-residue tryptic peptide from the active site of the [Ca++]-transporting adenosine triphosphatase of rabbit sarcoplasmic reticulum. FEBS Lett. *63*, 188-192.

Antonny, B., Beraud-Dufour, S., Chardin, P., and Chabre, M. (1997). N-terminal hydrophobic residues of the G-protein ADP-ribosylation factor-1 insert into membrane phospholipids upon GDP to GTP exchange. Biochemistry *36*, 4675-4684.

Audhya, A., Foti, M., and Emr, S.D. (2000). Distinct roles for the yeast phosphatidylinositol 4-kinases, Stt4p and Pik1p, in secretion, cell growth, and organelle membrane dynamics. Mol. Biol. Cell *11*, 2673-2689.

Austin, C., Boehm, M., and Tooze, S.A. (2002). Site-specific cross-linking reveals a differential direct interaction of class 1, 2, and 3 ADP-ribosylation factors with adaptor protein complexes 1 and 3. Biochemistry *41*, 4669-4677.

Ayscough, K.R., Stryker, J., Pokala, N., Sanders, M., Crews, P., and Drubin, D.G. (1997). High rates of actin filament turnover in budding yeast and roles for actin in establishment and maintenance of cell polarity revealed using the actin inhibitor latrunculin-A. J. Cell Biol. *137*, 399-416.

Baggett, J.J., and Wendland, B. (2001). Clathrin function in yeast endocytosis. Traffic *2*, 297-302.

Barik, S., and Galinski, M.S. (1991). "Megaprimer" method of PCR: increased template concentration improves yield. Biotechniques *10*, 489-490.

Becherer, K.A., Rieder, S.E., Emr, S.D., and Jones, E.W. (1996). Novel syntaxin homologue, Pep12p, required for the sorting of lumenal hydrolases to the lysosome-like vacuole in yeast. Mol. Biol. Cell *7*, 579-594.

Bell, R.M., Ballas, L.M., and Coleman, R.A. (1981). Lipid topogenesis. J. Lipid Res. *22*, 391-403.

Bensen, E.S., Costaguta, G., and Payne, G.S. (2000). Synthetic genetic interactions with temperature-sensitive clathrin in *Saccharomyces cerevisiae*. Roles for synaptojanin-like Inp53p and dynamin-related Vps1p in clathrin-dependent protein sorting at the *trans*-Golgi network. Genetics *154*, 83-97.

Bishop, A.C., Shah, K., Liu, Y., Witucki, L., Kung, C., and Shokat, K.M. (1998). Design of allele-specific inhibitors to probe protein kinase signaling. Curr. Biol. *8*, 257-266.

Black, M.W., and Pelham, H.R. (2000). A selective transport route from Golgi to late endosomes that requires the yeast GGA proteins. J. Cell Biol. *151*, 587-600.

Boehm, M., Aguilar, R.C., and Bonifacino, J.S. (2001). Functional and physical interactions of the adaptor protein complex AP-4 with ADP-ribosylation factors (ARFs). EMBO J. *20*, 6265-6276.

Boehm, M., and Bonifacino, J.S. (2002). Genetic analyses of adaptin function from yeast to mammals. Gene *286*, 175-186.

Bollen, I.C., and Higgins, J.A. (1980). Phospholipid asymmetry in rough- and smooth-endoplasmic-reticulum membranes of untreated and phenobarbital-treated rat liver. Biochem. J. *189*, 475-480.

Bonifacino, J.S., and Lippincott-Schwartz, J. (2003). Coat proteins: shaping membrane transport. Nat. Rev. Mol. Cell. Biol. *4*, 409-414.
Borst, P., Zelcer, N., and van Helvoort, A. (2000). ABC transporters in lipid transport. Biochim. Biophys. Acta *1486*, 128-144.
Bradford, M.M. (1976). A rapid and sensitive method for the quantitation of microgram quantities of protein utilizing the principle of protein-dye binding. Anal. Biochem. *72*, 248-254.
Burger, K.N., Demel, R.A., Schmid, S.L., and de Kruijff, B. (2000). Dynamin is membrane-active: lipid insertion is induced by phosphoinositides and phosphatidic acid. Biochemistry *39*, 12485-12493.
Catty, P., de Kerchove d'Exaerde, A., and Goffeau, A. (1997). The complete inventory of the yeast *Saccharomyces cerevisiae* P-type transport ATPases. FEBS Lett. *409*, 325-332.
Chantalat, S., Park, S.K., Hua, Z., Liu, K., Gobin, R., Peyroche, A., Rambourg, A., Graham, T.R., and Jackson, C.L. (2004). The Arf activator Gea2p and the P-type ATPase Drs2p interact at the Golgi in *Saccharomyces cerevisiae*. J. Cell Sci. *117*, 711-722.
Chardin, P., Paris, S., Antonny, B., Robineau, S., Beraud-Dufour, S., Jackson, C.L., and Chabre, M. (1996). A human exchange factor for ARF contains Sec7- and pleckstrin-homology domains. Nature *384*, 481-484.
Chen, C.-Y., Ingram, M.F., Rosal, P.H., and Graham, T.R. (1999). Role for Drs2p, a P-type ATPase and potential aminophospholipid translocase, in yeast late Golgi function. J. Cell Biol. *147*, 1223-1236.
Chen, L., and Davis, N.G. (2000). Recycling of the yeast a-factor receptor. J. Cell Biol. *151*, 731-738.
Chu, D.S., Pishvaee, B., and Payne, G.S. (1996). The light chain subunit is required for clathrin function in *Saccharomyces cerevisiae*. J. Biol. Chem. *271*, 33123-33130.
Chvatchko, Y., Howald, I., and Riezman, H. (1986). Two yeast mutants defective in endocytosis are defective in pheromone response. Cell *46*, 355-364.
Conibear, E., and Stevens, T.H. (1998). Multiple sorting pathways between the late Golgi and the vacuole in yeast. Biochim. Biophys. Acta *1404*, 211-230.
Cooper, A.A., and Stevens, T.H. (1996). Vps10p cycles between the late-Golgi and prevacuolar compartments in its function as the sorting receptor for multiple yeast vacuolar hydrolases. J. Cell Biol. *133*, 529-541.
Cope, M.J., Yang, S., Shang, C., and Drubin, D.G. (1999). Novel protein kinases Ark1p and Prk1p associate with and regulate the cortical actin cytoskeleton in budding yeast. J. Cell Biol. *144*, 1203-1218.
Cowles, C.R., Odorizzi, G., Payne, G.S., and Emr, S.D. (1997). The AP-3 adaptor complex is essential for cargo-selective transport to the yeast vacuole. Cell *91*, 109-118.
Cox, R., Mason-Gamer, R.J., Jackson, C.L., and Segev, N. (2004). Phylogenetic analysis of Sec7-domain-containing Arf nucleotide exchangers. Mol. Biol. Cell *15*, 1487-1505.
Cremona, O., Di Paolo, G., Wenk, M.R., Luthi, A., Kim, W.T., Takei, K., Daniell, L., Nemoto, Y., Shears, S.B., Flavell, R.A., McCormick, D.A., and De Camilli, P. (1999). Essential role of phosphoinositide metabolism in synaptic vesicle recycling. Cell *99*, 179-188.
Daleke, D.L., and Lyles, J.V. (2000). Identification and purification of aminophospholipid flippases. Biochim. Biophys. Acta *1486*, 108-127.
Darsow, T., Burd, C.G., and Emr, S.D. (1998). Acidic di-leucine motif essential for AP-3-dependent sorting and restriction of the functional specificity of the Vam3p vacuolar t-SNARE. J. Cell Biol. *142*, 913-922.
Davis, R.H. (1986). Compartmental and regulatory mechanisms in the arginine pathways of *Neurospora crassa* and *Saccharomyces cerevisiae*. Microbiol. Rev. *50*, 280-313.

de Heuvel, E., Bell, A.W., Ramjaun, A.R., Wong, K., Sossin, W.S., and McPherson, P.S. (1997). Identification of the major synaptojanin-binding proteins in brain. J. Biol. Chem. *272*, 8710-8716.

Dell'Angelica, E.C., Klumperman, J., Stoorvogel, W., and Bonifacino, J.S. (1998). Association of the AP-3 adaptor complex with clathrin. Science *280*, 431-434.

Deloche, O., Yeung, B.G., Payne, G.S., and Schekman, R. (2001). Vps10p transport from the *trans*-Golgi network to the endosome is mediated by clathrin-coated vesicles. Mol. Biol. Cell *12*, 475-485.

Deshaies, R.J., Sanders, S.L., Feldheim, D.A., and Schekman, R. (1991). Assembly of yeast Sec proteins involved in translocation into the endoplasmic reticulum into a membrane-bound multisubunit complex. Nature *349*, 806-808.

Devaux, P.F. (1991). Static and dynamic lipid asymmetry in cell membranes. Biochemistry *30*, 1163-1173.

DeWitt, N.D., dos Santos, C.F., Allen, K.E., and Slayman, C.W. (1998). Phosphorylation region of the yeast plasma-membrane H+-ATPase. Role in protein folding and biogenesis. J. Biol. Chem. *273*, 21744-21751.

D'Hondt, K., Heese-Peck, A., and Riezman, H. (2000). Protein and lipid requirements for endocytosis. Annu. Rev. Genet. *34*, 255-295.

Donaldson, J.G., and Jackson, C.L. (2000). Regulators and effectors of the ARF GTPases. Curr. Opin. Cell Biol. *12*, 475-482.

Dove, S.K., Piper, R.C., McEwen, R.K., Yu, J.W., King, M.C., Hughes, D.C., Thuring, J., Holmes, A.B., Cooke, F.T., Michell, R.H., Parker, P.J., and Lemmon, M.A. (2004). Svp1p defines a family of phosphatidylinositol 3,5-bisphosphate effectors. EMBO J. *23*, 1922-1933.

Drees, B.L., Sundin, B., Brazeau, E., Caviston, J.P., Chen, G.C., Guo, W., Kozminski, K.G., Lau, M.W., Moskow, J.J., Tong, A., Schenkman, L.R., McKenzie, A., 3rd, Brennwald, P., Longtine, M., Bi, E., Chan, C., Novick, P., Boone, C., Pringle, J.R., Davis, T.N., Fields, S., and Drubin, D.G. (2001). A protein interaction map for cell polarity development. J. Cell Biol. *154*, 549-571.

Duncan, M.C., Cope, M.J., Goode, B.L., Wendland, B., and Drubin, D.G. (2001). Yeast Eps15-like endocytic protein, Pan1p, activates the Arp2/3 complex. Nat. Cell Biol. *3*, 687-690.

Engqvist-Goldstein, A.E., and Drubin, D.G. (2003). Actin assembly and endocytosis: from yeast to mammals. Annu. Rev. Cell Dev. Biol. *19*, 287-332.

Enyedi, A., Flura, M., Sarkadi, B., Gardos, G., and Carafoli, E. (1987). The maximal velocity and the calcium affinity of the red cell calcium pump may be regulated independently. J. Biol. Chem. *262*, 6425-6430.

Enyedi, A., Verma, A.K., Filoteo, A.G., and Penniston, J.T. (1993). A highly active 120-kDa truncated mutant of the plasma membrane Ca2+ pump. J. Biol. Chem. *268*, 10621-10626.

Esmon, B., Novick, P., and Schekman, R. (1981). Compartmentalized assembly of oligosaccharides on exported glycoproteins in yeast. Cell *25*, 451-460.

Fadok, V.A., Bratton, D.L., Rose, D.M., Pearson, A., Ezekewitz, R.A., and Henson, P.M. (2000). A receptor for phosphatidylserine-specific clearance of apoptotic cells. Nature *405*, 85-90.

Fagan, M.J., and Saier, M.H., Jr. (1994). P-type ATPases of eukaryotes and bacteria: sequence analyses and construction of phylogenetic trees. J. Mol. Evol. *38*, 57-99.

Farge, E., and Devaux, P.F. (1992). Shape changes of giant liposomes induced by an asymmetric transmembrane distribution of phospholipids. Biophys. J. *61*, 347-357.

Farge, E., Ojcius, D.M., Subtil, A., and Dautry-Varsat, A. (1999). Enhancement of endocytosis due to aminophospholipid transport across the plasma membrane of living cells. Am. J. Physiol. *276*, C725-733.
Farsad, K., Ringstad, N., Takei, K., Floyd, S.R., Rose, K., and De Camilli, P. (2001). Generation of high curvature membranes mediated by direct endophilin bilayer interactions. J. Cell Biol. *155*, 193-200.
Farsad, K., and De Camilli, P. (2003). Mechanisms of membrane deformation. Curr. Opin. Cell Biol. 15, 372-381.
Fazi, B., Cope, M.J., Douangamath, A., Ferracuti, S., Schirwitz, K., Zucconi, A., Drubin, D.G., Wilmanns, M., Cesareni, G., and Castagnoli, L. (2002). Unusual binding properties of the SH3 domain of the yeast actin-binding protein Abp1: structural and functional analysis. J. Biol. Chem. *277*, 5290-5298.
Ferrell, J.E., Lee, K.J., and Huestis, W.H. (1985). Membrane bilayer balance and erythrocyte shape: a quantitative assessment. Biochemistry *24*, 2849-2857.
Fields, S., and Song, O. (1989). A novel genetic system to detect protein-protein interactions. Nature *340*, 245-246.
Ford, M.G., Mills, I.G., Peter, B.J., Vallis, Y., Praefcke, G.J., Evans, P.R., and McMahon, H.T. (2002). Curvature of clathrin-coated pits driven by epsin. Nature *419*, 361-366.
Gad, H., Ringstad, N., Low, P., Kjaerulff, O., Gustafsson, J., Wenk, M., Di Paolo, G., Nemoto, Y., Crun, J., Ellisman, M.H., De Camilli, P., Shupliakov, O., and Brodin, L. (2000). Fission and uncoating of synaptic clathrin-coated vesicles are perturbed by disruption of interactions with the SH3 domain of endophilin. Neuron *27*, 301-312.
Gadella, B.M., and Harrison, R.A. (2002). Capacitation induces cyclic adenosine 3',5'-monophosphate-dependent, but apoptosis-unrelated, exposure of aminophospholipids at the apical head plasma membrane of boar sperm cells. Biol. Reprod. *67*, 340-350.
Gall, W.E., Geething, N.C., Hua, Z., Ingram, M.F., Liu, K., Chen, S.I., and Graham, T.R. (2002). Drs2p-dependent formation of exocytic clathrin-coated vesicles in vivo. Curr. Biol. *12*, 1623-1627.
Gallusser, A., and Kirchhausen, T. (1993). The beta 1 and beta 2 subunits of the AP complexes are the clathrin coat assembly components. EMBO J. *12*, 5237-5244.
Gary, J.D., Wurmser, A.E., Bonangelino, C.J., Weisman, L.S., and Emr, S.D. (1998). Fab1p is essential for PtdIns(3)P 5-kinase activity and the maintenance of vacuolar size and membrane homeostasis. J. Cell Biol. *143*, 65-79.
Godi, A., Pertile, P., Meyers, R., Marra, P., Di Tullio, G., Iurisci, C., Luini, A., Corda, D., and De Matteis, M.A. (1999). ARF mediates recruitment of PtdIns-4-OH kinase-beta and stimulates synthesis of PtdIns(4,5)P_2 on the Golgi complex. Nat. Cell Biol. *1*, 280-287.
Goffeau, A., Barrell, B.G., Bussey, H., Davis, R.W., Dujon, B., Feldmann, H., Galibert, F., Hoheisel, J.D., Jacq, C., Johnston, M., Louis, E.J., Mewes, H.W., Murakami, Y., Philippsen, P., Tettelin, H., and Oliver, S.G. (1996). Life with 6000 genes. Science *274*, 546, 563-547.
Gomes, E., Jakobsen, M.K., Axelsen, K.B., Geisler, M., and Palmgreen, M.G. (2000). Chilling tolerance in Arabidopsis involves *ALA1*, a member of a new family of putative aminophospholipid translocases. The Plant Cell *12*, 2441-2453.
Goode, B.L., Rodal, A.A., Barnes, G., and Drubin, D.G. (2001). Activation of the Arp2/3 complex by the actin filament binding protein Abp1p. J. Cell Biol. *153*, 627-634.
Gruenberg, J. (2001). The endocytic pathway: a mosaic of domains. Nat. Rev. Mol. Cell. Biol. *2*, 721-730.
Gruenberg, J. (2003). Lipids in endocytic membrane transport and sorting. Curr. Opin. Cell Biol. *15*, 382-388.

Guo, S., Stolz, L.E., Lemrow, S.M., and York, J.D. (1999). SAC1-like domains of yeast *SAC1*, *INP52*, and *INP53* and of human synaptojanin encode polyphosphoinositide phosphatases. J. Biol. Chem. *274*, 12990-12995.
Ha, S., Torabinejad, J., DeWald, D.B., Wenk, M.R., Lucast, L., De Camilli, P., Newitt, R.A., Aebersold, R., and Nothwehr, S.F. (2003). The synaptojanin-like protein Inp53/Sjl3p functions with clathrin in a yeast TGN-to-endosomes pathway distinct from the GGA protein-dependent pathway. Mol. Biol. Cell *14*, 1319-1333.
Haffner, C., Takei, K., Chen, H., Ringstad, N., Hudson, A., Butler, M.H., Salcini, A.E., Di Fiore, P.P., and De Camilli, P. (1997). Synaptojanin 1: localization on coated endocytic intermediates in nerve terminals and interaction of its 170 kDa isoform with Eps15. FEBS Lett. *419*, 175-180.
Halleck, M.S., Pradhan, D., Blackman, C., Berkes, C., Williamson, P., and Schlegel, R.A. (1998). Multiple members of a third subfamily of P-type ATPases identified by genomic sequences and ESTs. Genome Res. *8*, 354-361.
Halleck, M.S., Lawler, J.J., Blackshaw, S., Gao, L., Nagarajan, P., Hacker, C., Pyle, S., Newman, J.T., Nakanishi, Y., Ando, H., Weinstock, D., Williamson, P., and Schlegel, R.A. (1999). Differential expression of putative transbilayer amphipath transporters. Physiol. Genomics *1*, 139-150.
Hanahan, D. (1983). Studies on transformation of *Escherichia coli* with plasmids. J. Mol. Biol. *166*, 557-580.
Hama, H., Schnieders, E.A., Thorner, J., Takemoto, J.Y., and DeWald, D.B. (1999). Direct involvement of phosphatidylinositol 4-phosphate in secretion in the yeast *Saccharomyces cerevisiae*. J. Biol. Chem. *274*, 34294-34300.
Harris, T.W., Hartwieg, E., Horvitz, H.R., and Jorgensen, E.M. (2000). Mutations in synaptojanin disrupt synaptic vesicle recycling. J. Cell Biol. *150*, 589-600.
Henry, K.R., D'Hondt, K., Chang, J., Newpher, T., Huang, K., Hudson, R.T., Riezman, H., and Lemmon, S.K. (2002). Scd5p and clathrin function are important for cortical actin organization, endocytosis, and localization of Sla2p in yeast. Mol. Biol. Cell *13*, 2607-2625.
Heuser, J.E., and Keen, J. (1988). Deep-etch visualization of proteins involved in clathrin assembly. J. Cell Biol. *107*, 877-886.
Higgins, J.A. (1984). The transverse distribution of phospholipids in the membranes of Golgi subfractions of rat hepatocytes. Biochem. J. *219*, 261-272.
Hitchcock, A.L., Auld, K., Gygi, S.P., and Silver, P.A. (2003). A subset of membrane-associated proteins is ubiquitinated in response to mutations in the endoplasmic reticulum degradation machinery. Proc. Natl. Acad. Sci. USA *100*, 12735-12740.
Holthuis, J.C., Nichols, B.J., Dhruvakumar, S., and Pelham, H.R. (1998). Two syntaxin homologues in the TGN/endosomal system of yeast. EMBO J. *17*, 113-126.
Hua, Z., Fatheddin, P., and Graham, T.R. (2002). An essential subfamily of Drs2p-related P-type ATPases is required for protein trafficking between Golgi complex and endosomal/vacuolar system. Mol. Biol. Cell *13*, 3162-3177.
Hua, Z., and Graham, T.R. (2003). Requirement for Neo1p in retrograde transport from the Golgi complex to the endoplasmic reticulum. Mol. Biol. Cell *14*, 4971-4983.
Huijbregts, R. P., L. Topalof, and V. A. Bankaitis. (2000). Lipid metabolism and regulation of membrane trafficking. Traffic *1*, 195-202.
Ito, H., Fukuda, Y., Murata, K., and Kimura, A. (1983). Transformation of intact yeast cells treated with alkali cations. J. Bacteriol. *153*, 163-168.
Jenness, D.D., and Spatrick, P. (1986). Down regulation of the alpha-factor pheromone receptor in *S. cerevisiae*. Cell *46*, 345-353.

Jochum, A., Jackson, D., Schwarz, H., Pipkorn, R., and Singer-Krüger, B. (2002). Yeast Ysl2p, homologous to Sec7 domain guanine nucleotide exchange factors, functions in endocytosis and maintenance of vacuole integrity and interacts with the Arf-like small GTPase Arl1p. Mol. Cell. Biol. *22*, 4914-4928.
Jones, E.W. (1984). The synthesis and function of proteases in *Saccharomyces*: genetic approaches. Annu. Rev. Genet. *18*, 233-270.
Jones, D.H., Bax, B., Fensome, A., and Cockcroft, S. (1999). ADP ribosylation factor 1 mutants identify a phospholipase D effector region and reveal that phospholipase D participates in lysosomal secretion but is not sufficient for recruitment of coatomer I. Biochem. J. *341 (Pt 1)*, 185-192.
Jones, D.H., Morris, J.B., Morgan, C.P., Kondo, H., Irvine, R.F., and Cockcroft, S. (2000). Type I phosphatidylinositol 4-phosphate 5-kinase directly interacts with ADP-ribosylation factor 1 and is responsible for phosphatidylinositol 4,5-bisphosphate synthesis in the Golgi compartment. J. Biol. Chem. *275*, 13962-13966.
Kaksonen, M., Sun, Y., and Drubin, D.G. (2003). A pathway for association of receptors, adaptors, and actin during endocytic internalization. Cell *115*, 475-487.
Katzmann, D.J., Stefan, C.J., Babst, M., and Emr, S.D. (2003). Vps27 recruits ESCRT machinery to endosomes during MVB sorting. J. Cell Biol. *162*, 413-423.
Kim, W.T., Chang, S., Daniell, L., Cremona, O., Di Paolo, G., and De Camilli, P. (2002). Delayed reentry of recycling vesicles into the fusion-competent synaptic vesicle pool in synaptojanin 1 knockout mice. Proc. Natl. Acad. Sci. USA *99*, 17143-17148.
Kölling, R., and Hollenberg, C.P. (1994). The ABC-transporter Ste6 accumulates in the plasma membrane in a ubiquitinated form in endocytosis mutants. EMBO J. *13*, 3261-3271.
Laemmli, U.K. (1970). Cleavage of structural proteins during the assembly of the head of bacteriophage T4. Nature *227*, 680-685.
Lee, F.J.S., Huang, C.F., Yu, W.L., Buu, L.M., Lin, C.Y., Huang, M.C., Moss, J., and Vaughan, M. (1997). Characterization of an ADP-ribosylation factor-like 1 protein in *Saccharomyces cerevisiae*. J. Biol. Chem. *272*, 30998-31005.
Lewis, M.J., Nichols, B.J., Prescianotto-Baschong, C., Riezman, H., and Pelham, H.R. (2000). Specific retrieval of the exocytic SNARE Snc1p from early yeast endosomes. Mol. Biol. Cell *11*, 23-38.
Lila, T., and Drubin, D.G. (1997). Evidence for physical and functional interactions among two *Saccharomyces cerevisiae* SH3 domain proteins, an adenylyl cyclase-associated protein and the actin cytoskeleton. Mol. Biol. Cell *8*, 367-385.
Machesky, L.M., and Gould, K.L. (1999). The Arp2/3 complex: a multifunctional actin organizer. Curr. Opin. Cell Biol. *11*, 117-121.
Martin, T.F. (2001). PI(4,5)P_2 regulation of surface membrane traffic. Curr. Opin. Cell Biol. *13*, 493-499.
McIntosh, T.J. (1996). Hydration properties of lamellar and non-lamellar phases of phosphatidylcholine and phosphatidylethanolamine. Chem. Phys. Lipids *81*, 117-131.
McPherson, P.S., Garcia, E.P., Slepnev, V.I., David, C., Zhang, X., Grabs, D., Sossin, W.S., Bauerfeind, R., Nemoto, Y., and De Camilli, P. (1996). A presynaptic inositol-5-phosphatase. Nature *379*, 353-357.
Mulholland, J., Konopka, J., Singer-Krüger, B., Zerial, M., and Botstein, D. (1999). Visualization of receptor-mediated endocytosis in yeast. Mol. Biol. Cell *10*, 799-817.
Muller, P., Pomorski, T., and Herrmann, A. (1994). Incorporation of phospholipid analogues into the plasma membrane affects ATP-induced vesiculation of human erythrocyte ghosts. Biochem. Biophys. Res. Commun. *199*, 881-887.
Natarajan, P., Wang, J., Hua, Z., and Graham, T.R. (2004). Drs2p-coupled aminophospholipid translocase activity in yeast Golgi membranes and relationship to *in vivo* function. Proc. Natl. Acad. Sci. USA *101*, 10614-10619.

Nelson, N. (1989). Structure, molecular genetics, and evolution of vacuolar H+-ATPases. J. Bioenerg. Biomembr. *21*, 553-571.
Nossal, R. (2001). Energetics of clathrin basket assembly. Traffic *2*, 138-147.
Novick, P., Field, C., and Schekman, R. (1980). Identification of 23 complementation groups required for post-translational events in the yeast secretory pathway. Cell *21*, 205-215.
Odorizzi, G., Babst, M., and Emr, S.D. (1998a). Fab1p PtdIns(3)P 5-kinase function essential for protein sorting in the multivesicular body. Cell *95*, 847-858.
Odorizzi, G., Cowles, C.R., and Emr, S.D. (1998b). The AP-3 complex: a coat of many colours. Trends Cell Biol. *8*, 282-288.
Odorizzi, G., Babst, M., and Emr, S.D. (2000). Phosphoinositide signaling and the regulation of membrane trafficking in yeast. Trends Biochem. Sci. *25*, 229-235.
Ohno, H., Stewart, J., Fournier, M.C., Bosshart, H., Rhee, I., Miyatake, S., Saito, T., Gallusser, A., Kirchhausen, T., and Bonifacino, J.S. (1995). Interaction of tyrosine-based sorting signals with clathrin-associated proteins. Science *269*, 1872-1875.
Palmgren, S., Ojala, P.J., Wear, M.A., Cooper, J.A., and Lappalainen, P. (2001). Interactions with PIP2, ADP-actin monomers, and capping protein regulate the activity and localization of yeast twinfilin. J. Cell Biol. *155*, 251-260.
Pasqualato, S., Renault, L., and Cherfils, J. (2002). Arf, Arl, Arp and Sar proteins: a family of GTP-binding proteins with a structural device for 'front-back' communication. EMBO Rep. *3*, 1035-1041.
Payne, G.S., Baker, D., van Tuinen, E., and Schekman, R. (1988). Protein transport to the vacuole and receptor-mediated endocytosis by clathrin heavy chain-deficient yeast. J. Cell Biol. *106*, 1453-1461.
Pelham, H.R. (1999). SNAREs and the secretory pathway-lessons from yeast. Exp. Cell Res. *247*, 1-8.
Pelham, H.R.B. (2002). Insights from yeast endosomes. Curr. Opin. Cell Biol. *14*, 454-462.
Perez-Victoria, F.J., Gamarro, F., Ouellette, M., and Castanys, S. (2003). Functional cloning of the miltefosine transporter. A novel P-type phospholipid translocase from *Leishmania* involved in drug resistance. J. Biol. Chem. *278*, 49965-49971.
Peterson, M.R., Burd, C.G., and Emr, S.D. (1999). Vac1p coordinates Rab and phosphatidylinositol 3-kinase signaling in Vps45p-dependent vesicle docking/fusion at the endosome. Curr. Biol. *9*, 159-162.
Piper, R.C., Cooper, A.A., Yang, H., and Stevens, T.H. (1995). *VPS27* controls vacuolar and endocytic traffic through a prevacuolar compartment in *Saccharomyces cerevisiae*. J. Cell Biol. *131*, 603-617.
Pomorski, T., Lombardi, R., Riezman, H., Devaux, P.F., van Meer, G., and Holthuis, C.M. (2003). Drs2p-related P-type ATPases Dnf1p and Dnf2p are required for phospholipid translocation across the yeast plasma membrane and serve a role in endocytosis. Mol. Biol. Cell *14*, 1240-1254.
Pomorski, T., Holthuis, J.C., Herrmann, A., and van Meer, G. (2004). Tracking down lipid flippases and their biological functions. J. Cell Sci. *117*, 805-813.
Portillo, F., de Larrinoa, I.F., and Serrano, R. (1989). Deletion analysis of yeast plasma membrane H+-ATPase and identification of a regulatory domain at the carboxyl-terminus. FEBS Lett. *247*, 381-385.
Prescianotto-Baschong, C., and Riezman, H. (1998). Morphology of the yeast endocytic pathway. Mol. Biol. Cell *9*, 173-189.
Prescianotto-Baschong, C., and Riezman, H. (2002). Ordering of compartments in the yeast endocytic pathway. Traffic *3*, 37-49.
Prezant, T.R., Chaltraw, W.E., Jr., and Fischel-Ghodsian, N. (1996). Identification of an overexpressed yeast gene which prevents aminoglycoside toxicity. Microbiology *142*, 3407-3414.

Prinz, W.A., Grzyb, L., Veenhuis, M., Kahana, J.A., Silver, P.A., and Rapoport, T.A. (2000). Mutants affecting the structure of the cortical endoplasmic reticulum in *Saccharomyces cerevisiae*. J. Cell Biol. *150*, 461-474.
Qualmann, B., Kessels, M.M., and Kelly, R.B. (2000). Molecular links between endocytosis and the actin cytoskeleton. J. Cell Biol. *150*, F111-116.
Radji, M., Kim, J.M., Togan, T., Yoshikawa, H., and Shirahige, K. (2001). The cloning and characterization of the *CDC50* gene family in *Saccharomyces cerevisiae*. Yeast *18*, 195-205.
Randazzo, P.A., and Hirsch, D.S. (2004). Arf GAPs: multifunctional proteins that regulate membrane traffic and actin remodelling. Cell Signal. *16*, 401-413.
Rapoport, I., Chen, Y.C., Cupers, P., Shoelson, S.E., and Kirchhausen, T. (1998). Dileucine-based sorting signals bind to the beta chain of AP-1 at a site distinct and regulated differently from the tyrosine-based motif-binding site. EMBO J. *17*, 2148-2155.
Riezman, H. (1985). Endocytosis in yeast: several of the yeast secretory mutants are defective in endocytosis. Cell *40*, 1001-1009.
Rigaut, G., Shevchenko, A., Rutz, B., Wilm, M., Mann, M., and Seraphin, B. (1999). A generic protein purification method for protein complex characterization and proteome exploration. Nat. Biotechnol. *17*, 1030-1032.
Rosenwald, A.G., Rhodes, M.A., Van Valkenburgh, H., Palanivel, V., Chapman, G., Boman, A., Zhang, C.J., and Kahn, R.A. (2002). *ARL1* and membrane traffic in *Saccharomyces cerevisiae*. Yeast *19*, 1039-1056.
Rosing, J., Tans, G., Govers-Riemslag, J.W., Zwaal, R.F., and Hemker, H.C. (1980). The role of phospholipids and factor Va in the prothrombinase complex. J. Biol. Chem. *255*, 274-283.
Rothman, J.E. (1994). Mechanisms of intracellular protein transport. Nature *372*, 55-63.
Rubino, M., Miaczynska, M., Lippe, R., and Zerial, M. (2000). Selective membrane recruitment of EEA1 suggests a role in directional transport of clathrin-coated vesicles to early endosomes. J. Biol. Chem. *275*, 3745-3748.
Saito, K., Fujimura-Kamada, K., Furuta, N., Kato, U., Umeda, M., and Tanaka, K. (2004). Cdc50p, a protein required for polarized growth, associates with the Drs2p P-type ATPase implicated in phospholipid translocation in *Saccharomyces cerevisiae*. Mol. Biol. Cell *15*, 3418-3432.
Sambrook, J., Fritsch, E.F., and Manniatis, T. (1989). Molecular Cloning-A Laboratory Manual. 2. edn, (Cold Spring Harbor Laboratory Press).
Sato, K., Sato, M., and Nakano, A. (2001). Rer1p, a retrieval receptor for endoplasmic reticulum membrane proteins, is dynamically localized to the Golgi apparatus by coatomer. J. Cell Biol. *152*, 935-944.
Schuske, K.R., Richmond, J.E., Matthies, D.S., Davis, W.S., Runz, S., Rube, D.A., van der Bliek, A.M., and Jorgensen, E.M. (2003). Endophilin is required for synaptic vesicle endocytosis by localizing synaptojanin. Neuron *40*, 749-762.
Segev, N., Mulholland, J., and Botstein, D. (1988). The yeast GTP-binding YPT1 protein and a mammalian counterpart are associated with the secretion machinery. Cell *52*, 915-924.
Seigneuret, M., and Devaux, P.F. (1984). ATP-dependent asymmetric distribution of spin-labeled phospholipids in the erythrocyte membrane: relation to shape changes. Proc. Natl. Acad. Sci. USA *81*, 3751-3755.
Sekiya-Kawasaki, M., Groen, A.C., Cope, M.J., Kaksonen, M., Watson, H.A., Zhang, C., Shokat, K.M., Wendland, B., McDonald, K.L., McCaffery, J.M., and Drubin, D.G. (2003). Dynamic phosphoregulation of the cortical actin cytoskeleton and endocytic machinery revealed by real-time chemical genetic analysis. J. Cell Biol. *162*, 765-772.

Sheetz, M.P., and Singer, S.J. (1974). Biological membranes as bilayer couples. A molecular mechanism of drug-erythrocyte interactions. Proc. Natl. Acad. Sci. USA *71*, 4457-4461.
Shih, S.C., Katzmann, D.J., Schnell, J.D., Sutanto, M., Emr, S., and Hicke, L. (2002). Epsins and Vps27p/Hrs contain ubiquitin-binding domains that function in receptor endocytosis. Nat. Cell Biol. *4*, 389-393.
Simonsen, A., Wurmser, A.E., Emr, S.D., and Stenmark, H. (2001). The role of phosphoinositides in membrane transport. Curr. Opin. Cell Biol. *13*, 485-492.
Singer, B., and Riezman, H. (1990). Detection of an intermediate compartment involved in transport of alpha-factor from the plasma membrane to the vacuole in yeast. J. Cell Biol. *110*, 1911-1922.
Singer-Krüger, B., Frank, R., Crausaz, F., and Riezman, H. (1993). Partial purification and characterization of early and late endosomes from yeast. Identification of four novel proteins. J. Biol. Chem. *268*, 14376-14386.
Singer-Krüger, B., Stenmark, H., Düsterhöft, A., Philippsen, P., Yoo, J.-S., Gallwitz, D., and Zerial, M. (1994). Role of three rab5-like GTPases, Ypt51p, Ypt52p, and Ypt53p, in the endocytic and vacuolar protein sorting pathways of yeast. J. Cell Biol. *125*, 283-298.
Singer-Krüger, B., Stenmark, H., and Zerial, M. (1995). Yeast Ypt51p and mammalian Rab5: counterparts with similar function in the early endocytic pathway. J. Cell Sci. *108*, 3509-3521.
Singer-Krüger, B., and Ferro-Novick, S. (1997). Use of a synthetic lethal screen to identify yeast mutants impaired in endocytosis, vacuolar protein sorting and the organization of the cytoskeleton. Europ. J. Cell Biol. *74*, 365-375.
Singer-Krüger, B., Nemoto, Y., Daniell, L., Ferro-Novick, S., and De Camilli, P. (1998). Synaptojanin family members are implicated in endocytic membrane traffic in yeast. J. Cell Sci. *111 (Pt 22)*, 3347-3356.
Slepnev, V.I., and De Camilli, P. (2000). Accessory factors in clathrin-dependent synaptic vesicle endocytosis. Nat. Rev. Neurosci. *1*, 161-172.
Smythe, E., and Ayscough, K.R. (2003). The Ark1/Prk1 family of protein kinases. Regulators of endocytosis and the actin skeleton. EMBO Rep. *4*, 246-251.
Srinivasan, S., Seaman, M., Nemoto, Y., Daniell, L., Suchy, S.F., Emr, S., De Camilli, P., and Nussbaum, R. (1997). Disruption of three phosphatidylinositol-polyphosphate 5-phosphatase genes from *Saccharomyces cerevisiae* results in pleiotropic abnormalities of vacuole morphology, cell shape, and osmohomeostasis. Eur. J. Cell Biol. *74*, 350-360.
Stamenova, S.D., Dunn, R., Adler, A.S., and Hicke, L. (2004). The Rsp5 ubiquitin ligase binds to and ubiquitinates members of the yeast CIN85-endophilin complex, Sla1-Rvs167. J. Biol. Chem. *279*, 16017-16025.
Stefan, C.J., Audhya, A., and Emr, S.D. (2002). The yeast synaptojanin-like proteins control the cellular distribution of phosphatidylinositol (4,5)-bisphosphate. Mol. Biol. Cell *13*, 542-557.
Stepp, J.D., Pellicena-Palle, A., Hamilton, S., Kirchhausen, T., and Lemmon, S.K. (1995). A late Golgi sorting function for *Saccharomyces cerevisiae* Apm1p, but not for Apm2p, a second yeast clathrin AP medium chain-related protein. Mol. Biol. Cell *6*, 41-58.
Stolz, L.E., Huynh, C.V., Thorner, J., and York, J.D. (1998). Identification and characterization of an essential family of inositol polyphosphate 5-phosphatases (*INP51*, *INP52* and *INP53* gene products) in the yeast *Saccharomyces cerevisiae*. Genetics *148*, 1715-1729.
Takei, K., Haucke, V., Slepnev, V., Farsad, K., Salazar, M., Chen, H., and De Camilli, P. (1998). Generation of coated intermediates of clathrin-mediated endocytosis on protein-free liposomes. Cell *94*, 131-141.

Takei, K., Slepnev, V.I., Haucke, V., and De Camilli, P. (1999). Functional partnership between amphiphysin and dynamin in clathrin-mediated endocytosis. Nat. Cell Biol. *1*, 33-39.
Tan, P.K., Davis, N.G., Sprague, G.F., and Payne, G.S. (1993). Clathrin facilitates the internalization of seven transmembrane segment receptors for mating pheromones in yeast. J. Cell Biol. *123*, 1707-1716.
Tang, X., Halleck, M.S., Schlegel, R.A., and Williamson, P. (1996). A subfamily of P-type ATPases with aminophospholipid transporting activity. Science *272*, 1495-1497.
Towbin, H., Staehelin, T., and Gordon, J. (1979). Electrophoretic transfer of proteins from polyacrylamide gels to nitrocellulose sheets: procedure and some applications. Proc. Natl. Acad. Sci. USA. *76*, 4350-4354.
Ungewickell, E., and Branton, D. (1981). Assembly units of clathrin coats. Nature *289*, 420-422.
Verstreken, P., Koh, T.W., Schulze, K.L., Zhai, R.G., Hiesinger, P.R., Zhou, Y., Mehta, S.Q., Cao, Y., Roos, J., and Bellen, H.J. (2003). Synaptojanin is recruited by endophilin to promote synaptic vesicle uncoating. Neuron *40*, 733-748.
Vida, T.A., and Emr, S.D. (1995). A new vital stain for visualizing vacuolar membrane dynamics and endocytosis in yeast. J. Cell Biol. *128*, 779-792.
Wang, L., Beserra, C., and Garbers, D.L. (2004). A novel aminophospholipid transporter exclusively expressed in spermatozoa is required for membrane lipid asymmetry and normal fertilization. Dev. Biol. *267*, 203-215.
Wang, Q., and Chang, A. (1999). Eps1, a novel PDI-related protein involved in ER quality control in yeast. EMBO J. *18*, 5972-5982.
Warren, D.T., Andrews, P.D., Gourlay, C.W., and Ayscough, K.R. (2002). Sla1p couples the yeast endocytic machinery to proteins regulating actin dynamics. J. Cell Sci. *115*, 1703-1715.
Watson, H.A., Cope, M.J., Groen, A.C., Drubin, D.G., and Wendland, B. (2001). *In vivo* role for actin-regulating kinases in endocytosis and yeast epsin phosphorylation. Mol. Biol. Cell *12*, 3668-3679.
Wendland, B., and Emr, S.D. (1998). Pan1p, yeast eps15, functions as a multivalent adaptor that coordinates protein-protein interactions essential for endocytosis. J. Cell Biol. *141*, 71-84.
Wendland, B., Steece, K.E., and Emr, S.D. (1999). Yeast epsins contain an essential N-terminal ENTH domain, bind clathrin and are required for endocytosis. EMBO J. *18*, 4383-4393.
Wesp, A., Hicke, L., Palecek, J., Lombardi, R., Aust, T., Munn, A.L., and Riezman, H. (1997). End4p/Sla2p interacts with actin-associated proteins for endocytosis in *Saccharomyces cerevisiae*. Mol. Biol. Cell *8*, 2291-2306.
Winter, D., Lechler, T., and Li, R. (1999). Activation of the yeast Arp2/3 complex by Bee1p, a WASP-family protein. Curr. Biol. *9*, 501-504.
Yin, H.L., and Janmey, P.A. (2003). Phosphoinositide regulation of the actin cytoskeleton. Annu. Rev. Physiol. *65*, 761-789.
Zachowski, A., Henry, J.P., and Devaux, P.F. (1989). Control of transmembrane lipid asymmetry in chromaffin granules by an ATP-dependent protein. Nature *340*, 75-76.
Zachowski, A. (1993). Phospholipids in animal eukaryotic membranes: transverse asymmetry and movement. Biochem. J. *294 (Pt 1)*, 1-14.
Zhao, L., Helms, J.B., Brugger, B., Harter, C., Martoglio, B., Graf, R., Brunner, J., and Wieland, F.T. (1997). Direct and GTP-dependent interaction of ADP ribosylation factor 1 with coatomer subunit beta. Proc. Natl. Acad. Sci. USA *94*, 4418-4423.
Ziman, M., Chuang, J.S., and Schekman, R.W. (1996). Chs1p and Chs3p, two proteins involved in chitin synthesis, populate a compartment of the *Saccharomyces cerevisiae* endocytic pathway. Mol. Biol. Cell *7*, 1909-1919.

Acknowledgements

I would like to start by thanking my Ph.D. advisor, Priv.-Doz. Dr. Birgit Singer-Krüger, who provided me with excellent support and scientific tutoring during the past three years. Thanks to her I had the opportunity to work on a particularly exciting project, to which she was extremely dedicated. Her enthusiasm and the innumerable pieces of advice she gave me greatly contributed to make this experience a very stimulating and enriching one.

Secondly, I would like to take this opportunity to thank Prof. Dr. Dieter Wolf, who gave me the possibility to accomplish my Ph.D. project at the institute for biochemistry and who accepted to be a member of my graduation committee.

I am also thankful to all the colleges I had the chance to work with during these three years: Claudia Böttcher, Maja Lasic, Yvonne Volkenstein, Alexandra Ziegler, Viola Günther, Dagmar Siele, and Alexandra Jochum. Having them around created an enjoyable work atmosphere. I thank Claudia and Maja in particular, with whom I had inspiring scientific discussions and who reviewed some parts of my thesis, thus greatly helping me.

I am also grateful to the numerous persons of the institute who helped me during the Ph.D. project and with whom I spent some social time. A particular thank to Elisabeth and Dragica for their logistical support.

On a more personal basis, I thank Cédric for continuously supporting me and believing in me, my mother, who made all of this possible by taking care of pretty much everything, and finally Paul, whose discreet but attentive presence helped me in the last months of the thesis.

Hiermit versichere ich, dass ich diese Arbeit selbständig und nur unter Verwendung der angegebenen Hilfsmittel angefertigt habe.

Stuttgart, den 15. Dezember 2004

Sidonie Wicky John